$\delta^{44/40}$Ca, Mg/Ca and δ^{18}O ratios of planktonic foraminifera from the Nordic Seas

Dissertation zur Erlangung des Doktorgrades

der Mathematisch-Naturwissenschaftlichen Fakultät

der Christian-Albrechts-Universität zu Kiel

Vorgelegt von

Reinhard Kozdon

Kiel, 2007

Referent:	Prof. Dr. Anton Eisenhauer
Koreferent:	Priv.-Doz. Dr. Mara Weinelt
Tag der mündlichen Prüfung:	7. Feb. 2007
Zum Druck genehmigt: Kiel, den	21. Mai 2007
	Prof. Dr. J. Grotemeyer
	Der Dekan

Hiermit erkläre ich an Eides statt, dass die vorliegende Abhandlung, abgesehen der Beratung durch meine akademischen Lehrer, nach Inhalt und Form meine eigene Arbeit darstellt. Ferner habe ich weder diese noch eine ähnliche Arbeit an einer anderen Abteilung oder Hochschule im Rahmen eines Prüfungsverfahrens vorgelegt.

Reinhard Kozdon

Abstract / Kurzfassung

Abstract

Sea surface temperatures (SSTs) contribute a vital element to our understanding of past and future climate dynamics. They strongly impact upon the global thermohaline circulation, a major driver of global climate variability on both millennial and orbital timescales. Reconstruction of SST history at key high latitude locations of hydrographic activity is essential for past climate understanding and modelling. A tremendous amount of these palaeoceanographic information is derived from proxy data from planktonic and benthic foraminifera. Reliable proxy data from higher latitudes are still relatively sparse, suggesting there may be complicating factors when comparing between multi-proxy reconstructions. In this context, the test of $\delta^{44/40}$Ca as a proxy for high latitude oceans is the main objective of this study.

In the **first chapter** (prepared for submission), a new approach for a solid $\delta^{44/40}$Ca temperature calibration of *N. pachyderma* (sin.) is presented, based on a broad sample pool comprising North and South Atlantic genotyped net catches and Nordic Seas core top sample material. We found that the calcium isotopic composition ($\delta^{44/40}$Ca) of calcite from genotyped and core top planktonic foraminifera *Neogloboquadrina pachyderma* (sin) is strongly related to temperature and independent of genetic variations providing an additional and independent proxy for the reconstruction of past SST in high latitude oceans.

The **second chapter** (submitted to GCA) addresses the issue of high latitude multi-proxy approaches comprising $\delta^{44/40}$Ca, Mg/Ca and δ^{18}O ratios in tests of the polar to subpolar planktonic foraminifera *N. pachyderma* (sin.) from Nordic Seas core top samples, covering an SST-range in between 0°C to 8°C. We found that tests of *N. pachyderma* (sin.) can be subdivided into two groups which differ significantly in their suitability as temperature proxy carrier. At water temperatures below about 3.5°C, the proxy to temperature relationship recorded in the Mg/Ca and $\delta^{44/40}$Ca signal simultaneously disappears. Based on these ‘cold-end‘ proxy-data we present a model demonstrating that the aberrant $\delta^{44/40}$Ca and Mg/Ca ratios in

N. pachyderma (sin.) calcified in cold polar waters can be interpreted by a two-step chemical modification of vacuolized seawater during its cytosolar transport to the calcification site.

The objective of the **third chapter** is a refinement of previous Mg/Ca temperature calibrations in combining $\delta^{44/40}$Ca, Mg/Ca and δ^{18}O ratios from Nordic Seas core top samples of the planktonic foraminifera *N. pachyderma* (sin.). Reference temperatures which were roughly estimated by hydrographic data in previous Mg/Ca temperature calibrations are now defined by parallel $\delta^{44/40}$Ca measurements. We found that in the Norwegian Sea, Mg/Ca as well as $\delta^{44/40}$Ca–inferred temperatures reflect hydrographic conditions strongly bound to the isopycnal defined by water densities σ_t of 27.7 to 27.8. As a result, the total amplitude of SST variations in the Nordic Seas recorded in the Mg/Ca and $\delta^{44/40}$Ca signal of *N. pachyderma* (sin.) is restricted to only about 4°, giving fairly constant values for the temperature difference between Late Holocene and LGM.

Kurzfassung

Die Rekonstruktion von Meerwassertemperaturen ist ein unverzichtbares Instrument, um vergangene Klimageschehen verstehen und zukünftige vorhersagen zu können. So beeinflussen sie beispielsweise die globale Thermohaline Zirkulation, die wiederum an den zyklischen globalen Klimaschwankungen maßgeblich beteiligt ist. Folglich muss der Rekonstruktion vergangener Wassertemperaturen, insbesondere in den Schlüsselregionen, eine große Bedeutung beigemessen werden. Ein wesentlicher Anteil der heute verfügbaren Temperaturinformationen der jüngeren Erdgeschichte wurde mithilfe von Proxy-Daten von planktischen und benthischen Foraminiferen gewonnen. Multiproxy Ansätze zeigen jedoch, dass die Vergleichbarkeit von Proxy-Daten aus hohen Breiten nicht immer gewährleistet ist. Basierend auf dieser Beobachtung ist es das Ziel dieser Arbeit, $\delta^{44/40}$Ca als einen neuen Proxy auf seine Eignung für die Anwendung in hohen Breiten zu überprüfen.

In dem **ersten Kapitel** wird eine neue, robuste Temperaturkalibrierung des $\delta^{44/40}$Ca Isotopensignals von *N. pachyderma* (sin.) vorgestellt, die sowohl genetisch kategorisierte Proben aus Netzfängen als auch fossile Sedimentoberflächenproben umfasst. Es hat sich gezeigt, dass die planktische Foraminifere *N. pachyderma* (sin.) unabhängig vom Genotyp eine

deutliche Temperaturabhängigkeit in der Ca-Isotopenfraktionierung aufweist. Dies ermöglicht die Anwendung von $\delta^{44/40}$Ca als einen ergänzenden Temperaturproxy in hohen Breiten.

In dem **zweiten Kapitel** werden Mg/Ca, $\delta^{44/40}$Ca sowie δ^{18}O Daten der planktischen, polar- bis subpolaren Foraminifere *N. pachyderma* (sin.) von Sedimentoberflächenproben aus dem Nordmeer verglichen. Der von den Wassermassen abgedeckte Temperaturbereich beträgt etwa 0°C bis 8°C. Der Multiproxy-Ansatz zeigt, dass sich *N. pachyderma* (sin.) in zwei Gruppen untergliedern lässt, die sich wesentlich in ihrer Eignung als Proxyträger unterscheiden. Beim Unterschreiten einer Kalzifizierungstemperatur von ca. 3.5°C wird die Temperaturabgängigkeit des Mg/Ca- Verhältnisses gemeinsam mit der $\delta^{44/40}$Ca -Isotopenfraktionierung aufgehoben. Basierend auf diesen Daten wurde ein Modell entwickelt, dass den abweichenden Chemismus des Kalkgehäuses durch eine zweifache Modifikation des vakuolisierten Meerwassers vor der biologisch induzierten Ausfällung erklärt.

Das **dritte Kapitel** befasst sich mit der Überarbeitung bestehender Mg/Ca Temperatur-kalibrierungen der Foraminiferenart *N. pachyderma* (sin.) mithilfe der Kombination von $\delta^{44/40}$Ca, Mg/Ca sowie δ^{18}O Daten. Während bisherige Kalibrierungen auf geschätzten Referenztemperaturen basieren, konnten nun erstmalig präzise Kalzifizierungstemperaturen mittels $\delta^{44/40}$Ca Parallelmessungen angewendet werden. Durch diesen neuen Ansatz zeigt sich, dass *N. pachyderma* (sin.) primär Wassermassensignale widerspiegelt, die dem Dichteintervall (σ_t) 27.7 bis 27.8 entsprechen. Infolgedessen stellt *N. pachyderma* (sin.) Variationen in den Oberflächenwassertemperaturen nur unvollständig mit einer maximalen Amplitude von etwa 4°C dar.

Contents

1. Introduction and goals

The knowledge of sea surface temperatures (SSTs) is most important for our understanding of past and future climate dynamics. This is because seawater temperature influences the release of trace and greenhouse gases at the interface between ocean and atmosphere, it controls the amount of global precipitation, the distribution of water vapour as well as the global thermohaline circulation as the major driver of global climate variability on both millennial and orbital timescales. Therefore, the reconstruction of the SST history at key locations of hydrographic activity is essential for climate modelling. A large part of palaeoceanographic information is derived from proxy data using benthic and planktonic foraminifera being among the most important proxy carriers. The advantage of using foraminifera for palaeoclimatic reconstructions lies in their high abundance in the marine realm and their excellent preservation in marine sediments. With a growing number of available proxies, many multi-proxy approaches have been published recently in order to test different proxies for consistency and to extract new environmental information. However, available data from multi-proxy approaches are mostly limited to low latitudes where they provide consistent values for temperature. Data from high latitude oceans with their various physical boundary conditions are still sparse and provide discrepant results, implying the presence of other controlling factors superimposing the pure temperature signal at the 'cold-end' of any given proxy-temperature calibration (Weinelt et al., 2003). Although it is already well known that none of the existing proxies is controlled by one environmental parameter only, proxy-specific uncertainties tend to increase with decreasing temperatures at high latitudes. This situation is very unsatisfactory as the high latitude oceans are considered to be the pacemaker for climate change. Hence, a lot of effort is spend in the development of new and the refinement of existing proxies in order to perform self-consistent multi-proxy approaches for high latitudes.

A first step in the development of geochemical proxies started with the study of Urey et al. (1947) who postulated that the temperature-response on the fractionation of the oxygen-isotopes between water and carbonates might become an important geological tool. Today it is known that the $\delta^{18}O$ signal in foraminifera is basically a combination of temperature, global ice volume, changes of salinity and seawater pH (Lea et al., 2001, Schrag et al., 1996, Schmidt et al., 2001).

Later, initiated by the study of Nürnberg (1995), Mg/Ca has become the second most important foraminiferal proxy-tool for the reconstruction of seawater temperatures within one decade. The temperature sensitivity of the Mg-content is best described by an exponential function with a strong biologic-mediated Mg-increase of about 10%°C^{-1} compared to only 3%°C^{-1} in inorganic precipitates (Oomori et al., 1987). As a result of this exponential temperature equation, foraminiferal Mg/Ca ratios are almost insensitive to temperature fluctuations in cold waters. Further restrictions of the application of Mg/Ca as palaeothermometer are coming from its pressure dependency within the water column as well as problems related to post-depositional changes and chemical alteration in sediments. With respect to long-term Mg/Ca reconstructions, insufficient knowledge of the initial Mg/Ca-ratios in the water column additionally restrict the precision of this proxy-tool.

As a consequence of the limited potential of Mg/Ca as palaeothermometer, efforts were made to develop complementary temperature proxies. In this regard, isotope proxies are highly recommended because they are supposed to be less sensitive to environmental changes than element-to-calcium ratios. It was Zhu & Macdougall in 1998 who first reported a temperature sensitivity in the Ca isotope fractionation of *N. pachyderma* of about 0.1 ‰°C^{-1}. A systematic study of Nägler at al., (2000) based on fossil and cultured *G. sacculifer* revealed a pronounced Ca isotope temperature sensitivity of about 0.2 ‰°C^{-1}. Subsequently, Hippler et al. (2004) verified the findings of Zhu & Macdougall (1998) and reported a $\delta^{44/40}$Ca temperature response of about 0.15‰°C^{-1} in genotyped *N. pachyderma* (sin.) from Nordic Seas plankton tow samples, qualifying the $\delta^{44/40}$Ca ratios of this polar to subpolar planktonic foraminifera as a sensitive recorder of past temperature fluctuations. Besides secular variations of the Ca-isotopic composition of seawater, no other environmental factor than water temperature is known so far to influence $\delta^{44/40}$Ca ratios in *N. pachyderma* (sin.). Therefore, $\delta^{44/40}$Ca can be regarded as a promising proxy-tool for high latitude oceans.

Based on these findings, the major goals of this study were:

(1) Verification of the $\delta^{44/40}$Ca temperature relation found in plankton tow samples with Holocene core top samples from the Nordic Seas

(2) Testing this new proxy at 'cold-end' conditions to gain information about its limitations

(3) To apply $\delta^{44/40}$Ca in a multi proxy approach in order to test its consistency by parallel δ^{18}O and Mg/Ca measurements.

References

Hippler, D., Darling, K.F., Eisenhauer, A., Nägler, T.F. 2004. Ca isotopes in high-latitude marine settings: Testing the limits of reliable SST estimates based on *N. pachyderma* (sin.). Abstract Swiss GeoScience Meeting

Lea D.W., Mashiotta T.A., Spero H.J., 1999. Controls on magnesium and strontium uptake in planktonic foraminifera determined by live culturing. Geochim. Cosmochim. Acta 63, 2369-2379

Nägler, T.F., Eisenhauer, A., Müller A.,. Hemleben, C., Kramers, J., 2000. The δ^{44}Ca–temperature calibration on fossil and cultured *Globigerinoides sacculifer*: new tool for reconstruction of past sea surface temperatures. Geochem. Geophys. Geosyst. 1

Nürnberg, D., 1995. Magnesium in tests of *Neogloboquadrina pachyderma* (sinistral) from high northern and southern latitudes. Journal of Foraminiferal Research 25, 350–368

Oomori, T., Kaneshima, H., Maezato, Y., Kitano, Y., 1987. Distribution coefficient of Mg^{2+} ions between calcite and solution at 10–50°C. Mar. Chem. 20, 327–336

Schmidt, G.A., Hoffman, G., Thresher, D., 2001. Isotopic tracers in coupled models: a new paleo-tool. PAGES News 9(1), 10-11

Schrag, D.P., Hampt, G., Murray, D.W., 1996. Pore fluid constrains on the temperature and oxygen isotopic composition of the glacial ocean. Science 272, 1930-1932

Urey H.C., 1947. The thermodynamic properties of isotopic substances. J. Chem. Soc., 562-581

Weinelt, M., Kuhnt, W., Sarnthein, M., Altenbach, A., Costello, O., Erlenkeuser, H., Matthiessen, J., Pflaumann, U., Simstich, J., Struck, U., Thies, A., Trauth, M., Vogelsang, E., 2001. Paleoceanographic proxies in the Northern North Atlantic. In: Schäfer, P., Ritzrau, W., Schlüter, M., Thiede, J. (Eds.), The Northern North Atlantic. Springer, Berlin, 319-352

Zhu, P., Macdougall, J.D., 1998. Calcium isotopes in the marine environment and the oceanic calcium cycle. Geochimica et Cosmochimica Acta 62, 1691–1698

.

2. Genetically constrained calcium isotope thermometry in high-latitude oceans

by

Hippler, D.[1*)]; Kozdon, R.[2)]; Darling, K.[3)]; Eisenhauer, A.[2)]; Nägler, T. F.[1)]

[1)]Institute of Geological Sciences, University of Bern, Baltzerstraße 1-3, 3012 Bern, Switzerland

[2)]Leibniz-Institut für Meereswissenschaften (IFM-GEOMAR), Wischhofstraße 1-3, 24148 Kiel, Germany

[3)]Grant Institute of Earth Science, University of Edinburgh, West Mains Road, Edinburgh EH9 3JW

*) Corresponding author: Tel.: +31 20 598 7365; fax: +31 20 598 99 41 (D. Hippler). Present address: Faculty of Earth and Life Sciences, Vrije Universiteit Amsterdam, De Boelelaan 1085, 1081 HV Amsterdam

Abstract

The accurate reconstruction of sea surface temperature (SST) history in climate-sensitive regions (e.g. tropical and polar oceans) became a challenging task in palaeoceanographic research. However, biogenic shell carbonate SST proxies successfully developed for tropical regions often fail in cool water environments. Their major regional shortcomings and the cryptic diversity now found within the major high latitude proxy carrier *Neogloboquadrina pachyderma* (sin.) highlight an urgent need to develop complementary SST proxies for these cool water regions. Here we incorporate the genetic component into a calibration study of a new SST proxy for the high latitudes. We found that the calcium isotopic composition ($\delta^{44/40}$Ca) of calcite from genotyped net catches and core top samples of the planktonic foraminifera *Neogloboquadrina pachyderma* (sin) is strongly related to temperature and unaffected by genetic variations providing an additional and independent proxy for the reconstruction of past SST in high latitude oceans.

Keywords: Ca isotopes, sea surface temperature proxy, planktonic foraminifera, *N. pachyderma* (left-coiling), genotype

2.1. Introduction

Sea surface temperatures (SSTs) contribute a vital element to our understanding of past and future climate dynamics [1]. They strongly impact upon the global thermohaline circulation, a major driver of global climate variability on both millennial and orbital timescales [2]. Reconstruction of SST history at key high latitude locations of hydrographic activity is essential for past climate modelling [3] yet accurate high latitude proxies for SSTs remain elusive.

The growing consensus on the reliability of biostatistical and geochemical SST proxies successfully utilized in the tropics [4-6] contrasts markedly with their application in the (sub-) polar oceans. The interpretation of $\delta^{18}O$-values in planktonic foraminiferal shell calcite from high latitudes is complicated by the fact that seawater $\delta^{18}O$ is altered significantly by frequent meltwater discharges related to the complex ice-sheet dynamics of this region [7]. Moreover, planktonic foraminiferal Mg/Ca ratios show little response to temperature in the cold-water areas of the Nordic Seas [8]. This is thought to be due to the difference in sea water carbonate chemistry specifically associated with Arctic polar water masses which are characterised by low salinities and annual sea ice cover. Alkenone proxies overestimate Last Glacial Maximum temperatures for these regions [9], possibly due to ice-rafted ancient alkenones masking the autochthonous biomarker signal [10]. Temperature overestimates are also a common problem in all transfer functions using the near-monospecific assemblages found in polar regions [11, 12]. These inherent shortcomings highlight the urgent need to develop complementary SST proxies for these high latitude regions of major climate change.

Previous studies reported variations in the calcium isotopic composition of planktonic foraminiferal species potentially related to temperature [13]. This relationship has now been successfully quantified and temperature calibrations of the Ca isotope fractionation of the tropical foraminifer *Globigerinoides sacculifer* have been established and applied as palaeothermometers in the tropical Atlantic Ocean on glacial-interglacial timescale [14, 15]. In the high latitudes, *N. pachyderma* (sin.) dominates the bipolar assemblages [12] and constitutes the major ecological and geochemical proxy carrier of modern and past polar ocean conditions in both hemispheres. Here we examine Ca isotope fractionation in *N. pachyderma* (sin.) and demonstrate its potential as a complementary tool for multi-proxy SST reconstruction in these regions. Several studies clearly

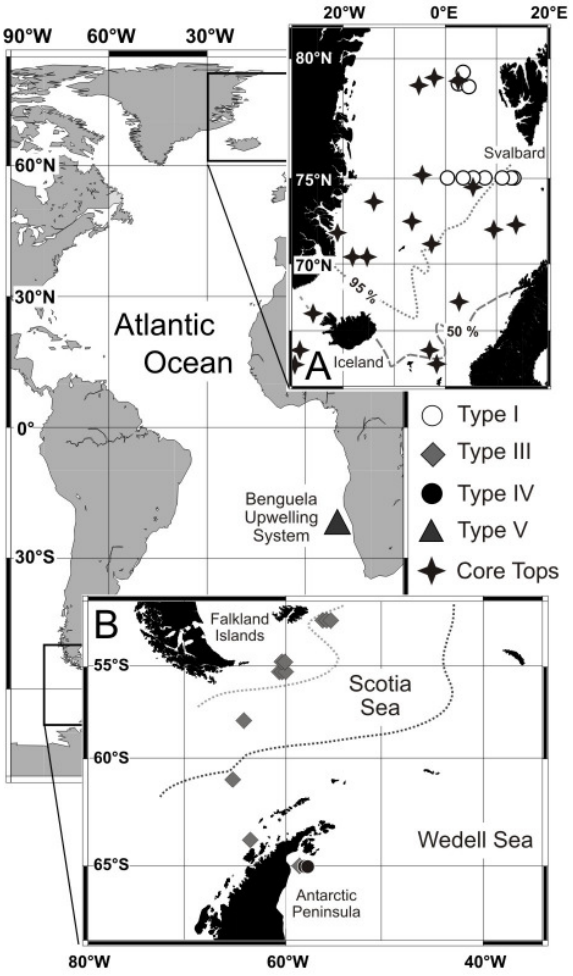

Fig. 1. Sampling localities of genotyped samples and distribution of the high-latitude and Benguela left-coiling (sin.) *N. pachyderma* genotypes. (a) Station chart of *N. pachyderma* (sin.) type I in the northern North Atlantic. The contour denotes the sediment "core top" coiling ratio (% sin coiling). (b) Distribution pattern of *N. pachyderma* (sin.) type II, III, and IV in the subpolar/polar Antarctic deduced from samples of cruise JR48. The contours delineate the approximate position of the Subantarctic Front and the Polar Front. The main map shows the location of *N. pachyderma* (sin.) type V samples from the Benguela upwelling system.

demonstrate that the Ca isotope fractionation in planktonic foraminifera is strongly species dependent and should be assessed separately [13, 15-17]. The morphospecies *N. pachyderma* represents several highly divergent genetic types (genotypes) in the Atlantic and Southern Ocean with different biogeographical distributions and environmental adaptations [18-22]. This implies that palaeoceanographic proxies based on this taxon should be calibrated independently.

2.2. Sample material and sample locations

We have successfully eliminated these genetically induced uncertainties in the Ca isotope study by using only genetically characterised individuals of *N. pachyderma* (sin.) for the calibration.

They were collected alive from all major surface water masses of the Atlantic Ocean inhabited by this morphospecies [21]. Ca isotope signatures in core top samples of *N. pachyderma* (sin.) from the Nordic Seas (Fig. 1) previously studied by [23] were investigated in parallel to demonstrate the palaeoceanographic applicability and robustness of the proxy against post-depositional processes.

2.3. Analytical methods

2.3.1. Molecular determinations

DNA extraction, amplification by polymerase chain reaction (PCR), cloning and automated sequencing of an ~1000-b.p. region of terminal 3' end of the foraminiferal small subunit ribosomal RNA (SSU rRNA) gene were carried out as described previously [21].

2.3.2. Ca isotope analysis

Ca isotope analyses were performed at the University of Bern (CH) and IFM-GEOMAR, Kiel (D) applying a chemical separation and mass spectrometric analysis with a ^{43}Ca-^{48}Ca double-spike technique [14, 15, 17]. Ca isotope variations are expressed in the δ-notation: $\delta^{44/40}$Ca [‰] = $\{(^{44}Ca/^{40}Ca)_{sample} / (^{44}Ca/^{40}Ca)_{standard} - 1\} * 1000$, where the standard is NIST SRM 915a [24]. A detailed compilation of reference materials is given in [24]. Prior to and after column chemistry it is essential that samples are treated with a HNO_3–H_2O_2 solution to remove residual organics. The long-term 2σ-sample reproducibility of $\delta^{44/40}$Ca is 0.2‰ in both laboratories and is equivalent to approximately ±1°C. An important advantage of our combined approach is that genetic determination and Ca isotope analysis were performed on the same individual. The sensitivity of the Ca isotope method allows replicate analysis of single shells resulting from the ability to measure very small quantities of Ca (200–500ng).

2.4. Results and discussion

2.4.1. The Ca isotopic composition

All Ca isotopic data are presented in Table 1 and 2. The $\delta^{44/40}$Ca values (‰ relative to NIST SRM 915a) of *N. pachyderma* (sin.) vary between –0.47 and 0.72 in Arctic specimen (Type I), and between –0.18 and 0.91 in Antarctic specimen (Type III, IV). Samples of the Benguela system

(Type V) yield values around 1.75. Holocene core top $\delta^{44/40}$Ca [‰] values of *N. pachyderma* (sin.) range from 0.36 to 1.05. Given the observations that the Ca isotopic composition of seawater is homogeneous throughout modern and Pleistocene oceans [13, 24] these variations do not reflect regional differences in seawater Ca isotopic composition.

2.4.2. The $\delta^{44/40}$Ca-temperature calibration

The Ca isotopic composition of *N. pachyderma* (sin.) is positively correlated to sea surface temperature above about 2°C (Fig. 2). We observe clear linear trends for both genetically characterized net catches and Holocene core top specimens, measured in two different laboratories, respectively. The $\delta^{44/40}$Ca-temperature relationship on modern specimen of *N. pachyderma* (sin.) can be expressed as follows: $\delta^{44/40}$Ca [‰] = 0.15 (±0.03)*SST [°C] – 0.20. (error-weighted regression, calculated using the tool Isoplot [34]). Thus a change in $\delta^{44/40}$Ca of 0.15 (±0.03) ‰ corresponds to a relative temperature change of 1°C. We found the identical correlation for North Atlantic core top samples representing a temperature range of 2.4 to 7.1°C.

The determination of both genotype and $\delta^{44/40}$Ca on the same shell of *N. pachyderma* (sin.) provides direct evidence that the genotype does not influence the temperature sensitivity of the Ca isotope fractionation. Arctic, Antarctic and Benguela genotypes all describe the same relationship within analytical uncertainties. The most significant consequence of the genotype-independency is the global validity of the $\delta^{44/40}$Ca-temperature calibration for down-core studies where sample classifications can only be carried out on the morphospecies level. Thus, even if there would be more than one genotype in the Arctic realm, genotype differences would have no impact on the core top calibration.

Samples characterised by low salinities (<33.0‰) as well as modern and core top samples collected in true polar surface waters characterised by temperatures below 2.0°C and salinities <33.5 ‰ plot offset from the trendline and overestimate local temperatures. Our data indicate that the breakdown of the $\delta^{44/40}$Ca-temperature relationship only occurs in these extreme low-temperature and low-salinity environments which are exclusively characterised by the occurrence of almost monospecific foraminifera assemblages [12]. Therefore, these findings do not affect SST reconstructions in all other open marine high-latitude settings.

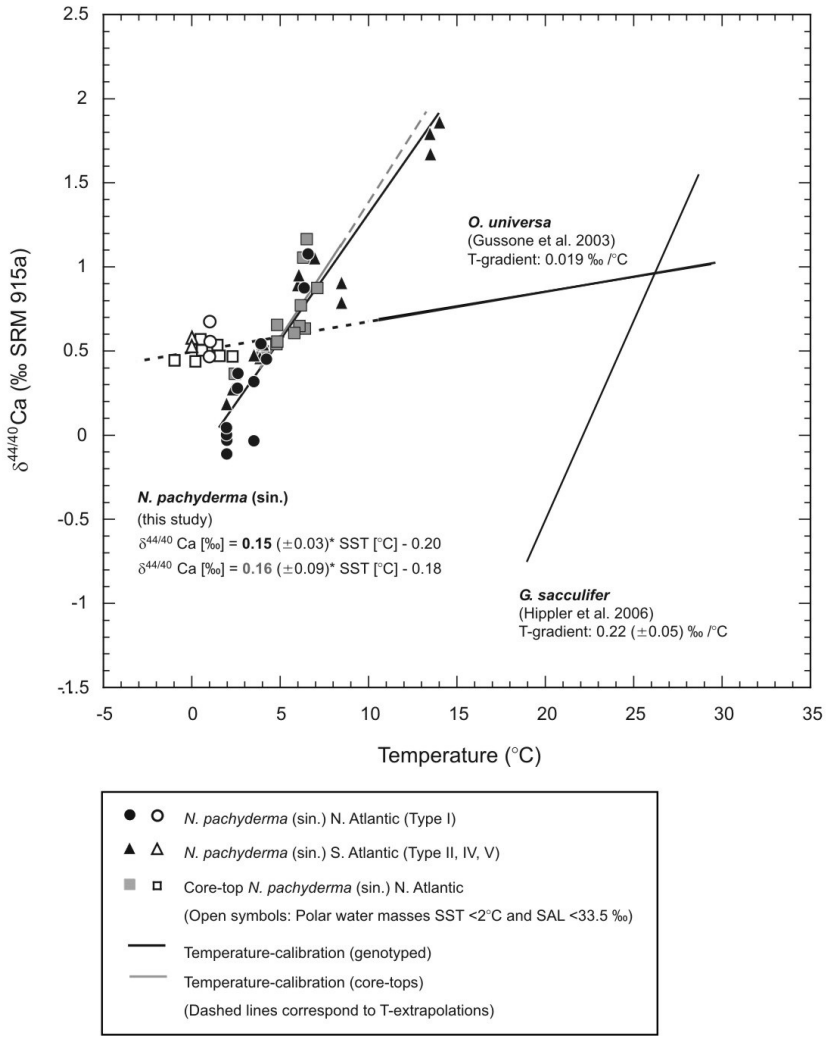

Fig. 2. Ca isotopic composition of genotyped (black) and core top (grey) *N. pachyderma* (sin.) in comparison to the $\delta^{44/40}$Ca-temperature relationships defined for *G. sacculifer* [15] and *O. universa* [17]. $\delta^{44/40}$Ca of *N. pachyderma* (sin.) is positively correlated to temperature and describes a clear $\delta^{44/40}$Ca-temperature-relationship independent of the genotype and post-depositional processes. Identical temperature gradients of *N. pachyderma* (sin.) and *G. sacculifer* point to the same Ca fractionation mechanism suggesting similar biocalcification processes in contrast to *O. universa*. Samples from the "cold end" (T<2°C and SAL<33.5‰) (open symbols) tend to plot on the extrapolation of the *O. universa*-trendline being potentially indicative for a switch in biocalcification mode.

The consistency of temperature-relationships using pristine genotyped shells in combination with core top shells, which could have been exposed to post-depositional processes, confirms that the Ca isotopic composition of foraminiferal calcite is well preserved in our samples and records the primary temperature signal. Especially crucial for the fossil record, our findings support earlier observations of partial dissolution experiments performed on shells of *N. pachyderma* (sin.) demonstrating that the degree of dissolution has no significant impact on the $\delta^{44/40}$Ca values [25].

These findings give robust support for the use of the core top calibration ($\delta^{44/40}$Ca [‰] = 0.16 (±0.09)*SST [°C] – 0.18) for future SST reconstructions in high-latitude settings.

Most observations suggest that *N. pachyderma* (sin.) calcifies at depth similar to other morphospecies used as recorders of SST. There is a general consensus that the vertical distribution of *N. pachyderma* (sin.) is related to local hydrography. An early direct study of the depth habitat of *N. pachyderma* (sin.) demonstrated that it lives above 100 m depth north of 83°N in the Arctic Ocean [26]. Peak abundances of *N. pachyderma* (sin.) were observed in the surface 20-80 m in the Northeast Water Polynya (East Greenland Current), in conjunction with the chlorophyll maximum zone [27] which is in agreement with δ^{18}O signatures suggesting that *N. pachyderma* (sin.) calcifies in the upper 25 m of the water column offshore Greenland [23]. The assumption of a depth habitat by proxy is the inherent weakness in such core top calibrations where summer SSTs for the respective core locations are calculated using estimated calcification depths. In this study, estimated calcification depths are based on the difference in the δ^{18}O ratios of the surface dwelling planktonic foraminifera *Turborotalita quinqueloba* and the deeper dwelling species *N. pachyderma* (sin.) according to the study of [23, 33] (Tab. 2). As recently reported by [35], $\delta^{18}O_{calcite}$ and Mg/Ca-inferred temperatures in downcore samples from *N. pachyderma* originating from the Norwegian Sea reflect different parameters, presumably due to significant temporal variations in $\delta^{18}O_{water}$. Hence, a calibration of $\delta^{44/40}$Ca ratios of our core top samples against the δ^{18}O ratios previously published in [23] is not straightforward for the Nordic Seas. Further, core top calibrations suffer from the sites' natural variability integrated over several hundred years. The recalculation of calcification temperatures of core top specimens of *N. pachyderma* (sin.) by using the $\delta^{44/40}$Ca-temperature relationship based on genotyped specimens independently re-assesses the estimated calcification depths [23] for the core top sites and provide strong evidence that they are within the correct range.

2.4.3. Interspecies comparison

The observed temperature gradient is within uncertainties identical to the one recently reported for modern specimens of planktonic foraminifera *G. sacculifer* [15] (Fig. 2). Although *N. pachyderma* (sin.) and *G. sacculifer* have different ecologies and temperature preferences [28], they exhibit highly similar relative temperature change. However, their trendlines of temperature

sensitivity are significantly offset, which emphasises the importance of species-specific calibrations for absolute temperature reconstruction. These findings render strong evidence that biocalcification in these two species is related to comparable biochemical mechanisms controlling Ca isotope fractionation. In contrast, the planktonic foraminifera *Orbulina universa*, which is widely distributed with respect to temperature [28], is interestingly much less sensitive to temperature [17], similar to inorganic precipitates [17, 29].

Insensitivity of Ca isotope fractionation to temperature was recently reported for a wide range of planktonic foraminiferal species collected from core top sediments [30]. The authors suggest that any temperature relationship is obscured by "unquantified metabolic and physiological processes in nature". Unexpectedly, their findings are inconsistent with recent studies on *G. sacculifer* for which a strong temperature response has been recently reported in cultures, catches and sediments [14, 15]. Further evidence for the temperature sensitivity of Ca isotope fractionation comes also from ODP site 999 in the Caribbean Sea [31] and from the western equatorial Pacific box core ERDC92 (2°13.5'S, 156°59.9'E Java plateau) [13], the latter reporting a difference in $\delta^{44/40}$Ca of 0.6‰ between Holocene and Last Glacial Maximum (LGM) samples of *G. sacculifer*. Applying the $\delta^{44/40}$Ca-temperature calibration based on *G. sacculifer* [15] this value would correspond to a temperature change of 2.7±0.6ºC between the LGM and the Holocene. Furthermore, a consistent SST change for this period of 2.8±0.7ºC has been estimated for the equatorial Pacific (including data from Java plateau ODP core 806B at 0º19.1'N, 159º21.7'E) based on Mg/Ca ratios in foraminifera [32] rendering strong support for a preserved temperature signal in the *G. sacculifer* data [13].

The reasons for these contrasting Ca isotope fractionation patterns observed in different planktonic foraminifera remain a highly interesting challenge for future research. On one hand, the temperature-dependent fractionation of Ca isotopes has been explained as a result of kinetic fractionation in investigations on different carbonate sources (inorganic precipitates, shells of *O. universa* and *G. sacculifer*) [17]. In contrast, equilibrium dynamics was proposed for Ca isotope fractionation based solely on observations on inorganic calcite precipitates [29]. The similarity of Ca isotope fractionation in inorganic precipitates and *O. universa* was attributed by these authors to similar equilibrium processes. The stronger temperature dependence of *G. sacculifer* is interpreted

as the result of a superimposed additional biological fractionation effect assuming different biomineralization processes for both species [29].

2.5. Conclusion

We have identified a new complementary SST proxy for the high latitudes based on the Ca isotopic composition of the planktonic foraminifera *N. pachyderma* (sin.). This is supported by evidence from both the plankton and the sediment. Further, the temperature sensitivity is independent of genetic variation observed within the major high latitude proxy carrier showing its potential for downcore applications in cool-water environment.

Acknowledgements

We would like to thank J. Kramers for his helpful comments on the manuscript. This work was supported by grants from the Swiss National Science Foundation (21-61644.00 and 21-60987.00, to D.H. and T.F.N.), the National Environmental Research Council (NER/J/S/2000/00860, to K.F.D.), the German Science Foundation within the Research Theme FOR 451 (GATEWAYS, WE 2679/3-1) and by the European Science Foundation, ESF (CASIOPEIA, to R.K. and A.E.).

Table 1: Calcium isotopic composition of genotyped *N. pachyderma* (sin.)

Northern Atlantic Ocean, *Polarstern* (ARK XV/1, 1999)

Station	No.	Longitude [°E/W]	Latitude [°N]	Genotype	SAL [‰]	SST [°C]	$\delta^{44/40}$Ca [‰][a]	Uncertainty[b]
A5	3	4 17.08E	79 3.73	Type I	33.5	1.0	0.55	0.28
	3	4 17.08E	79 3.73	(")	33.5	1.0	0.46	0.18
	4	4 17.08E	79 3.73	(")	33.5	1.0	0.67	0.20
B5	1	2 31.00E	79 7.14	(")	33.4	2.0	0.04	0.19
	2	2 31.00E	79 7.14	(")	33.4	2.0	-0.01	0.16
C5	3	2 31.00E	79 7.14	(")	33.4	2.0	-0.04	0.21
	4	2 31.00E	79 7.14	(")	33.4	2.0	-0.12	0.18
D5	1	2 59.71E	79 28.15	(")	33.7	2.0	-0.04	0.19
F5	2	12 44.72W	74 59.49	(")	32.7	2.5	0.27	0.13
	3	12 44.72W	74 59.49	(")	32.7	2.5	0.36	0.30
H5	3	7 23.80W	75 0.08	(")	34.8	4.0	0.45	0.23
I5	2	3 33.82W	75 0.84	(")	34.8	4.0	0.54	0.22
J5	2	0 22.17E	75 0.21	(")	34.7	3.5	-0.04	0.23
	2	0 22.17E	75 0.21	(")	34.7	3.5	0.31	0.17
K5	5	5 9.05E	75 1.06	(")	35.0	6.5	1.07	0.24
L5	1	10 37.25E	74 59.66	(")	35.1	6.5	1.07	0.20
M5	1	12 33.57E	75 0.39	Type I	35.0	6.0-6.5	0.87	0.18

Southern Atlantic Ocean, British Antarctic Survey *James Clark Ross* (JR 48, 2000)

Station	No.	Longitude [°W]	Latitude [°S]	Genotype	SAL [‰]	SST [°C]	$\delta^{44/40}$Ca [‰][a]	Uncertainty[b]
8	69	60°53’	54° 81’	Type III	34.1	7.0	0.89	0.25
	71	60°53’	54° 81’	Type III	34.1	7.0	1.05	0.16
10	121	60° 79’	55° 22’	Type III	33.9	6.0	0.88	0.25
	129	60° 79’	55° 22’	Type III	33.9	6.0	0.95	0.14
	129	60° 79’	55° 22’	Type III	33.9	6.0	0.89	0.15
13	165	64° 31’	57° 98’	Type III	33.9	4.0	0.53	0.24
17	223	65° 32’	61° 00’	Type III	33.7	3.5	0.47	0.20
23	265	63° 74’	63° 92’	Type III	33.7	2.0	0.17	0.30
30	297	58° 45’	62° 63’	Type III	34.3	2.0-2.5	0.27	0.30
36	309	59° 61’	64° 74’	Type IV	32.4	0.0	0.67	0.19
	313	59° 61’	64° 74’	Type IV	32.4	0.0	0.57	0.21
	321	59° 61’	64° 74’	Type III	32.4	0.0	0.52	0.14
85	649	56° 75’	52° 21’	Type III	34.0	8.5	0.80	0.14
	649	56° 75’	52° 21’	Type III	34.0	8.5	0.79	0.16
	651	56° 75’	52° 21’	Type III	34.0	8.5	0.91	0.15

Benguela System (offshore Namibia), *RV Welwitscha* (2001)

Station	No.	Longitude [°E]	Latitude [°S]	Genotype	SAL [‰]	SST [°C]	$\delta^{44/40}$Ca [‰][a]	Uncertainty[b]
10	13	14 13.26	23.00	Type V	35.0	13.5	1.67	0.22
	23	14 23.26	23.00	Type V	35.0	13.5	1.79	0.26
20	35	14 02.45	23.00	Type V	35.0	14.0	1.85	0.29

[a] $\delta^{44/40}$Ca values are given in [‰] relative to NIST SRM 915a. [b]Uncertainties reflect the 2σ standard error of single analysis. Samples were obtained either by pumping continually from the surface water layer (6m, 63-µm filter) or from vertical plankton tows (≤100m, 63µm mesh).

Table 2: Calcium isotopic composition of *N. pachyderma* (sin.) from Holocene core tops, Nordic Seas

Core[a]	Longitude [°E/W]	Latitude [°N]	Water depth [m]	$\Delta\delta^{18}O_{Nps\text{-}quinqueloba}$[b]	Inferred depth [m][b]	SAL [‰][c]	SST [°C][c]	$\delta^{44/40}Ca$ [‰][d]	*n*[e]	2SEM[f]
Nordic Seas (Norwegian Current) core tops samples										
23071-1	2 54.60E	67 04.80	1306	0.53	150-200 m	35.1	6.1	0.64	11	0.11
23259-3	9 18.00E	72 01.20	2518	0.66	150-200 m	35.1	4.8	0.65	4	0.03
23261-2	13 06.60E	72 10.80	1667	0.44	100-150 m	35.0	5.1	0.54	4	0.21
23514-3	25 57.00W	66 40.20	713	-0.05	0-50 m	33.8	4.8	0.55	2	0.14
23523-3	30 13.20W	62 15.00	2156	1.88	> 250 m	35.1	6.3	1.05	2	0.16
23528-3	28 50.40W	63 09.60	1632	1.79	> 250 m	35.0	6.4	0.63	2	0.11
23538-1	2 10.20W	62 00.60	1667	1.32	> 250 m	35.2	7.1	0.87	7	0.39
23540-2	2 30.60W	62 46.20	1126	1.19	> 250 m	35.1	5.8	0.60	4	0.04
HM94-12	3 33.00W	71 19.20	1816	0.63*)	150-200 m	35.0	2.4	0.36	2	0.09
HM94-18	5 42.00W	74 30.00	2469	0.52*)	150-200 m	35.0	4.0	0.48	3	0.20
Nordic Seas (Arctic Domain and polar waters) core top samples										
23231-2	3 59.40W	78 54.00	1979	0.17	0-50 m	34.0	0.2	0.43	2	0.23
23232-1	1 37.20W	79 01.80	2642	0.64	150-200 m	34.9	1.1	0.44	2	0.03
23235-1	1 23.40E	78 52.20	2500	0.24	50-100 m	34.7	1.5	0.46	4	0.06
23347-4	16 04.80W	70 26.40	1375	-0.05	0-50 m	33.8	1.4	0.53	3	0.02
23348-2	18 57.00W	70 25.20	737	-0.33	0-50 m	33.3	0.5	0.56	2	0.13
23506-1	7 36.00W	72 23.40	2670	0.15	0-50 m	34.2	2.3	0.46	2	0.16
23509-1	13 30.00W	73 49.80	2576	0.11	0-50 m	33.2	0.6	0.50	6	0.08
23549-9	4 36.00W	75 03.60	3624	-0.05	0-50 m	34.1	1.6	0.47	2	0.27
PS2638-6	22 45.00W	72 05.40	428	–	0-50 m	31.7	-1.0	0.44	3	0.08

[a] Source: see reference [8 and 23]. [b] Average calcification depth are estimated using the $\delta^{18}O$-difference between shallow-dwelling *T. quinqueloba* and deep-dwelling *N. pachyderma* (sin.): $\Delta depth = -86 + \Delta\delta^{18}O*300$ [33]. Negative values are set to 0-50 m. *)$\Delta\delta^{18}O_{Nps}$ ratios from adjacent cores 23277 and 23254, see [23]. [c] Summer salinities and SSTs are averaged using depth corresponding hydrographic data from July-September (main planktonic bloom in the Nordic Seas [27]) from the World Ocean Atlas, NOAA, 2001 (http://www.nodc.noaa.gov/OC5/WOA01/pr_woa01.html). [d] $\delta^{44/40}Ca$ values are given in [‰] relative to NIST SRM 915a. [e]Number of repeated measurements of each sample. [f] $2SEM = 2\sigma/n^{0.5}$.

Appendix

Concerning the expression of the calculated $\delta^{44/40}$Ca-temperature relationship (chapter 4.2) the following considerations have been addressed in view of originally independent sample sets (see Table 2 and Table 4):

1) The $\delta^{44/40}$Ca-temperature relationship defined exclusively for core top samples (excluding samples from Arctic and polar water masses) could be expressed as follows:

[1] $\delta^{44/40}Ca\ [‰] = 0.16\ (\pm 0.09) * SST\ [°C] - 0.18$

2) The $\delta^{44/40}$Ca-temperature relationship defined for pooled modern genotyped samples could be expressed as:

[2] $\delta^{44/40}Ca\ [‰] = 0.15\ (\pm 0.03) * SST\ [°C] - 0.20$

We propose the use of equation [1] for future applications of past sea surface temperature reconstruction in high-latitude oceans. This calibration is based exclusively on core top specimen of *N. pachyderma* (sin.). The slope of pooled genotyped samples [2] is slightly shallower and identical within uncertainty. The bigger uncertainty on the core top data [1] is less related to biology (or else values from modern samples would scatter to the same extent) than to external factors that might complicate the exact estimation of past core top temperatures, which represent average temperatures over several hundred years. The consistency of temperature-relationships using pristine genotyped shells in combination with core top specimen, which could have been exposed to post-depositional processes, render strong evidence for equations [1] applicability and reliability.

References

[1] W. S. Broecker, Thermohaline circulation, the Achilles heel of our climate system: Will man-made CO_2 upset the current balance? , Science 278 (1997) 1582-1588.

[2] W. S. Broecker, Paleocean circulation during the last deglaciation: a bipolar seesaw? Paleoceanography 13 (1998) 119-121.

[3] S. Rahmstorf, Ocean circulation and climate during the past 120.000 years, Nature 419, (2002) 207-214.

[4] C. Rühlemann, S. Mulitza, P. J. Müller, G. Wefer, R. Zahn, Warming of the tropical Atlantic Ocean and slowdown of thermohaline circulation during the last deglaciation, Nature 402 (1999) 511-514.

[5] D. W. Lea, D. K. Pak, L. C. Peterson, K. A. Hughen, Synchroneity of tropical and high-latitude Atlantic temperatures over the last glacial termination, Science 301 (2003) 1361-1364.

[6] K. Visser, R. Thunell, L. Stott, Magnitude and timing of temperature change in the Indo-Pacific warm pool during deglaciation, Nature 421 (2003) 152-155.

[7] G. A. Jones, L. D. Keigwin, Evidence from Fram Strait (78°N) for early deglaciation, Nature 336 (1988) 56-59.

[8] M. Y. Meland, E. Jansen, H. Elderfield, T. M. Dokken, A. Olsen, R. G. J. Bellerby, Mg/Ca ratios in the planktonic foraminifer *Neogloboquadrina pachyderma* (sinistral) in the northern North Atlantic/Nordic Seas, G3 7 (2006) 2005GC001078.

[9] A. Rosell-Mele, P. Comes, Evidence for a warm Last Glacial Maximum in the Nordic Seas or an example of shortcomings in U^{K}_{37}‘ and U^{K}_{37} to estimate low sea surface temperatures, Paleoceanography 14 (1999) 770-776.

[10] P. P. E. Weaver, M. R. Chapman, G. Eglinton, M. Zhao, D. Rutledge, G. Read, Combined coccolith, foraminiferal, and biomarker reconstruction of paleoceanographic conditions over the last 120 kyr in the northern Atlantic (59°N, 23°W), Paleoceanography 14 (1999) 336-349.

[11] R. Huber, H. Meggers, K.-H. Baumann, M. E. Raymo, R. Henrich, Shell size variation of the planktonic foraminifer *Neogloboquadrina pachyderma* (sin.) in the Norwegian-Greenland Sea during the last 1.3Myrs: implications for paleoceanographic reconstructions, Palaeogeogr. Palaeoclimatol. Palaeoecol. 160 (2000) 193-212.

[12] M. Kucera, A. Rosell-Melé, R. Schneider, C. Waelbroeck, M. Weinelt, Reconstruction of sea-surface temperatures from assemblages of planktonic foraminifera: multi-technique approach based on geographically constrained calibration data sets and its application to glacial Atlantic and Pacific Oceans, Quat. Sci. Rev. 24 (2005) 951-998.

[13] P. Zhu, J. D. MacDougall, Calcium isotopes in the marine environment and the oceanic calcium cycle, Geochim. Cosmochim. Acta 62 (1998) 1691-1698.

[14] T. F. Nägler, A. Eisenhauer, A. Müller, C. Hemleben, J. Kramers, The δ^{44}Ca-temperature calibration on fossil and cultured *Globigerinoides sacculifer*: New tool for reconstruction of past sea surface temperatures, G3 1 (2000) 2000GC000091.

[15] D. Hippler, A. Eisenhauer, T. F. Nägler, Tropical SST history inferred from Ca isotope thermometry over the last 140ka, Geochim. Cosmochim. Acta 70 (2006) 90-100.

[16] J. Skulan, D. J. DePaolo, T. L. Owens, Biological control of calcium isotopic abundances in the global calcium cycle, Geochim. Cosmochim. Acta 61 (1997) 2505-2510.

[17] N. Gussone, A. Eisenhauer, A. Heuser, M. Dietzel, B. Bock, F. Böhm, H. J. Spero, D. W. Lea, J. Bijma, T. F. Nägler, Model for kinetic effects on calcium isotope fractionation (δ^{44}Ca) in inorganic aragonite and cultured planktonic foraminifera, Geochim. Cosmochim. Acta 67 (2003) 1375-1382.

[18] K. F. Darling, C. M. Wade, I. A. Stewart, D. Kroon, R. Dingle, A. J. L. Brown, Molecular evidence for genetic mixing of arctic and Antarctic subpolar populations of planktonic foraminifers, Nature 405 (2000) 43-47.

[19] I. A. Stewart, K. F. Darling, D. Kroon, C. M. Wade, S. R. Troelstra, Genotypic variability in subarctic Atlantic planktic foraminifera, Mar. Micropaleontol. 43 (2001) 143-153.

[20] D. Bauch, K. F. Darling, H. A. Bauch, H. Erlenkeuser, D. Kroon, Palaeoceanographic implications of genetic variation in living North Atlantic *Neogloboquadrina pachyderma*, Nature 424 (2003) 299-302.

[21] K. F. Darling, M. Kucera, C. J. Pudsey, C. M. Wade, Molecular evidence links cryptic diversification in polar planktonic protists to Quaternary climate dynamics, Proc. Natl. Acad. Sci. U.S.A. 101 (2004) 7657-7662.

[22] K. F. Darling, M. Kucera, D. Kroon, C. M. Wade, A resolution for the coiling direction paradox in *Neogloboquadrina pachyderma*, Paleoceanography 21 (2006) 2005PA001189.

[23] J. Simstich, M. Sarnthein, H. Erlenkeuser, Paired δ^{18}O signals of *Neogloboquadrina pachyderma* (sin.) and *Turborotalia quinqueloba* show thermal stratification structure in Nordic Seas, Mar. Micropaleontol. 48 (2003) 107-125.

[24] D. Hippler, A.-D. Schmitt, N. Gussone, A. Heuser, P. Stille, A. Eisenhauer, T. F. Nägler, Calcium isotopic composition of various reference materials and seawater, Geostandard Newsl. 27 (2003) 13-19.

[25] B. Hönisch, Stable isotope and trace element composition of foraminiferal calcite - from incorporation to dissolution, Thesis, University of Bremen, 2002.

[26] J. Carstens, G. Wefer, Recent distribution of planktonic foraminifera in the Nansen basin, Arctic Ocean, Deep-Sea Res. 39 (1992) S507-S524.

[27] K. E. Kohfeld, R. G. Fairbanks, S. L. Smith, I. D. Walsh, Neogloboquadrina pachyderma (sinistral coiling) as paleoceanographic tracers in polar oceans: evidence from Northeast Water Polynya plankton tows, sediments traps, and surface sediments, Paleoceanography 11 (1996) 679-699.

[28] S. Zaric, , B. Donner, G. Fischer, S. Mulitza, G. Wefer, Sensitivity of planktonic foraminifera to sea surface temperature and export production as derived from sediment trap data, Mar. Micropaleontol. 55, (2005) 75-105.

[29] C. S. Marriott, G. M. Henderson, N. S. Belshaw, A. W. Tudhope, Temperature dependence of δ^{7}Li, δ^{44}Ca and Li/Ca during growth of calcium carbonate, Earth Planet. Sci. Lett. 222 (2004) 615-624.

[30] N. G. Sime, C. L. De La Rocha, A. Galy, Negligible temperature dependence of calcium isotope fractionation in 12 species of planktonic foraminifera, Earth Planet. Sci. Lett. 232 (2005) 51.

[31] N. Gussone, A. Eisenhauer, R. Tiedemann, G. H. Haug, A. Heuser, B. Bock, T. F. Nägler, A. Müller, Reconstruction of Caribbean Sea surface temperature and salinity fluctuations in response to the Pliocene closure of the Central American Gateway and radiative forcing, using $\delta^{44/40}$Ca, δ^{18}O and Mg/Ca ratios, Earth Planet. Sci. Lett. 227 (2004) 201-214.

[32] D. W. Lea, D. K. Pak, H. J. Spero, Climate impact of late quaternary equatorial Pacific sea surface temperature variations, Science 289 (2000) 1719-1724.

[33] Simstich, J, Die ozeanische Deckschicht des Europäischen Nordmeers im Abbild stabiler Isotope von Kalkgehäusen unterschiedlicher Planktonforaminiferenarten. Berichte – Reports, Institut für Geowissenschaften, 2, Christian-Albrechts-Universität, Kiel (1999).

[34] K. R. Ludwig, Isoplot/Ex 2.45, a geochronological toolkit for Microsoft Excel: Berkeley Geochronology Center (2000).

[35] B. Nyland, E. Jansen, H. Elderfield, C. Andersson, Neogloboquadrina pachyderma (dex. and sin.) Mg/Ca and δ^{18}O records from the Norwegian Sea. Geochem. Geophys. Geosyst. (2006).

3. A $\delta^{44/40}$Ca, Mg/Ca and δ^{18}O multi-proxy approach reveals a two phase calcification process in *N. pachyderma* (sin.)

by

Kozdon, R.[1,2)]; Eisenhauer, A.[1*)]; Weinelt, M.[2)]; Fietzke, J.[1)], Meland, M.[3)]; Hippler, D.[4)]

[1)]Leibniz-Institut für Meereswissenschaften (IFM-GEOMAR), 24148 Kiel, Germany

[2)]Institut für Geowissenschaften an der Christian-Albrechts-Universität zu Kiel, 24118 Kiel, Germany

[3)]Bjerknes Centre for Climate Research, 5007, Bergen, Norway

[4)]Faculty of Earth and Life Sciences, Vrije Universiteit, 1081 HV Amsterdam, The Netherlands

* Corresponding Author: A. Eisenhauer, Tel.: +49-431-600-2282; e-mail: aeisenhauer@ifm-geomar.de

Abstract

A multi-proxy approach comprising $\delta^{44/40}$Ca, Mg/Ca and δ^{18}O ratios was applied on tests of the polar to subpolar planktonic foraminifer *N. pachyderma* (sin.) from Holocene core tops originating from the Nordic Seas, covering an SST-range in between 0°C to 7°C. We found that tests of *N. pachyderma* (sin.) can be subdivided into two groups which differ significantly in their suitability as temperature proxy recorder. Mg/Ca and $\delta^{44/40}$Ca ratios of '*Group I*' specimens from the Norwegian Sea are positively correlated ($\delta^{44/40}$Ca = 1.32 (±0.40)*Mg/Ca [mmol/mol] – 0.70 (±0.37); R^2 = 0.75, n = 20) and match existing Mg/Ca and $\delta^{44/40}$Ca temperature calibrations. In particular, the temperature dependent slopes of $\delta^{44/40}$Ca and Mg/Ca are identical pointing to a binary mixing process of two distinctively different calcite endmembers within the foraminifera. In contrast, Mg/Ca and $\delta^{44/40}$Ca proxy data of '*Group II*' specimens originating from the cold, low saline Arctic Domain and polar waters tend to be inversely related to temperature and are decoupled from each other, forming an almost parabolic Mg/Ca temperature relation. The threshold water temperature with lowest Mg/Ca ratios is at about 3.5°C corresponding to a

salinity of about 34.5 ‰. This highly nonpassive character of *Group I* and *II* specimens at the 'cold end' of existing proxy temperature calibrations can be reconciled by a model assuming that the final test composition is defined by temperature dependent proportions of two different calcite phases present in *N. pachyderma* (sin.). The temperature response of the Mg-content by mixing is more temperature sensitive than that of a single calcite endmember alone. A 'normal' mixing process (*NMP* = Normal Mode Process) active in *N. pachyderma* (sin.) at water temperatures above about 3.5°C with Mg/Ca ratios being positively correlated to temperature may represent part of the trace metal homeostasis during moderate temperatures. However, the inverse Mg/Ca-temperature response of the *Group II* data below about 3.5°C may then be interpreted to reflect a biomineralisation mode (*CMP* = Cold Mode Process) meant to inhibit the decrease of the Mg-content below a certain threshold value with decreasing temperatures. *NMP* and *CMP* may then be alternating tools to compensate for the influence of the temperature in order to keep the Mg/Ca ratio within narrow limits set by the foraminiferal physiology.

3.1. Introduction

Shells of foraminifers are among the most important archives for the proxy-based reconstruction of past physical and chemical oceanographic conditions such as temperature, salinity, pH and ocean circulation (cf. Lea et al., 2003). Early studies in foraminiferal proxy research were limited in their instrumental and analytical possibilities, mainly focusing on faunal assemblages and the fractionation of the stable isotopes of oxygen ($\delta^{18}O$) and carbon ($\delta^{13}C$) (e.g. Emiliani, 1955; Imbrie and Kipp, 1971). Using these approaches, some proxy information could not be reconstructed with sufficient precision and reliability as proxy data do not depend on one single physical or ecological parameter only rather integrate over several ones. Moreover, foraminiferal calcite shows significant offsets relative to inorganic calcium carbonate precipitated in thermodynamic equilibrium from seawater. This is attributed to the physiological control of the foraminiferal metabolism strongly influencing the material fluxes between seawater, cytosol and the site of calcification. Many of these isotopic and trace metal related "vital effects" are still enigmatic because the chemical and biological processes underlying foraminiferal calcification as well as the entire process of material uptake is still not understood in detail yet (e.g. Erez et al., 2003). As a consequence of the observation that none of the existing proxies is controlled by one environmental variable only, modern foraminiferal proxy research focuses on the combination of

several proxies to extract the pure and anticipated signal. A positive correlation of two or more independent proxy information can then be considered to be a self-consistent criteria for the robustness and quality of the proxy reconstruction. Following this approach, Mg/Ca and $\delta^{44/40}$Ca together with δ^{18}O ratios have already been tested to be an excellent set of multi-proxy tracers to reconstruct salinity and seawater temperature fluctuations in the tropical oceans using *G. sacculifer* as a foraminiferal archive (Nägler et al., 2000; Gussone et al.; 2004, Hippler et al., 2005).

In contrast to the tropical oceans, multiproxy data from higher latitudes are sparse, suggesting that the temperature to proxy relationship is less reliable at the 'cold-end' and does therefore not necessarily reflect true calcification temperatures (Barker at al., 2005). With respect to Mg/Ca, the first systematic foraminiferal temperature calibration of Nürnberg (1995) already indicates that in the western part of the Nordic Seas which is characterized by cold (summer SST <3.5°C), low saline (<34.5 ‰) Arctic Domain and polar waters, Mg/Ca ratios of *Neogloboquadrina pachyderma* (sin. = sinistral, left coiling) are higher than expected. Restrictions in the adaptability of foraminiferal Mg/Ca as high latitude temperature proxy were also reported in Meland et al. (2005) for the Last Glacial Maximum and in Meland et al. (2006) for Holocene core top samples with a remarkably low temperature sensitivity of the Mg/Ca signal in *N. pachyderma* (sin). Similar to Mg/Ca, the use of foraminiferal δ^{18}O as a reliable palaeothermometer for the Nordic Seas is restricted due to the lack of information about the dynamics of salinity changes in the past (cf. Weinelt et al., 2001; Simstich et al., 2003). In order to overcome these restrictions of foraminiferal temperature proxies in the Nordic Seas, the Mg/Ca and δ^{18}O thermometry of *N. pachyderma* (sin.) might be used in conjunction with $\delta^{44/40}$Ca. Then the positive correlation between $\delta^{44/40}$Ca- and Mg/Ca-derived temperatures provides a self-consistent criteria for a robust temperature reconstruction.

It was Zhu and Macdougall (1998) who first proposed a pronounced $\delta^{44/40}$Ca temperature sensitivity of about 0.1 ‰°C^{-1} in *N. pachyderma* (sin.). Later, this species was recalibrated more precisely on the basis of a broad plankton tow and core top sample pool by Hippler et al. (2004; Hippler et al., in prep.) who found a $\delta^{44/40}$Ca temperature sensitivity of about 0.16 ± 0.09 ‰°C^{-1} in core top samples and 0.15 ± 0.03 ‰°C^{-1} in net catches. Both gradients are almost as sensitive as the δ^{18}O-thermometer, qualifying the $\delta^{44/40}$Ca ratios as a recorder of past temperature

fluctuations of high latitude ocean seawater. Besides secular variations of the Ca-isotopic composition of seawater, no other environmental factor than water temperature is known so far to influence the $\delta^{44/40}$Ca ratios in *N. pachyderma* (sin.). In contrast to the pronounced Ca-temperature sensitivity of *G. sacculifer* and *N. pachyderma* (sin.), Gussone et al. (2003) reported a Ca isotope temperature relation of only 0.019 ‰°C^{-1} in *O. universa* which is similar to the temperature sensitivity of the Ca isotope fractionation in inorganic precipitates (Gussone et al., 2005; Lemarchand et al., 2004) but almost an order of magnitude lower than for *G. sacculifer* and *N. pachyderma* (sin.). All foraminifera tested so far for their $\delta^{44/40}$Ca-temperature relation fall along two distinctively different slopes. A shallow $\delta^{44/40}$Ca-temperature slope indicating a relatively weak temperature sensitivity similar to inorganic precipitates and a steep $\delta^{44/40}$Ca-temperature slope reflecting a pronounced temperature sensitivity almost similar to the one of δ^{18}O. The reason for this species dependent bimodal behaviour of the Ca isotope fractionation in foraminifera is still enigmatic pointing to unique and species related calcification processes probably adopted to the species' ecological niche.

The goal of this study is to test the applicability of Mg/Ca, $\delta^{44/40}$Ca and δ^{18}O in a multi proxy approach for the temperature reconstruction of Nordic seawater and to examine the abnormal behaviour of Mg/Ca ratios at the 'cold end' of the temperature calibration.

3.2. Material and methods

3.2.1. Hydrography, core locations and sample material

The modern surface hydrography of the Nordic Seas (Fig. 3) is characterized by the Norwegian Current which carries warm (summer SST = 13 to 14°C) and saline (summer SSS = 34.9 to 35.3‰) waters northwards at the eastern side and the East Greenland Current which transports polar (summer SST = 1.5 to 2°C), partly ice-covered and low-saline (summer SSS = 31 to 33‰) waters southwards at the western side (e.g. Weinelt et al., 2001). Mixing between both water masses creates the extremely dense Arctic Domain water, forming gyres in the central Greenland Sea.

A station chart of North Atlantic sediment surface samples selected for paired $\delta^{44/40}$Ca and Mg/Ca temperature estimates is presented in Fig 3. Adjacent core tops were dated by AMS ^{14}C

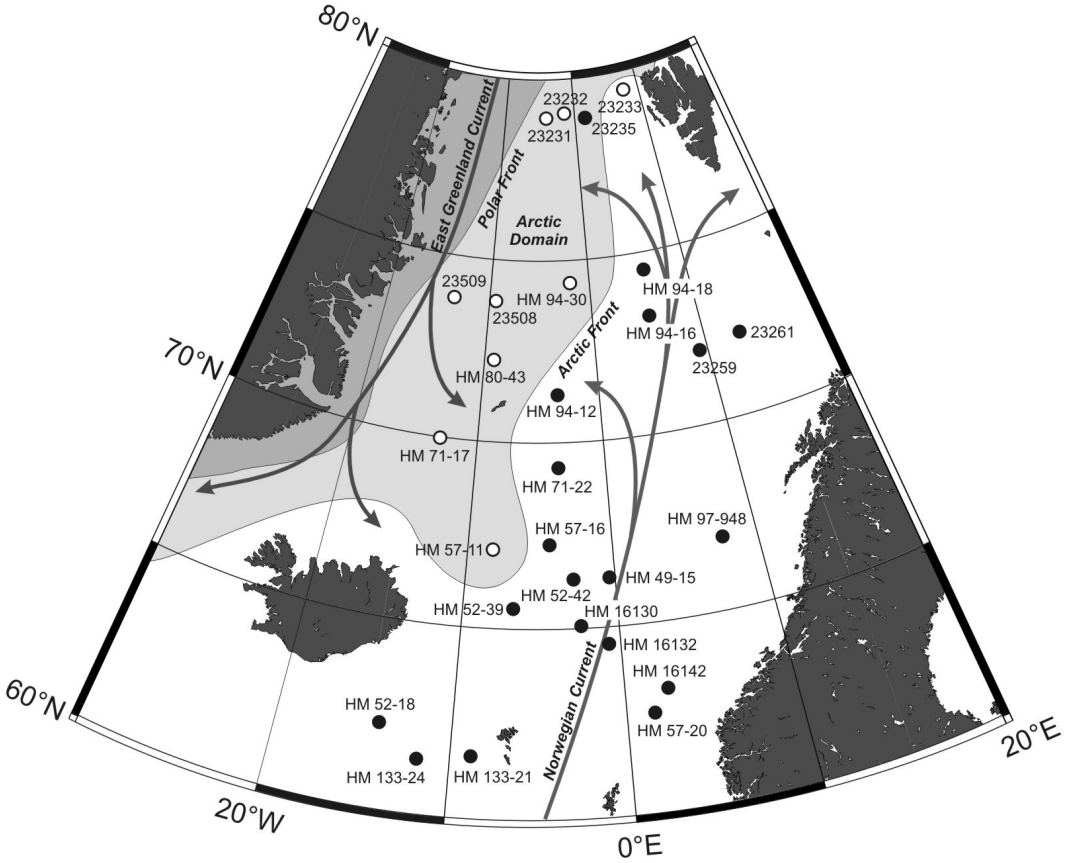

Fig. 3. Simplified surface hydrography of the Nordic Seas. Arctic Domain waters are light gray, polar waters dark gray. Black circles mark samples where Mg/Ca and $\delta^{44/40}$Ca proxy temperature estimates show consistent water temperatures in calcification depth (*Group I* specimens). Core locations with inconsistent $\delta^{44/40}$Ca and Mg/Ca temperatures are marked by white circles (*Group II* specimens).

(compilation of all data in Simstich et al., 2003) and corrected for a ^{14}C reservoir effect of 400 years (Bard et al., 1994). Most core top dates are younger than 2500 years before present and can therefore be considered to represent modern conditions, assuming that the major hydrographic parameters in the Nordic Seas did not change significantly over this time span (Koç et al., 1993; Sarnthein et al., 2001). It is notable that *N. pachyderma* (sin.) originating from the Nordic Seas represent one genotype only ([Type I, (sin.)]; Bauch et al., 2003; Darling et al., 2006). This means that differences in elemental or isotopic ratios may be controlled environmentally rather than genetically.

3.2.2. Sample preparation

Ca isotopes and Mg/Ca ratios were measured on the polar to subpolar planktonic foraminifer *N. pachyderma* (sin.). Samples were taken from sediment surface samples which have previously

been used by Horwege et al. (1987), Hohnemann et al. (1996) and Simstich et al. (2003) for $\delta^{18}O$ and $\delta^{13}C$ measurements. Approximately 60 to 80 species were hand-picked in the size fraction of 125 to 250 µm. The foraminiferal tests were gently crushed between glass plates and cleaned using the Mg-cleaning protocol of Barker et al. (2003). After cleaning, the shell fragments were dissolved in ultrapure 2.5N HCl. About 80% of the sample solution was separated for the determination of Mg/Ca ratios, the residual still provided sufficient material for $\delta^{44/40}Ca$ runs.

3.2.3. Ca isotope measurements and temperature estimates ($T_{\delta 44/40Ca}$)

In order to correct for isotope fractionation during the course of the Ca isotope analysis, an isotopically well defined $^{43}Ca/^{48}Ca$-double spike was added to an aliquot of the sample solution (Heuser at al., 2002). The sample-spike mixture was dried down in order to guarantee a homogenous distribution and later recovered in 2 µl of ultrapure 2.5N HCl. Subsequently, the mixture was loaded with a Ta_2O_5-activator solution using the "sandwich-technique" (activator-sample-activator) onto a previously outgassed zone refined rhenium single filament, following a method previously published by Birck et al., (1986). After evaporating to dryness, the filament with the sample-spike mixture was briefly glowed. The total amount of Ca loaded on the filament (spike and sample) is about 300 ng.

Ca isotope measurements were performed on a TRITON thermal ionization mass-spectrometer at the IFM-GEOMAR mass spectrometer facilities in Kiel, Germany. The isotopic variations are expressed as $\delta^{44/40}Ca$-values ($(^{44/40}Ca_{sample}/^{44/40}Ca_{standard} - 1) * 1000$, using NIST SRM 915a $CaCO_3$ reference powder as standard material and following the Ca-notations as proposed in Eisenhauer et al. (2004). In order to monitor our long-term reproducibility, we repeatedly measured an additional CaF_2 standard previously used in Nägler et al. (2000) and further discussed in Hippler et al. (2003). Control runs of selected unspiked samples were performed using an AXIOM MC-ICP-MS in cool plasma mode (Fietzke et al., 2004). As the sample consumption of the MC-ICP-MS in cool plasma mode is significantly higher relative to the TIMS technique, we used this method to perform control runs on core locations with sufficient sample material only. In order to guarantee statistical significance, all samples were measured at least twice. Both methods achieve a long term analytical uncertainty in the order of 0.2 ‰ (2σ).

The $\delta^{44/40}$Ca-based temperature reconstructions ($T_{\delta 44/40Ca}$) presented in Tab. 4 were calculated using the equation given by Hippler et al. (chapter 1 in this work) for core top samples:

[1] $\delta^{44/40}$Ca [‰] = 0.16*SST (±0.09) [°C] – 0.18.

3.2.4. Mg/Ca-measurements and temperature estimates ($T_{Mg/Ca}$)

Cleaned subsamples for Mg/Ca determinations were dissolved in ultrapure 0.075 M HNO_3 and diluted to Ca concentrations of 30 to 70 ppm. Analyses were performed on a simultaneous radially viewing ICP-OES (Ciros CCD SOP, Spectro A.I., Germany) at the "Geologisch-Paläontologisches Institut und Museum der Universität Kiel", Germany, following standard procedures (Nürnberg et al., 2000). During the course of the measurements, the total drift is less than 0.2 % as determined by analyzing an internal consistency standard after every 5 samples. Replicate analyses on the same samples, which were cleaned and analyzed during different sessions, showed a standard deviation of 0.09 mmol/mol, introducing a temperature error of about 0.5°C. Samples labelled "HM" and "JM" were prepared and analyzed for Mg/Ca at the Department of Earth Sciences, University of Cambridge, UK (Meland et al., 2006). The foraminiferal tests were cleaned following identical cleaning protocols (Barker et al., 2003) and measured using an ICP-AES with a relative precision of <0.3 % (de Villiers et al., 2002). For additional $\delta^{44/40}$Ca determinations, approximately 20 tests of *N. pachyderma* (sin.) in the size fraction 150 to 212 µm of the remaining sample material were hand-picked and sent to IFM-GEOMAR (Kiel, Germany) where they were cleaned and analyzed as described above. Mg/Ca ratios from adjacent core tops reflecting identical water masses measured in Cambridge and Kiel are within analytical error indistinguishable from each other. Moreover, the Mg/Ca to $\delta^{44/40}$Ca relationship is consistent between these groups, implying that there are no systematic offsets due to measurements in different laboratories. The Mg/Ca-based temperatures ($T_{Mg/Ca}$) in Tab. 4 were calculated by the equation of Mashiotta et al. (1999) for *N. pachyderma* (sin.) ($Mg/Ca = 0.549*e^{0.099*T}$), based on the microprobe data set of Nürnberg (1995).

3.2.5. $\delta^{18}O$-measurements and temperature estimates

The δ^{18}O values of our core top foraminifera presented in Tab. 4 as well as the corresponding calcification depths, salinities and the time span of the main planktonic bloom have already been

measured, published and discussed in Simstich et al. (2003) and Meland et al. (2006), respectively. The reconstruction of absolute Nordic Seas palaeotemperatures from core top $\delta^{18}O$ values is not straightforward as they integrate several decades or even centuries whereas only modern precise salinity data are available. Moreover, the correlation between salinity and $\delta^{18}O_{water}$ is poor (Weinelt et al., 2001; Simstich et al., 2003), mainly due to the influence of different (melt-)water sources with unknown $\delta^{18}O_{water}$ endmembers. Hence, in a first order approach, water temperature can be estimated assuming that the change of the hydrographic regime was small and that the salinity distribution has not changed significantly throughout the last 2500 years (Sarnthein et al., 2001). Foraminiferal $\delta^{18}O$ temperature estimates presented in Tab. 4 have therefore been calculated based on the palaeoequation of Shackleton et al. (1974) ($T(°C) = (\delta^{18}O_{calcite} - \delta^{18}O_{water}) + 0.1*(\delta^{18}O_{calcite} - \delta^{18}O_{water})$) using the previously published $\delta^{18}O$ measurements of Simstich et al. (2003), Meland et al. (2006) and taking modern salinity data from the World Ocean Atlas 2001 (Conkright et al., 2002) into account.

3.3. Results

3.3.1. Consistency of Mg/Ca and $\delta^{44/40}Ca$ ratios

The measured $\delta^{44/40}Ca$ ratios were plotted as a function of their corresponding Mg/Ca values (Fig. 4) We found that tests of *N. pachyderma* (sin.) can be subdivided into two groups which differ significantly in their suitability as temperature proxy recorder. In '*Group I*' specimens from the Norwegian Sea, Mg/Ca and $\delta^{44/40}Ca$ ratios are positively correlated´:

[3] $\delta^{44/40}Ca_{SRM915a}$ [‰] = 1.32 (±0.40)*Mg/Ca [mmol/mol] – 0.70 (±0.37) (R^2 = 0.75, n = 20)

Although slightly shallower but within statistical uncertainties, *Group I* data match the $\delta^{44/40}Ca$ temperature relation of Hippler et al. (2004) as well as the Mg/Ca temperature calibrations of Mashiotta et al. (1999) and Elderfield and Ganssen (2000) (dotted lines in Fig. 4). The positive correlations reveal that $\delta^{44/40}Ca$ and Mg/Ca ratios of *Group I* specimens are controlled by the same environmental parameter, supposingly integrating ambient seawater temperatures from the period of foraminiferal chamber formation and wall thickening. Furthermore, the good correlation of $\delta^{44/40}Ca$ and Mg/Ca respectively provides a self-consistent criterion for the robustness of the temperature approximation. In contrast, the correlation between $\delta^{44/40}Ca$ and

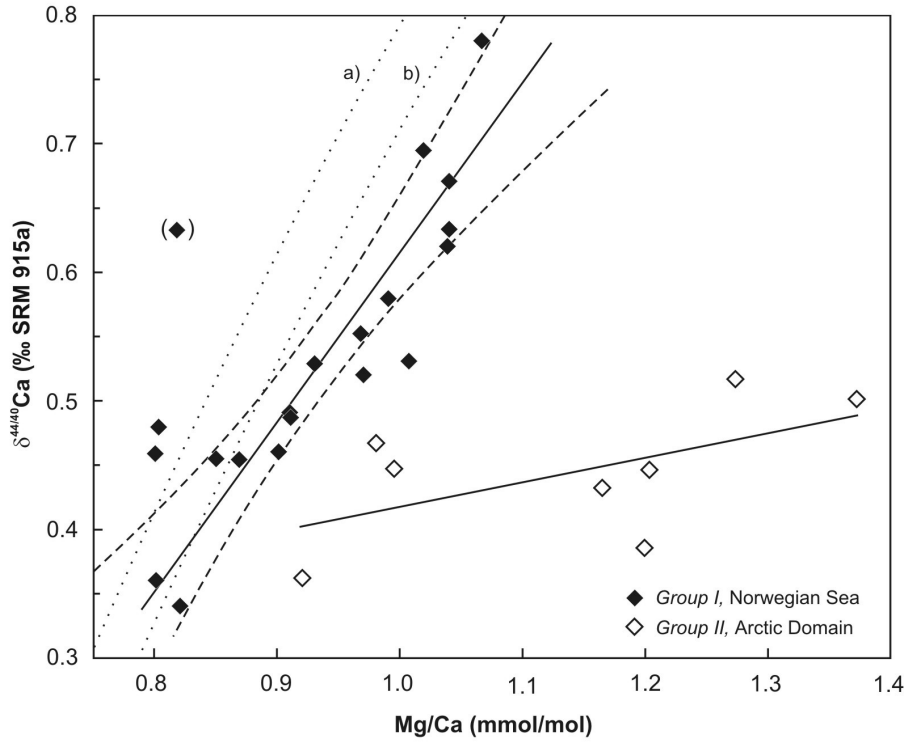

Fig. 4. The measured $\delta^{44/40}$Ca are plotted as a function of their corresponding Mg/Ca ratios. It can be seen that the *Group I* (filled diamonds) are positively correlated. The dashed line marks the 2σ-confidence band. One sample in brackets (core JM97-948) falls significantly off the correlation curve for the *Group I* data and was not considered in the calculations. In contrast, the *Group II* data (open diamonds) scatter to a large extent and do not show any significant correlation at all. The expected intersection lines of the Mg/Ca calibration of Elderfield and Ganssen, 2000 (a) and of Mashiotta et al., 1999 (b) with the $\delta^{44/40}$Ca temperature calibration of Hippler et al. [1] are plotted together with our data. Note that the measured $\delta^{44/40}$Ca and Mg/Ca ratios of *Group I* are close to (b) as predicted from the temperature calibrations.

Mg/Ca data of *Group II* originating from Arctic Domain and polar waters (Fig. 4) is less robust by a factor of almost three (equation 3, $R^2 = 0.33$). This indicates that the temperature response of the Mg/Ca and $\delta^{44/40}$Ca ratios are superimposed by other parameters than temperature.

[4] $\delta^{44/40}CaS_{RM915a}$ [‰] = 0.32 (±0.16)*Mg/Ca [mmol/mol] +0.09 (±0.17) ($R^2 = 0.33$, $n = 8$)

3.3.2. Comparison of $T_{\delta 44/40Ca}$, $T_{Mg/Ca}$ and $T_{\delta 18O}$ from core top samples

In order to further verify the proxy potential of $\delta^{44/40}$Ca and Mg/Ca for the reconstruction of past seawater temperatures, we subtracted $T_{\delta 44/40Ca}$ from $T_{Mg/Ca}$ (Fig. 5a). Given that the difference of two proxy temperature estimates $\Delta T = (T_{Mg/Ca} - T_{\delta 44/40Ca})$ is statistically undistinguishable

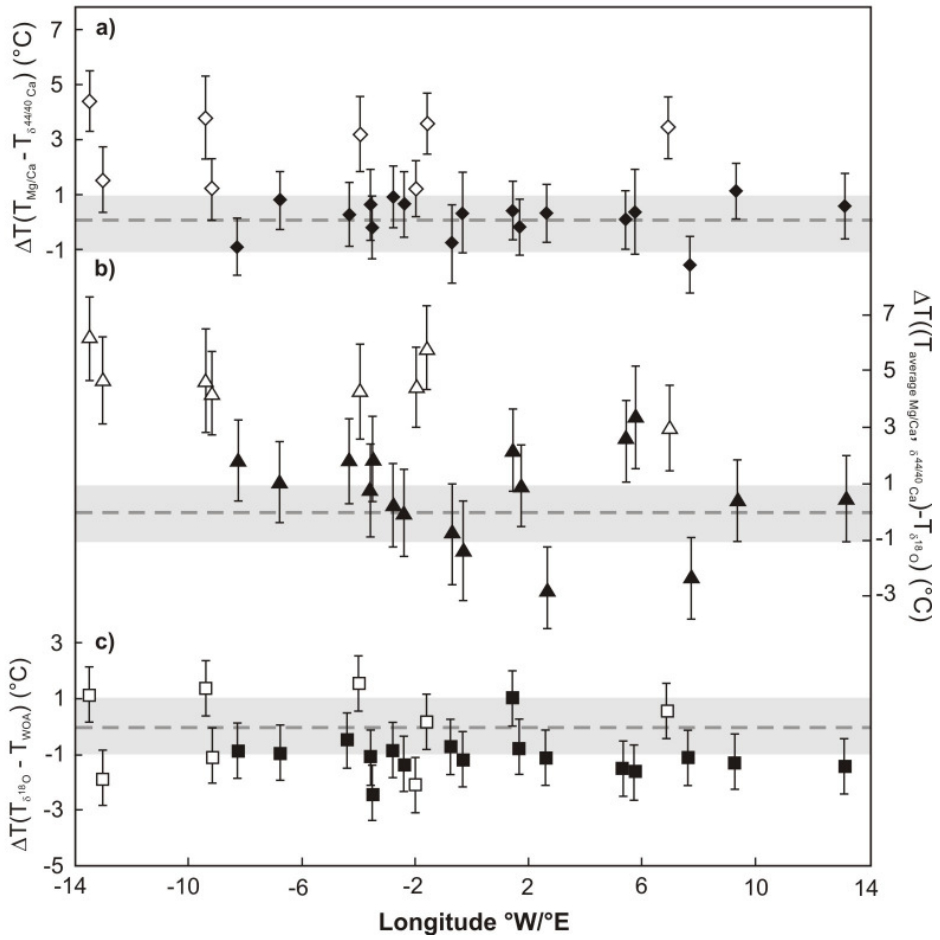

In **Fig. 5a**, the difference ($\Delta T = (T_{Mg/Ca} - T_{\delta 44/40Ca})$) of Mg/Ca-based ($T_{Mg/Ca}$) and $\delta^{44/40}$Ca-based ($T_{\delta 44/40Ca}$) temperature estimates is plotted on a meridional projection. *Group I* data are marked by black squares, *Group II* data by white squares. *Group I* data are within about ±1°C indistinguishable from zero and can thus be considered to reflect a robust approximation of calcification temperatures. *Group II* data scatter to a large extent and do not fulfil the proxy criteria of consistency, therefore, they have to be considered to be less reliable.

In **Fig. 5b,** δ^{18}O-inferred temperatures ($T_{\delta 18O}$) are subtracted from averaged Mg/Ca and $\delta^{44/40}$Ca temperature estimates ($\Delta T = (T_{average\ Mg/Ca,\ \delta 44/40Ca}) - T_{\delta 18O}$). It can be seen that the data scatter to a larger extent than in Fig 5a. Group *I* data are within about ±2°C indistinguishable from zero whereas *Group II* data deviate up to 7°C from the zero line, mainly due to Mg/Ca and $\delta^{44/40}$Ca temperatures overestimates.

In **Fig. 5c,** the difference ($\Delta T = T_{\delta 18O} - T_{WOA}$) of $T_{\delta 18O}$ and instrumental data from the World Ocean Atlas (T_{WOA}) is plotted on a meridional projection. It can be seen that the scatter of the data around zero is only about ±1°C for both *Group I* and *Group II* data.

from zero, both proxies reliably predict the same temperature within distinct uncertainties. In the opposite case, the use of Mg/Ca and $\delta^{44/40}$Ca in a multi-proxy approach must be challenged. It can be seen from our data projected meridionally onto a SEE – NWW transect line (Fig. 5a) that

$T_{\delta 44/40Ca}$ and $T_{Mg/Ca}$ provide consistent results for those data corresponding to the Norwegian Current (*Group I*). All *Group I* data are within about ±1°C indistinguishable from zero and can thus be considered to reflect robust calcification temperature estimates. In contrast, most ($\Delta T = T_{Mg/Ca} - T_{\delta 44/40Ca}$) estimates from sediment cores west of about 0°E (*Group II*) deviate between about 1°C to 4°C from zero. Therefore, *Group II* data corresponding oceanographically to Arctic Domain and polar waters do not fulfil proxy criterion and have to be considered to be less or even not reliable.

In order to further assess the reliability of $T_{Mg/Ca}$ and $T_{\delta 44/40Ca}$ we compare their average value ($T_{average\ Mg/Ca - \delta 44/40Ca}$) with their corresponding $T_{\delta 18O}$. From Fig. 5b it can be seen that $\Delta T = (T_{average\ Mg/Ca - \delta 44/40Ca} - T_{\delta 18O})$ for *Group I* data is equal to zero within about 2°C which is a factor of 2 worse than for $T_{\delta 44/40Ca}$ and $T_{Mg/Ca}$. This indicates that the salinity changes or the mixture of water masses with different $\delta^{18}O_{water}$ values may have been larger than expected from our assumptions. However, much larger deficiencies exist for *Group II* data where average Mg/Ca and $\delta^{44/40}$Ca- inferred temperatures ($\Delta T = (T_{average\ Mg/Ca,\ \delta 44/40Ca} - T_{\delta 18O})$) overestimate $T_{\delta 18O}$ by up to 7°C (Fig. 5b). From Fig 5a and 5b it can not be decided whether $T_{average\ Mg/Ca,\ \delta 44/40Ca}$ or $T_{\delta 18O}$ is the better approximation of the true water temperature for *Group II* data. However, it is apparent from Fig 5c that $T_{\delta 18O}$ and T_{WOA} (present day temperatures taken from the World Ocean Atlas 2001) are in general accordance within 2°C which is significantly more reliable than the *Group II* deficiencies for $T_{\delta 44/40Ca}$ and $T_{Mg/Ca}$ seen in Fig. 5a. This indicates first that the assumption of minor past salinity changes relative to the present day values is reasonable for the $\delta^{18}O$ data and second that at least in the case of *Group II* data, $T_{\delta 18O}$ and T_{WOA} reflect calcification temperatures more closely than $T_{Mg/Ca}$ and $T_{\delta 44/40Ca}$, respectively. Therefore, for further discussion, we take T_{WOA} to be the best approximation of foraminiferal calcification temperatures for *Group II* data whereas for *Group I*, we assume that $T_{\delta 44/40Ca}$ and $T_{Mg/Ca}$ are the best approximation due to their consistency and reproducibility within about 1°C.

3.3.3. Temperature dependency of $\delta^{44/40}$Ca and Mg/Ca ratios in core top samples

In Fig. 6, all $\delta^{44/40}$Ca ratios of our core top samples are plotted as a function of their corresponding calcification temperatures as presented in Tab. 4. The *Group I* data are plotted as a function of $T_{Mg/Ca}$. This is justified because $T_{Mg/Ca}$ has been determined completely independent

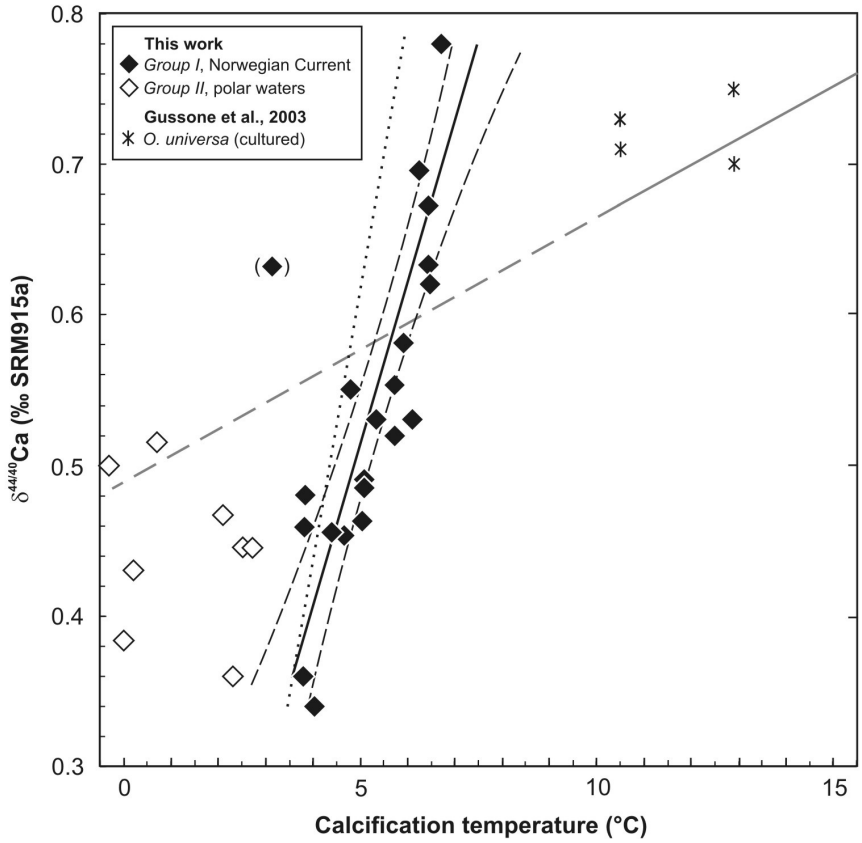

Fig. 6. $\delta^{44/40}$Ca ratios are plotted as a function of their calcification temperature ($T_{Mg/Ca}$ for *Group I* (filled diamonds) and T_{WOA} for *Group II* (open diamonds)). *Group I* match the Hippler et al. 2006 calibration (dotted line) whereas *Group II* data plot in between the temperature equation of *N. pachyderma* (sin.) and the calibration line of *O. universa* (Gussone et al. 2003).

from the Ca isotope temperature relation. In addition, $T_{Mg/Ca}$ is a close approximation of the calcification temperature because $T_{\delta 44/40Ca}$ and $T_{Mg/Ca}$ are in good agreement. The same arguments are also valid when plotting *Group I* Mg/Ca ratios as a function of $T_{\delta 44/40Ca}$. In contrast, *Group II* data are plotted as a function of T_{WOA} which has been shown to be the best approximation for their calcification temperature.

From Fig 6 it can be seen that *Group I* data closely follow the expected $\delta^{44/40}$Ca-temperature calibration curve for *N. pachyderma* (sin.) as proposed by Hippler et al. (2004; chapter I, this work). In contrast, *Group II* data scatter in between the $\delta^{44/40}$Ca temperature calibration curves for *O. universa* (Gussone et al., 2003) and the $\delta^{44/40}$Ca -temperature equation for *N. pachyderma* (sin.). This indicates that the $\delta^{44/40}$Ca ratios of *Group II* specimens are higher then predicted by the Ca-temperature equation of Hippler et al. (2004).

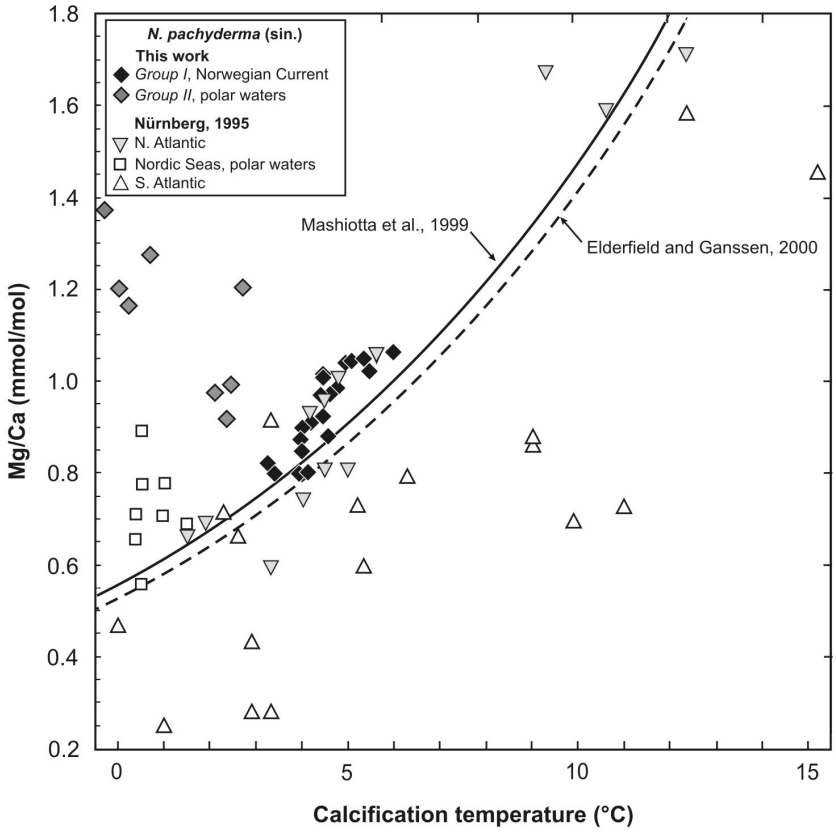

Fig. 7. Mg/Ca ratios of *N. pachyderma* (sin.) from various locations are plotted as a function of their expected calcification temperature ($T_{\delta 44/40Ca}$ for *Group I;* T_{WOA} for *Group II*). In addition, the Mg/Ca-temperature calibrations of Mashiotta et al. (1999) and of Elderfield and Ganssen (2000) are shown for comparison. *Group I* Mg/Ca ratios fall along the Mg/Ca calibration data set of Nürnberg, 1995. However, *Group II* Mg/Ca ratios show an offset plotting distinctively above the calibration curve.

In a similar plot presenting Mg/Ca values as a function of their corresponding water temperatures $T_{\delta 44/40Ca}$ (Fig. 7), it can be seen that *Group I* data match the existing Mg/Ca-temperature calibrations of Mashiotta et al (1999) and Elderfield and Ganssen (2000). However, *Group II* data plotted as a function of T_{WOA} fall off the calibration line towards significant higher Mg/Ca ratios than predicted from the temperature equations, forming an almost parabolic function with lowest Mg/Ca ratios at about 3 to 4°C.

Both foraminiferal Mg/Ca and $\delta^{44/40}$Ca ratios are plotted against their corresponding calcification temperatures in Fig. 8. The slopes of the Mg/Ca and $\delta^{44/40}$Ca ratios of *Group I* data are identical, indicating that Mg/Ca and $\delta^{44/40}$Ca values of *Group I* specimens change in equal proportions similar to binary mixing processes of two independent phases. In contrast, $\delta^{44/40}$Ca and even more pronounced Mg/Ca data of *Group II* specimens point towards an inverse

temperature response with increasing values at decreasing temperatures as well as they do not show any significant relationship to each other. In general, *Group I* are separated from *Group II* data by a distinct temperature threshold value of about 3.5°C which is also associated with a salinity threshold value of about 34.5 ‰, representing the boundary between the Norwegian Current and the Arctic Domain in the central Nordic Seas.

In summary, the comparison of our data reveals that the temperature response of the trace element as well as of the Ca isotope fractionation is significantly different in *Group I* and *Group II* samples. The only obvious discriminating factor between these two groups is their original occurrence from different water masses characterized by different temperature and salinity ranges. *Group I N. pachyderma* (sin.) calcify above and *Group II N. pachyderma* (sin.) below the temperature salinity threshold values of 3.5°C and 34.5 ‰ (Fig 8).

3.4. Discussion

The multiproxy approach with the objective to test the 'cold-end' behaviour of *N. pachyderma* (sin.) revealed a bivalent calcification pattern as a function of the ambient water temperature. Above about 3.5°C characterizing *Group I* samples, Mg/Ca and $\delta^{44/40}$Ca ratios are very well correlated reflecting consistent calcification temperature estimates compared to modern oceanographic data. However, in *Group II* samples corresponding to water temperatures below about 3.5°C the proxy to temperature relation is obscured even showing an inverse temperature trend. Hence, $T_{\delta 44/40Ca}$ and $T_{Mg/Ca}$ overestimate given water temperatures accompanied by the total loss of any proxy temperature sensitivity.

The effect which causes this discrepant behaviour of the foraminifera cannot be explained by any of the usual ecological, environmental and diagenetic processes because these usual controlling factors affect the temperature-Mg/Ca and temperature-$\delta^{44/40}$Ca relationship in different ways. In particular $\delta^{44/40}$Ca as an isotopic proxy is relatively insensitive to those parameters influencing Mg/Ca ratios beside temperature. Rather the simultaneous loss of correlation and individual temperature-calibration as a function of temperature point to the likelihood that changes of the calcification mechanism of *N. pachyderma* (sin.) itself has to be involved. In this regard, it is notable that the slopes of the temperature sensitivity of the $\delta^{44/40}$Ca and Mg/Ca ratios are identical (Fig. 8). This indicates that any change is equally recorded in same

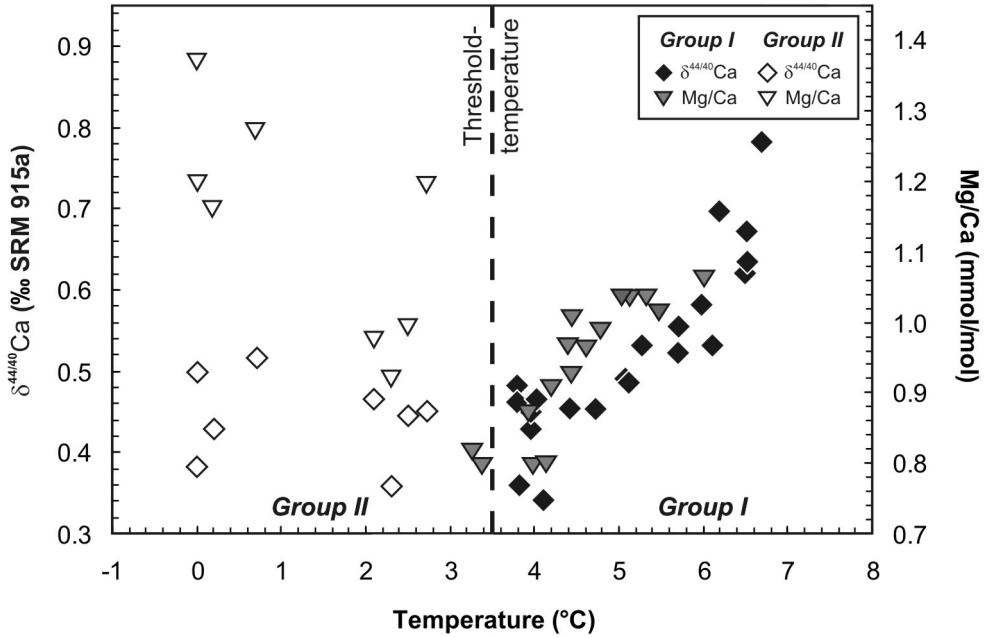

Fig. 8. Mg/Ca (right axis) and $\delta^{44/40}$Ca (left axis) ratios of *N. pachyderma* (sin.) are plotted together as a function of their calcification temperatures (Mg/Ca vs. $T_{\delta 44/40Ca}$ and $\delta^{44/40}$Ca vs. $T_{Mg/Ca}$ for *Group I* data; T_{WOA} for *Group II*). *Group I* data are well correlated and characterized by identical slopes. *Group II* data show a large scatter and are insensitive to calcification temperature. *Group I* and *II* data are well distinguished by a distinct temperature threshold value of about 3.5°C and a salinity of about 34.5°C (not shown here).

proportions for both proxies as we would expect from a binary mixing process of two calcite endmembers with distinctively different $\delta^{44/40}$Ca and Mg/Ca ratios. A model describing the temperature response of the Mg content in low-Mg foraminifera as a temperature dependent mixture between two calcite phases has recently been reported by Bentov and Erez, 2006. These authors describe two calcite endmembers, *phase I* and *phase II* calcite, which are produced by significantly different biomineralisation processes and intracellular pathways and form the final foraminiferal tests by varying proportions. In order to understand our apparently discrepant data, we will first discuss qualitatively and quantitatively a model for the pathways of Mg and Ca from the adjacent seawater to the site of calcification for *Group I* data comprising *N. pachyderma* (sin.) calcifying above the threshold temperature of about 3.5 °C. Subsequently we will apply this model to discuss the "cold-end" biomineralisation pathways in *N. pachyderma* (sin.) from water temperatures below about 3.5°C.

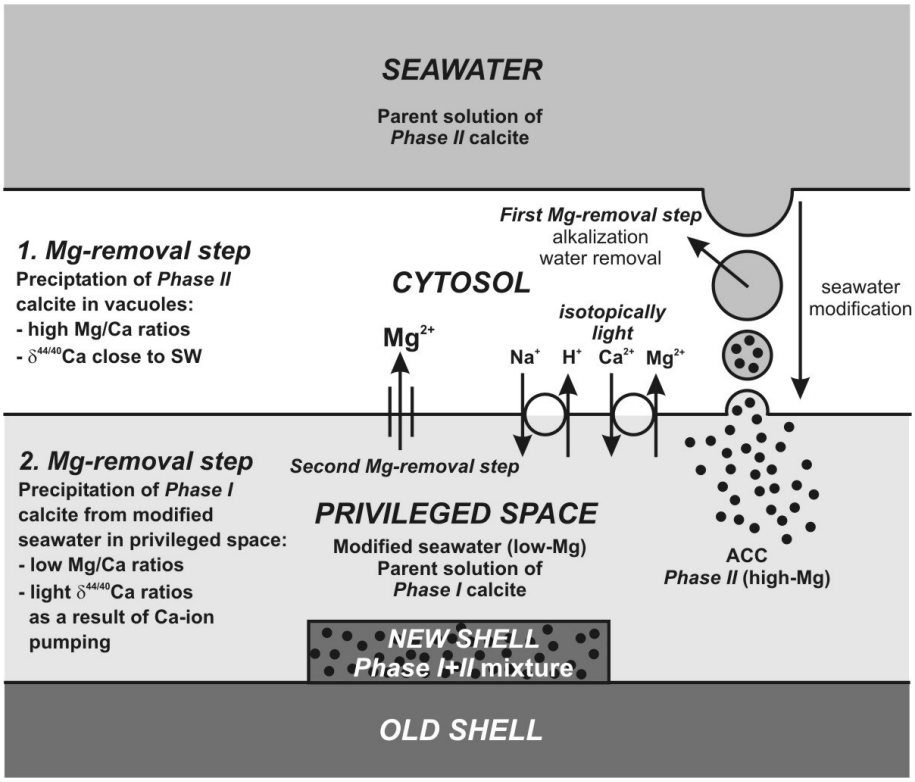

Fig. 9. Model of a 2-step removal of Mg^{2+} in perforate foraminifera, modified after Bentov and Erez (2006). Seawater is vacuolised by the cytoplasm and chemically modified. After a first Mg-removal step, *Phase II* calcite (high Mg- and high $\delta^{44/40}$Ca ratios) is precipitated in the vacuoles in the form of amorphous calcite (AAC) granules and provides a temporary calcium storage in the cytosol, probably stabilized by some organic compound ("Ca-pool", Bentov and Erez, 2005). The modified seawater is subsequently transferred to the privileged space where it is further modified by a second Mg-removal step, accompanied by the input of isotopically light Ca to the privileged space by ion pumping.

3.4.1. Impact of biomineralization processes on the Mg/Ca ratio of foraminifera

In earlier studies it has been speculated that beside temperature controlled inorganic processes, related temperature controlled physiological processes may dominate the incorporation of Mg in foraminiferal calcite (Rosenthal et al., 1997). Recently, Bentov and Erez (2006) proposed that the high variability of the Mg/Ca ratios in foraminifera (c.f. Nürnberg, 1996; Sadekov and Eggins, 2005; Eggins et al., 2003) represent different biomineralisation pathways for Mg that developed during the evolution of foraminifera. The authors suggested that the high-Mg calcite (>10 mol% Mg) in shells and their sublayers may precipitate from transient amorphous $CaCO_3$ (AAC) granules with the influence of an organic matrix (*primary calcite*, *Phase II*). In contrast, the low-

Mg calcite (~3 mol% Mg) precipitates from a confined seawater parent solution that is strongly modified and depleted in Mg (*secondary calcite*, *Phase I*). *Phase II* calcite is supposed to delineate the shape of a new chamber on both sides of an organic matrix, termed the primary organic membrane (POM, Hemleben et al., 1986) which is subsequently covered and thickened by *Phase I* calcite (Bentov and Erez, 2005). Consequently, when evaluating the final Mg content of a shell, the Mg/Ca ratios of the two phases and their relative proportion must be taken into consideration. Besides environmental parameters such as the temperature of the ambient seawater, the distribution of *Phase I* and *Phase II* calcite may also change as a result of a physiological control (Bentov and Erez, 2006). Hence, the strong temperature sensitivity in Mg/Ca of about 10%°C^{-1} in low-Mg foraminifera (e.g. Mashiotta et al., 1999) compared to only about 3%°C^{-1} in inorganic precipitates (Oomori et al., 1987) may then be caused by a temperature-mediated binary mixing of *Phase II* calcite with *Phase I* calcite. The relative contribution of *Phase I* and *Phase II* fluxes may then reflect the physiological response of the foraminifera to a changing hydrographic environment.

3.4.2. 'Two Phase Model' for biomineralization in order to explain the bivalent behaviour of Mg/Ca and $\delta^{44/40}Ca$

The main and trace element homeostasis of foraminifera requests to keep the Ca- and Mg concentrations and fluxes controlled within narrow limits. Hence the Mg/Ca ratio has to be fixed between an upper and a lower limit. Presumably the best mechanism to keep the Mg/Ca ratio in the desired interval is the mixing of two different calcite endmembers in suitable proportions. Therefore, closely following the model of Bentov and Erez (2006) we assume the presence of two calcite phases in *N. pachyderma* (sin.), low-Mg *Phase I* calcite (secondary calcite) and high-Mg *Phase II* calcite (primary calcite). Their production is a two-step-process of purification and extraction of Mg from vacuoles (precipitation of *Phase II* calcite) and the privileged space (precipitation of *Phase I* calcite) in which the ion concentration can be regulated (Fig. 9). We assume that the main purpose of this two-step-process is generally directed towards the lowering of the Mg/Ca ratio present in seawater (~5.2 mol/mol) to values below about 2 mmol/mol in order to permit the precipitation of calcite in an aragonite ocean.

Phase I (secondary) calcite is produced in a "privileged space" from a parental solution that originates from seawater but was already chemically altered along its transport through the cytosol to the privileged space via vacuoles (Fig. 9). In these vacuoles, Ca and Mg may already precipitate in the form of ACC (Bentov and Erez, 2006) which are subsequently transported to the privileged space where they can be redissolved for further chemical alteration and purification of Mg. Tracer experiments (Bentov, 1997) reveal that these ACC granules (*Phase II calcite*) might act as an internal carbon pool as already reported for *G. sacculifer* (Anderson and Faber, 1984). Although not known in detail, the removal of Mg from the vacuoles as well as from the privileged space must be performed via diffusion across Mg-channels and/or by spending energy via ADT-ADP reactions across Mg-pumps (Bentov and Erez, 2006). Alternatively, the Mg/Ca ratio can also be lowered by pumping extra Ca^{2+} ions from other sources located in the cytosol into the privileged space. Principally, we assume that the ion transport processes modifying the parental solution in the vacuoles forming *Phase II* (primary) calcite are similar to the ion transport processes employed at the privileged space creating *Phase I* (secondary) calcite (Bentov and Erez, 2006). Concerning the element and isotope partitioning between liquid and solid phase it is important to note that *Phase II* calcite experiences only one Mg-removal step whereas *Phase I* experiences a second Mg removal step in the privileged space resulting in higher Mg/Ca ratios of *Phase II* relative to *Phase I* calcite (Fig. 9). According to the model of Bentov and Erez the Mg/Ca difference between *Phase I* and *II* calcite is in the order of a factor of four.

With respect to the Ca isotope fractionation we assume that the ACC of the vacuoles forming the *Phase II* (primary) calcite is enriched in the light isotope (^{40}Ca) relative to seawater due to kinetic isotope fractionation (Gussone et al., 2003; Lemarchand et al., 2004) showing the relative insensitive temperature relationship of ~0.019 ‰°C^{-1}. According to Gussone et al. (2003) the isotopic difference ($\Delta^{44/40}Ca$) between seawater and precipitated carbonates is about 1.5 ‰ in *O. universa* but may be much smaller as a function of an increasing calcite precipitation rate (Lemarchand et al., 2004). Eventually, the vacuoles empty their ACC into the privileged space (Fig 9) where it can become redissolved. In this case, the ACC present in the privileged space and later forming *Phase I* calcite is then isotopically distinctively lighter than seawater. It may also become lighter than *Phase II* (primary) calcite when the redissolved ACC precipitates again form *Phase I* (secondary) calcite. The isotopic contrast between *Phase I* and *II* calcite may even be enhanced due to the input of isotopically light Ca added to the privileged space by Ca ion-

pumping which is related to kinetic processes preferring the light relative to the heavy isotopes (Gussone et al., 2003). In particular, Ca channels and pumps cause a Ca isotope fractionation between ^{44}Ca and ^{40}Ca in the order of about ±1 ‰ (Gussone et al., 2005).

Following these model approaches we may predict that *Phase I* (secondary) calcite has to be isotopically lighter then *Phase II* (primary) calcite. Similar to that, the Mg/Ca ratios of *Phase I* (secondary) calcite have to be lower than those of *Phase II* (primary) calcite. However, concerning the Ca isotopes, the actual isotopic difference between seawater and *Phase II* (primary) calcite as well as the isotopic difference between *Phase II* and *Phase I* (secondary) calcite may be a function of the precipitation rate.

3.4.3. Model description

According to the model approach it may be predicted that the mixing between the two calcite endmembers with their distinct different Mg/Ca- and $\delta^{44/40}Ca$-characteristics are physiologically or enzymatically controlled in a way that the proportion of *Phase I* (secondary) calcite as the low Mg/Ca mixing endmember decreases, whereas *Phase II* (primary) calcite as the high Mg/Ca mixing endmember increases as a function of temperature (Fig 10). In general, temperature dependent binary mixing of two phases can be quantitatively described as followed:

[5] $$y(T) = a(T) + \frac{b}{c \cdot e^{d \cdot T} + 1}$$

y(T) = either Mg/Ca(T) or $\delta^{44/40}Ca(T)$; T = Temperature(°C).
a(T) = lower endmember for Mg/Ca(T) or $\delta^{44/40}Ca(T)$
a(T)+b = upper endmember for Mg/Ca(T) or $\delta^{44/40}Ca(T)$
c = initial value
d = slope of the exponential function

The function y(T) may describe the temperature dependent variation of the Mg/Ca and $\delta^{44/40}Ca$ ratios between the lower endmember a(T) and the upper endmember a(T) + b. Note, that both functions a(T) and a(T)+b are temperature dependent but different by an offset of "b". Given that $T \rightarrow -\infty$, the function y(T) approaches a(T) and for $T \rightarrow \infty$, y(T) approaches a(T) + b. As long as the slope "d" is set to a negative number, y(T) will increase as a function of temperature from

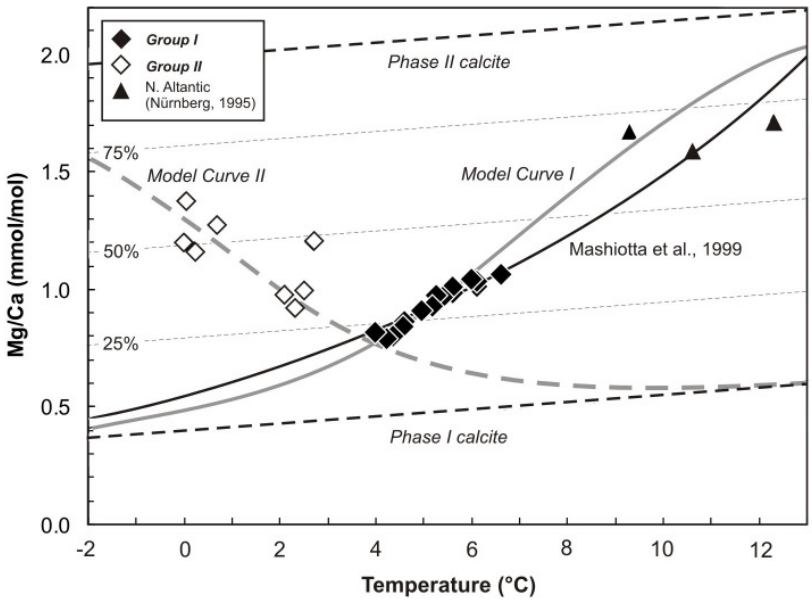

Fig. 10. The Mg/Ca composition of *N. pachyderma* (sin.) at the 'cold end' can be described by a temperature or physiologically mediated change in the proportions in *Phase I* and *Phase II* calcite. The equations selected for *Phase I* and *Phase II* calcite are close to the functions given by Bentov and Erez (2006) and Oomori et al., (1987). The triangles represent the highest Mg/Ca ratios found in North Atlantic *N. pachyderma* (sin.) (Nürnberg, 1995).

the low mixing endmember a(T) towards the high mixing endmember a(T) + b. In contrast, a positive "d" will cause y(T) to decrease towards a(T).

In the case of the Mg/Ca ratios of our *N. pachyderma* (sin.) tests, the low endmember a(T) can be set to meet the *Phase I* (secondary) calcite characteristics and a(T)+b can be set to closely meet the characteristics of the *Phase II* (primary) calcite originally given by Bentov and Erez (2006). Both calcite endmembers are temperature dependent showing a slope in the order of ~3%°C^{-1}. According to their model, we assume a four fold difference in the Mg content between the two phases. The values "c" and "d" can be selected in order to approximate the empirical Mg/Ca values (for details see Tab. 3).

In the case of $\delta^{44/40}$Ca(T), *Phase I* calcite corresponding to a(T) can arbitrarily be set to the function for the inorganic Ca isotope fractionation curve given by Gussone et al. (2003). The $\delta^{44/40}$Ca(T) characteristics of *Phase II* calcite is yet not known and has arbitrarily to be chosen to be about 1.2 ‰ higher than *Phase I* calcite in order to closely approach our data (Fig. 11).

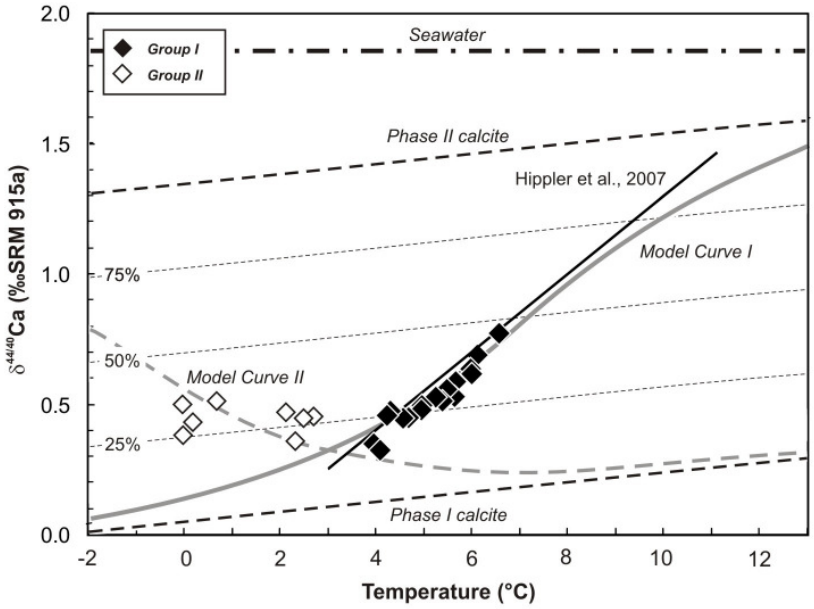

Fig. 11. Model describing the $\delta^{44/40}$Ca temperature sensitivity of *N. pachyderma* (sin.) at the 'cold end' by a temperature or physiologically mediated change in the proportions in *Phase I* and *Phase II* calcite. *N. pachyderma* (sin) is successfully calibrated to above about 10°C (Hippler at al., 2004).

It is important to emphasize that there are two model curves necessary in order to describe the temperature dependent behaviour of our empirical data corresponding to *Group I* and *II N. pachyderma (sin.)* calcifying above and below the temperature threshold value of about 3.5°C. In Tab. 5 (appendix), a(T), b and c for the two model curves (*I* and *II*) are calculated to closely approximate our empirical data for *Group I* and *Group II* samples. As a major characteristics of the data approximation by model curve *I* and *II,* the model curve *I* approximating the *Group I* data increase as a function of increasing temperatures whereas model curve *II* approximating the *Group II* data decrease as a function of increasing temperatures. From Fig. 10 and 11 it can be seen that the model curves *I* and *II* fit the empirical data closely within statistical uncertainties. Because of the fact that *Group I* and *II* data have to be described by two different model curves, both data groups will be discussed separately in the section below.

3.4.4. Comparison of the model predictions with Group I data (>3.5°C)

The characteristics of the *Group I* data is that Mg/Ca and the $\delta^{44/40}$Ca ratios increase as a function of temperature (Figs. 8, 10, 11) as predicted by Mg/Ca-temperature calibrations. In particular, Model curve *I* (Fig. 10) is in general accordance with the Mg/Ca-temperature

calibration of Mashiotta et al. (1999) and also fits the high Mg/Ca values of *N. pachyderma* (sin.) from the North Atlantic, almost representing the upper thermal limit of this species (Nürnberg 1995). Simultaneously, model curve *I* fits the measured $\delta^{44/40}$Ca values as well as the approximating function of Hippler et al., 2006 (Fig. 11). It can be seen in Fig. 10 and 11 that the amount of *Phase I* (secondary) calcite reaches a minimum proportion of about 25% in the temperature range of 3.5°C. At increasing temperatures, *Group I* data show a maximum contribution of *Phase I* (secondary) calcite of about 50 % at about 7°C. At temperatures below 3.5°C the foraminiferal physiology switches from *process I* to *process II*, resulting in an increase of the proportion of *phase II* (primary) calcite with decreasing temperatures.

3.4.5. Comparison of the model predictions with Group II data (<3.5°C)

From Figs. 10 and 11 it can be seen that model curve *II* fits the Mg/Ca and $\delta^{44/40}$Ca ratios of the *Group II* data. However, in contrast to the model curve *I*, it is characterized by an inverse relationship between calcification temperature and proxy-response. We interpret this observation as a switch of the foraminiferal physiology from one biomineralization process active at moderate temperatures (normal mode process, *NMP*) to an alternative mode active below 3.5°C only (cold mode process, *CMP*). Obviously, *Group I* data correspond to NMP whereas *Group II* data correspond to *CMP*. It may be speculated that the switch from *NMP* to *CMP* at a certain temperature threshold may reflect the Ca and Mg homeostasis which tend to keep a balance between *Phase I* (secondary) and *Phase II* (primary) calcite. In particular it may be speculated that the foraminiferal physiology inhibits a decrease of the relative contribution of *Phase I* (secondary) calcite to fall below about 25%, probably under the aspect of an energy efficient calcification process.

3.4.6. The origin of the temperature dependency of Mg/Ca- and $\delta^{44/40}$Ca in the shell of N. pachyderma (sin.)

Our model describing the temperature sensitivity of the Mg/Ca ratio in *N. pachyderma* (sin.) by a mixing process between two different calcite phases challenges earlier arguments by Lea et al. (1999) and Mashiotta et al. (1999) proposing that the temperature response of the Mg/Ca ratios in foraminifera can be described by the van't Hoff equation which predicts an exponential temperature response similar to the observations made from inorganic calcite precipitation

studies (Oomori et al., 1987). The van't Hoff equation certainly approaches the temperature dependency correctly for inorganic systems as assumed for *Phase I* (secondary) and *Phase II* (primary) calcite. However, this equation can not simply be transferred to biological systems which have a strong physiological control over their trace metal budgets. In particular, the inverse temperature response at the "cold-end" of the Mg/Ca temperature calibration cannot be explained by the van't Hoff equation. Instead, we have to assume that the foraminiferal physiology actively controls, mainly lowers the Mg/Ca ratio in order to initiate calcite precipitation. Because of a yet unknown biochemical reason, the foraminiferal physiology may inhibit any drop of the Mg/Ca ratio below a certain threshold value by switching from *NMP* to *CMP*. The *CMP* operates inversely to the *NMP* increasing the Mg/Ca ratio as a function of decreasing temperature. As soon as a high end Mg/Ca threshold is achieved with decreasing temperatures, the biomineralisation pathways may switch again to the opposite direction from the *CMP* to the *NMP* comparable to a control circuit in order to keep the Mg/Ca ratios within narrow limits as requested by the trace metal homeostasis of the foraminiferal physiology.

3.5. Summary of results and conclusion

A multi-proxy approach applying Mg/Ca and $\delta^{44/40}$Ca ratios in *N. pachyderma* (sin.) with the objective to test their consistency for the reconstruction of past seawater temperatures revealed discrepant results. *Group I* samples originating from the Norwegian Sea characterized by water temperatures above about 3.5°C show well correlated $\delta^{44/40}$Ca and Mg/Ca data in accordance with existing temperature calibrations (Mashiotta et al., 1999; Elderfield and Ganssen, 2000; Hippler et al., 2004, in prep.). In contrast, *Group II* $\delta^{44/40}$Ca and Mg/Ca data originating from Arctic Domain and polar waters characterized by water temperatures below about 3.5°C are not correlated to each other and show no significant response to calcification temperature. Instead, opposed to existing temperature calibrations, *Group II* $\delta^{44/40}$Ca and Mg/Ca data tend to increase with decreasing temperatures, forming almost parabolic temperature relations with lowest Mg/Ca and $\delta^{44/40}$Ca ratios at about 3.5°C.

In order to reconcile our $\delta^{44/40}$Ca and Mg/Ca ratios and the discrepant behaviour of *Group I* and *Group II* data we presented a "two-step-model" to describe the final test chemistry by the temperature-mediated mixture of two calcite endmembers (*Phase I and II*) formed by *N. pachyderma* (sin.) in different biomineralisation pathways. The arbitrarily selected model

curves *I* and *II* closely approximating our data for *Phase I* and *II* calcite are in general accordance with earlier findings of Gussone et al. (2003), Bentov and Erez (2006) and the existing temperature calibrations for Mg/Ca and $\delta^{44/40}$Ca in planktonic foraminifera. The non-linear mixing of two calcite endmembers produces a final test chemistry with a significantly higher temperature response in the Mg/Ca and $\delta^{44/40}$Ca signal than in pure *Phase I* and *II* calcite alone. Our observation challenges earlier assumptions that the van´t Hoff equation can be unambiguously transferred to biological systems in order to explain the temperature sensitivity of foraminiferal Mg/Ca ratios. Rather we have to assume that the foraminiferal physiology actively controls their trace element incorporation within narrow limits. It is speculated that there are two modes present which are able to increase (*NMP*) or decrease (*CMP*) the Mg/Ca ratio as a function of temperature. Hence, our *Group I* and *II* data may reflect this alternation between *NMP* and *CMP* as a function of temperature.

Acknowledgement

This study was supported by the German Science foundation within the Research Theme FOR 451 and the CASIOPEIA project (Ei272/20-1, DFG). Mara Weinelt, Florian Böhm, Volker Liebetrau, Folkmar Hauff and Ana Kolevica are acknowledged for their general support, interest and ongoing discussions concerning this project.

Appendix: Model parameters for Mg/Ca(T) and $\delta^{44/40}$Ca(T)

Table 3a: Model Parameters set for Mg/Ca(T)

	***Group I* data**	***Group II* data**
a(T)	$0.4*e^{0.03T}$	$0.4*e^{0.03T}$
b	1.6	1.6
c	20	0.4
d	-0.4	0.4

Table 3b: Model Parameters set for $\delta^{44/40}$Ca(T)

	***Group I* data**	***Group II* data**
a(T)	0.019*T + 0.05	0.019*T + 0.05
b	1.3	1.3
c	18	1.5
d	-0.4	0.4

Table 4: $\delta^{44/40}$Ca, Mg/Ca and δ^{18}O records of *N. pachyderma* (sin.) and proxy temperature estimates

Nr.	Core	Group	Latitude °N	Longitude °W/°E	Water depth [m]	Inferred calcification depth [m][1)]	Temp in calc depth (July-Sept.) [°C][2)]	Sal. in calc. depth (July-Sept.) [‰][2)]	Mg/Ca [mmol/mol][3)]	$\delta^{44/40}$Ca [‰ SRM 915a]	*n*	$\delta^{18}O_{Nps}$ [‰ PDB][4)]	$T_{Mg/Ca}$	$T_{\delta 44/40Ca}$	$T_{\delta 18O}$
1	HM16130	I	65.10	-2.42	3182	60	7.0	35.1	0.99	0.58 ± 0.11	4	2.40	6.0	4.8	5.7
2	HM16132	I	64.57	-0.72	2798	150	5.7	35.1	0.80	0.46 ± 0.18	5	2.58	3.8	4.0	5.0
3	HM16142	I	63.25	2.60	1100	70	9.0	35.1	0.93	0.53 ± 0.07	5	1.83	5.3	4.4	8.0
4	HM49-15	I	66.34	-0.36	3260	40	7.5	35.1	0.91	0.49 ± 0.18	2	2.23	5.1	4.2	6.3
5	HM52-18	I	62.27	-14.14	1672	50[1)]	9.8	35.2	0.82	0.34 ± 0.08	5	3.09	4.1	3.3	3.2
6	HM52-39	I	65.57	-6.79	2305	70	5.2	35.0	0.97	0.52 ± 0.06	2	2.73	5.7	4.4	4.3
7	HM52-42	I	66.34	-2.80	3104	50	6.6	35.1	1.04	0.62 ± 0.08	3	2.38	6.5	5.0	5.6
8	HM57-11	I	67.12	-8.30	1617	60	3.3	34.9	0.80	0.48 ± 0.06	2	3.19	3.8	4.1	2.4
9	HM57-16	I	67.28	-4.37	2816	40	5.3	35.0	1.07	0.78 ± 0.09	3	2.59	6.7	6.0	4.8
10	HM57-20	I	62.65	1.67	750	400	4.3	35.0	0.85	0.46 ± 0.05	2	2.92	4.4	4.0	3.8
11	HM71-17	II	70.00	-13.02	1460	20	2.5	34.1	1.00	0.45 ± 0.11	6	3.40	6.0	3.9	2.5
12	HM71-22	I	69.34	-3.61	1833	20	6.5	35.0	1.04	0.67 ± 0.14	5	2.44	6.5	5.3	5.4
13	HM80-43	II	72.25	-9.19	2448	10	2.1	34.1	0.98	0.47 ± 0.08	5	3.50	5.9	4.0	2.1
14	HM94-12	I	71.32	-3.55	1816	30	4.4	34.7	0.80	0.36 ± 0.09	2	3.23	3.8	3.4	0.4
15	HM94-16	I	73.23	5.37	2356	60	3.6	35.0	0.87	0.45 ± 0.06	3	3.32	4.7	4.0	2.1
16	HM94-18	I	74.50	5.70	2469	50	3.2	35.0	0.91	0.48 ± 0.20	3	3.47	5.1	4.2	1.4
17	HM94-30	II	74.38	-2.00	3599	30	2.3	34.5	0.92	0.36 ± 0.03	3	3.67	5.2	3.4	0.2
18	JM97-948	I	66.97	7.64	1048	50	8.3	35.1	0.82	0.63 ± 0.05	5	2.01	4.1	5.1	7.2
19	HM133-21	I	61.62	-8.86	891	50[1)]	9.6	35.2	1.04	0.63 ± 0.09	4	-	6.5	5.1	
20	HM133-24	I	61.42	-11.87	1468	50[1)]	9.9	35.2	1.02	0.70 ± 0.03	2	-	6.2	5.5	
21	23231-2	II	78.90	-3.99	1979	50[1)]	0.2	34.0	1.17	0.43 ± 0.16	2	3.06	7.6	3.8	2.5
22	23232-1	II	79.03	-1.62	2642	50[1)]	0.7	34.3	1.27	0.52 ± 0.08	4	3.37	8.5	4.3	1.3
23	23233-1	II	79.41	6.88	1264	50[1)]	2.7	34.7	1.20	0.45 ± 0.09	2	2.37	7.9	3.9	5.2
24	23235-1	I	78.87	1.39	2500	50[1)]	1.6	34.6	0.90	0.46 ± 0.07	7	3.03	5.0	4.0	1.8
25	23259-3	I	72.02	9.3	2518	50[1)]	6.4	35.0	1.01	0.53 ± 0.05	4	2.50	6.1	4.4	5.2
26	23261-2	I	72.18	13.11	2224	50[1)]	6.4	35.0	0.97	0.55 ± 0.11	4	2.55	5.7	5.1	5.1
27	23508-1	II	73.86	-9.40	3202	50[1)]	0.0	34.5	1.20	0.38 ± 0.20	3	3.35	7.9	4.1	0.4
28	23509-1	II	73.83	-13.50	2576	50[1)]	-0.3	34.3	1.37	0.50 ± 0.08	6	3.41	9.3	4.8	0.4

[1)] Samples 1 to 20 were provided from Meland et al., 2006, samples 21 to 28 were provided from Simstich et al., (2003) and references therein. The calcification depth was set according to these sources.

[2)] Depth corresponding salinity and temperature data taken from World Ocean Data Atlas 2001 (averaged July-September, main planktonic bloom).

[3)] Mg/Ca ratio measurements for samples 1 to 20 was performed in Cambridge, UK. Mg/Ca ratios of samples 21 to 28 were measured in Kiel, Germany.

[4)] δ^{18}O values were taken from Hohnemann, 1996, Horwege, 1987, Meland et al. 2006 and Simstich et al., 2003

[5)] Mg/Ca temperature equation of Mashiotta, 1999 ($Mg/Ca\ [mmol/mol] = 0.549*\exp^{0.099T}$).

[6)] $\delta^{44/40}$Ca temperature equations of Hippler et al. 2004 for Holocene core top samples ($\delta^{44/40}Ca\ [‰] = 0.16\ (\pm 0.09)*SST\ [°C] - 0.18$)

[7)] δ^{18}O paleotemperature equation of Shackleton et al., 1974: $T(°C) = 16.9 - 4.38*(\delta^{18}O_{calcite} - \delta^{18}O_{water}) + 0.1*(\delta^{18}O_{calcite} - \delta^{18}O_{water})^2$

References

Anderson O. R. and Faber W. W. J. (1984) An estimation of calcium carbonate deposition rate in a planktonic foraminifer *Globigerinoides sacculifer* using ^{45}Ca as a tracer: A recommended procedure for improved accuracy: *Journal of Foraminiferal Research* **14**, 303–308.

Bauch D., Darling K. F., Simstich J., Bauch H. A., Erlenkeuser H., and Kroon D. (2003) Palaeoceanographic implications of genetic variation in living North Atlantic *N. pachyderma*. *Nature* **424**, 299–302.

Bard E., Arnold M., Mangerud J., Paterne M., Labeyrie L., Duprat J., Mélières M.-A., Sønstegaard E. and Duplessy J.-C. (1994) The North Atlantic atmosphere-sea surface ^{14}C gradient during the Younger Dryas climatic event. *Earth Planet. Sci. Lett*. **126**, 275–287.

Barker S., Greaves M. and Elderfield H. (2003) A study of cleaning procedures used for foraminiferal Mg/Ca paleothermometry. *Geochem. Geophys. Geosyst* **4**.

Barker S., Cacho I., Benway H. and Tachikawa K. (2005) Planktonic foraminiferal Mg/Ca as a proxy for past oceanic temperatures: a methodological overview and data compilation for the Last Glacial Maximum. *Quarternary Science Reviews* **24**, 821-834.

Bentov S. (1997) Biomineralization processes in foraminifera. M.S. thesis, Hebrew University, Jerusalem.

Bentov S. and Erez J. (2005) Novel observations on biomineralization processes in foraminifera and implications for Mg/Ca ratio in the shell. *Geology* **33**, 841–844.

Bentov S. and Erez J. (2006) Impact of biomineralization processes on the Mg content of foraminiferal shells: A biological perspective. *Geochem. Geophys. Geosyst*. **7**.

Birck J. L. (1986) Precision K-Rb-Sr isotopic analysis: Application to Rb-Sr chronology. *Chem. Geol*. **56**, 73–83.

Conkright M. E., Locarnini R. A., Garcia H. E., O'Brien T. D., Boyer T. P., Stephens C. and Antonov J. I. (2002) World Ocean Atlas 2001: Objective Analyses, Data Statistics, and Figures, CD-ROM Documentation. *National Oceanographic Data Center*, Silver Spring, MD, 17 pp.

Darling K. F., Kucera M., Kroon D. and Wade C. M. (2006) A resolution for the coiling direction paradox in *Neogloboquadrina pachyderma. Paleoceanography* **21**.

de Villiers S., Greaves M. and Elderfield H. (2002) An intensity ratio calibration method for the accurate determination of Mg/Ca and Sr/Ca of marine carbonates by ICP-AES. *Geochem. Geophys. Geosyst.* **3**.

Eggins S., DeDeckker P. and Marshall A. T. (2003) Mg/Ca variation in planktonic foraminifera tests: implications for reconstructing palaeoseawater temperature and habitat migration. *Earth Planet. Sci. Lett.* **212**, 291–306.

Eisenhauer A., Nägler T. F., Stille P., Kramers J., Gussone N., Bock B., Fietzke J., Hippler D. and Schmitt A.-D. (2004) Proposal for an international agreement on Ca notation as a result of the discussions from the workshops on stable isotope measurements in Davos (Goldschmidt 2002) and Nice (EGS-AGU-EUG 2003), *Geostand. Geoanalytical Res*. **28** (1), 149–151.

Elderfield H. and Ganssen G. (2000) Past temperature and $\delta^{18}O$ of surface ocean waters inferred from foraminiferal Mg/Ca ratios. *Nature* **405**, 442–445.

Emiliani C. (1955) Pleistocene temperatures, *J. Geol*. **63**, 538–578.

Erez J. (2003) The source of ions for biomineralization in foraminifera and their implications for paleoceanographic proxies. *Reviews in Mineralogy and Geochemistry* **54**, 115–149.

Fietzke J., Eisenhauer A., Gussone N., Bock B., Liebetrau V., Nägler T. F., Spero H. J., Bijma J and Dullo W.-C. (2004) Direct measurement of $^{44}Ca/^{40}Ca$ ratios by MC-ICP-MS using the cool plasma technique. *Chem. Geol.* **206** (1–2), 11–20.

Gussone N., Eisenhauer A., Heuser A., Dietzel M., Bock B., Böhm F., Spero H. J., Lea D. W., Bijma J. and Nägler T. F. (2003) Model for kinetic effects on calcium isotope fractionation ($\delta^{44}Ca$) in inorganic aragonite and cultured planktonic foraminifera. *Geochimica et Cosmochimica Acta* **67**, 1375–1382.

Gussone N., Eisenhauer A., Tiedemann R., Haug G. H., Heuser A., Bock B., Nägler T. F. and Müller A. (2004) Reconstruction of Caribbean sea surface temperature and salinity fluctuations in response to the Pliocene closure of the Central American Gateway and radiative forcing, using $\delta^{44/40}Ca$, $\delta^{18}O$ and Mg/Ca ratios. *Earth Planet. Sci. Lett*. **227**, 201–214.

Gussone N., Böhm F., Eisenhauer A., Dietzel M., Heuser A., Teichert B. M. A., Reitner J., Wörheide G. and Dullo W.-C. (2005) Calcium isotope fractionation in calcite and aragonite. *Geochimica et Cosmochimica Acta* **69**, 4485–4494.

Hemleben C., Anderson O. R., Berthold W. and Spindler M. (1986) Calcification and chamber formation in foraminifera - A brief overview. In Leadbeater B.S.C. and Riding R. (Eds.), *Biomineralization in lower plants and animals*, 237–249.

Heuser A., Eisenhauer A., Gussone N., Bock B., Hansen B. T. and Nägler T. F. (2002) Measurement of calcium isotopes ($\delta^{44}Ca$) using a multicollector TIMS technique. *Int. J. Mass Spectrom.* **220**, 387–399.

Hippler D., Schmitt A.-D., Gussone N., Heuser A., Stille P., Eisenhauer A. and Nägler T. F. (2003) Calcium isotopic composition of various reference materials and seawater. *Geostand. Newsl.* **27** (1), 13–19.

Hippler D., Darling K. F., Eisenhauer A. and Nägler T. F. (2004) Ca isotopes in high-latitude marine settings: Testing the limits of reliable SST estimates based on *N. pachyderma* (sin.). Abstract Swiss GeoScience Meeting 2004.

Hippler D., Eisenhauer A., and Nägler T. F. (2005) Tropical Atlantic SST history inferred from Ca isotope thermometry over the last 140ka. *Geochimica et Cosmochimica Acta* **70**, 90–100.

Hohnemann C. (1996) Zur Paläoozeanographie der südlichen Dänemarkstraße. Diploma Thesis, Geologisch-Paläontologisches Institut, Christian-Albrechts-Universität, Kiel.

Horwege S. (1987) Oberflächentemperaturen (und -strömungen) der Norwegisch- Grönländischen See im Abbild stabiler Kohlenstoff und Sauerstoffisotope rezenter planktischer Foraminiferen. Diploma Thesis, Geologisch-Paläontologisches Institut, Christian-Albrechts Universität, Kiel.

Imbrie J. and Kipp N. (1971) The Agulhas Current during the Late Pleistocene: Analysis of modern faunal analogs. *Science* **207**, 64–66.

Koç N., Jansen E. and Haflidason H. (1993) Paleoceanographic reconstructions of surface ocean conditions in the Greenland, Iceland, Norwegian Seas through the last 14 ka based on diatoms. *Quat. Sci. Rev*. **12**, 115–140.

Lea D. W. (2003) Elemental and Isotopic Proxies of Past Ocean Temperatures. In: *Treatise on Geochemistry* **6**, 365–390.

Lemarchand D., Wasserburg G. J. and Papanastassiou D. A. (2004) Rate controlled calcium isotope fractionation in synthetic calcite. *Geochimica et Cosmochimica Acta* **68**, 4665–4678.

Mashiotta T. A., Lea D. W. and Spero H. J. (1999) Glacial-interglacial changes in Subantarctic sea surface temperature and δ^{18}O-water using foraminiferal Mg. *Earth Planet. Sci. Lett.* **170**, 417–432.

McKenna, V. S. and Prell W. L. (2004) Calibration of the Mg/Ca of *Globorotalia truncatulinoides* (R) for the reconstruction of marine temperature gradients. *Paleoceanography* **19.**

Meland M. Y., Jansen E. and Elderfield H. (2004) Constraints on SST estimates for the northern North Atlantic/Nordic Seas during the LGM. *Quaternary Science Review* **24**, 835–852**.**

Meland M. Y., Jansen E., Elderfield H., Dokken T. M., Olsen A. and Bellerby R. G. J. (2006) Mg/Ca ratios in the planktonic foraminifer *Neogloboquadrina pachyderma* (sinistral) in the northern North Atlantic/Nordic Seas. *Geochem. Geophys. Geosyst*. **7.**

Nägler T. F., Eisenhauer A., Müller A.,. Hemleben C. and Kramers J. (2000) The δ^{44}Ca–temperature calibration on fossil and cultured *Globigerinoides sacculifer*: new tool for reconstruction of past sea surface temperatures. *Geochem. Geophys. Geosyst*. **1**.

Nürnberg D. (1995) Magnesium in tests of *Neogloboquadrina pachyderma* (sinistral) from high northern and southern latitudes. *Journal of Foraminiferal Research* **25**, 350–368.

Nürnberg D., Bijma J. and Hemleben C., (1996) Assessing the reliability of magnesium in foraminiferal calcite as a proxy for water mass temperatures. *Geochimica et Cosmochimica Acta* **60**, 803–814.

Nürnberg D., Müller A. and Schneider R. R. (2000) Paleo-sea surface temperature calculations in the equatorial east Atlantic from Mg/Ca ratios in planktic foraminifera: a comparison to sea surface temperature estimates from $U^{K'}_{37}$, oxygen isotopes, and foraminiferal transfer function. *Paleoceanography* **15**, 124–134.

Oomori T., Kaneshima H., Maezato Y. and Kitano Y. (1987) Distribution coefficient of Mg^{2+} ions between calcite and solution at 10–50°C. *Mar. Chem*. **20**, 327–336.

Rosenthal Y., Boyle E. A. and Slowey N. (1997) Temperature control on the incorporation of magnesium, strontium, flourine, and cadmium into benthic foraminiferal shells from Little Bahama Bank: prospects for thermocline paleoceanography. *Geochimica et Cosmochimica Acta* **61**, 3633–3644.

Sadekov A. Y., Eggins S. M. and Deckker P. D. (2005) Characterization of Mg/Ca distributions in planktonic foraminifera species by electron microprobe mapping. *Geochem. Geophys. Geosyst*. **6**.

Sarnthein M., Stattegger K. and 17 others (2001) Fundamental modes and abrupt changes in North Atlantic circulation and climate over the last 60 ky - Concepts, reconstruction, and numerical modelling. In: Schäfer P., Ritzrau W., Schlüter M., Thiede J. (Eds.) *The northern North Atlantic: A changing environment*, Springer, Berlin, 365–410.

Shackleton N. J. (1974) Attainment of isotopic equilibrium between ocean water and the benthonic foraminifera genus *Uvigerina*: Isotopic changes in the ocean during the last glacial. *Coll. Int. C.N.R.S*. **219**, 203–209.

Simstich J., Sarnthein M. and Erlenkeuser H. (2003) Paired $\delta^{18}O$ signals of *Neogloboquadrina pachyderma* (s) and *Turborotalita quinqueloba* show thermal stratification structure in Nordic Seas. *Mar. Micropaleontol*. **48**, 107–125.

Weinelt M., Kuhnt W., Sarnthein M., Altenbach A., Costello O., Erlenkeuser H., Matthiessen J., Pflaumann U., Simstich J., Struck U., Thies A., Trauth M. and Vogelsang E. (2001) Paleoceanographic proxies in the Northern North Atlantic. In: Schäfer P., Ritzrau W., Schlüter M., Thiede J. (Eds.) *The northern North Atlantic: A changing environment*. Springer, Berlin, 319–352.

Zhu P. and Macdougall J. D. (1998) Calcium isotopes in the marine environment and the oceanic calcium cycle. *Geochimica et Cosmochimica Acta* **62**, 1691–1698.

4. Reassessing cold-end Mg/Ca temperature calibrations of *N. pachyderma* (sin.) using paired $\delta^{44/40}$Ca and Mg/Ca measurements

by

Kozdon, R.[1,2)]; Eisenhauer, A.[1*)]; Weinelt, M.[2)]; Nürnberg, D.[1)]

[1)]Leibniz-Institut für Meereswissenschaften (IFM-GEOMAR), 24148 Kiel, Germany

[2)]Institut für Geowissenschaften an der Christian-Albrechts-Universität zu Kiel, 24118 Kiel, Germany

* Corresponding Author: A. Eisenhauer, Tel.: +49-431-600-2282; e-mail: aeisenhauer@ifm-geomar.de

Abstract

Previous Mg/Ca temperature calibrations of the polar to subpolar planktonic foraminifera *N. pachyderma* (sin.) were refined using a multi-proxy approach combining $\delta^{44/40}$Ca, Mg/Ca and δ^{18}O ratios from Nordic Seas sediment surface samples. Mg/Ca reference temperatures are defined by parallel $\delta^{44/40}$Ca measurements. Despite thermodynamic consideration requiring an exponential temperature dependence of the Mg-uptake into foraminiferal calcite, our data can be best described by a linear Mg/Ca temperature equation for the narrow temperature range of 3.5–7°C (Mg/Ca mmol/mol] = 0.12 * T [°C] + 0.42) which produces slightly lower temperatures than previous calibrations. This narrow temperature range independently confirmed by Mg/Ca and $\delta^{44/40}$Ca temperature estimates reflects hydrographic conditions bound to the isopycnal layer defined by water densities (σ_t) between of 27.7 to 27.8 in the Norwegian Sea. As a result of the density-driven habitat migration of *N. pachyderma* (sin.) in the Norwegian Sea, the total amplitude of SST variations recorded in the Mg/Ca and $\delta^{44/40}$Ca signal is reduced to only about 4°, giving fairly constant values for the temperature difference between Late Holocene and LGM. In the colder waters of the Arctic Domain and the East Greenland Current, the proxy to temperature relation disappears, resulting in significant temperature overestimates. Foraminiferal Mg/Ca ratios

from these region measured with the ICP-AES/OES techniques commonly applied today deviate by more than 0.2 mmol/mol from the existing electron microprobe data set.

4.1. Introduction

Although Mg/Ca has proven to be a robust tool for the reconstruction of SSTs in low latitudes, the application in subpolar to polar regions is critical due to the low temperature sensitivity of the exponential Mg/Ca temperature equation. To date, several multi- and single species Mg/Ca as well as multi-proxy reconstructions are published from transitional to tropical foraminiferal provinces, but data from higher latitudes remain sparse. Moreover, all planktonic foraminiferal Mg/Ca calibrations comprising data from water temperatures below about 7°C (e.g. Mashiotta et al., 1999, Elderfield and Ganssen, 2000) are based on the Mg/Ca electron microprobe dataset of Nürnberg (1995). Aside from some recent studies using laser ablation ICP-MS or electron microprobe technique (e.g, Eggins et al., 2004; McKenna and Prell, 2004; Sadekov et al.; 2005), Mg/Ca ratios for palaeoceanographic applications are routinely determined by ICP-OES/AES instruments today. Hence, the Mg/Ca temperature equations commonly applied in high latitude oceans today are based on data determined by different analytical approaches which results are not necessarily in agreement to each other. Moreover, the *N. pachyderma* (sin.) calibration of Nürnberg (1995) is based on reference temperatures from hydrographic data as independent temperature measurements were not available for these sample locations at this time. Therefore, the overall precision of this calibration is restricted as sediment surface samples integrate the hydrographic conditions at core location over decades or even centuries whereas reliable reference data for temperature or salinity represent a distinct "snapshot". Although ocean temperatures and the positions of the oceanic fronts in the Nordic Seas are assumed to be subject to minor changes only, recent work (e.g. Meland et al., 2006, Nyland et al., 2006) have demonstrated that the correlation between modern Mg/Ca inferred temperatures and their corresponding hydrographic data is poor. This implies that the Mg/Ca calibration data of Nürnberg (1995) might be attributed to incorrect calcification temperatures. In order to avoid these calibration problems, Elderfield and Ganssen (2000) calibrated Mg/Ca ratios against "true" $\delta^{18}O_c - \delta^{18}O_w$ (c = calcite, w = water) calculated calcification temperatures. However, in the cold temperature range from 0°C to 6°C the data set of Nürnberg (1995) was reused again without any correction for true calcification temperatures, mainly because the uncertainty of $\delta^{18}O$ inferred temperatures in high latitude oceans is probably

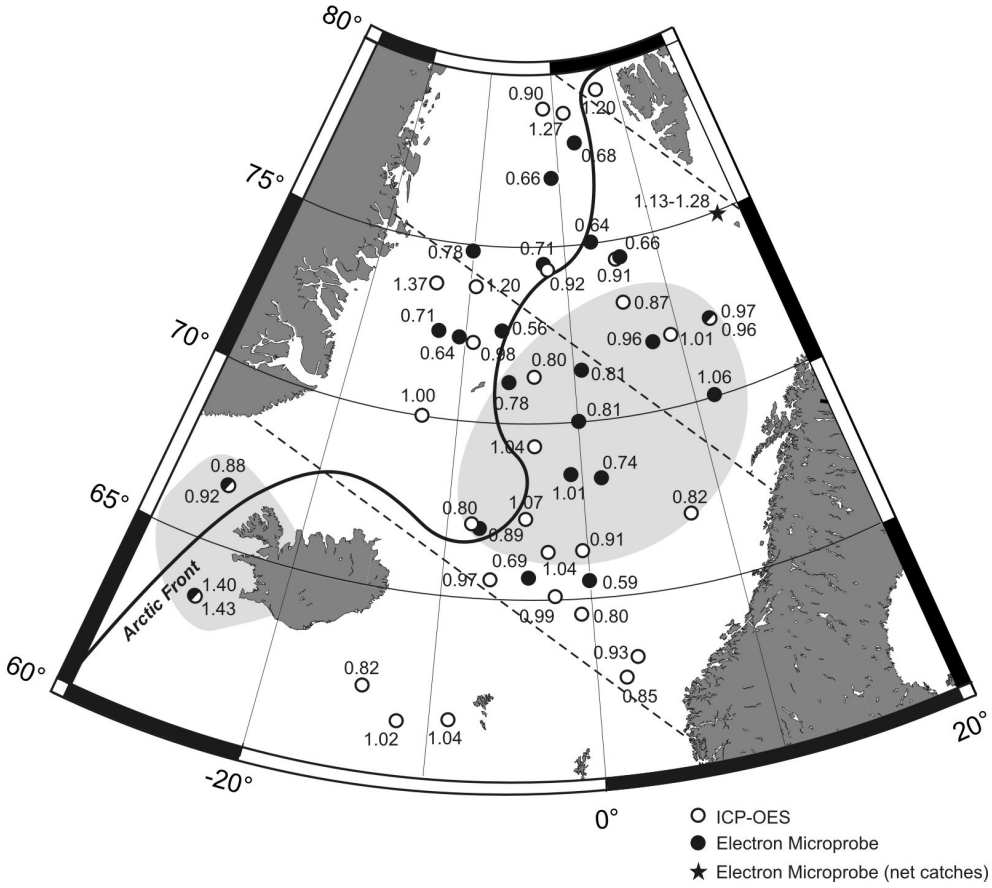

Fig. 12. Station chart of sediment surface samples with their corresponding Mg/Ca ratios (mmol/mol).The dashed lines mark the transect discussed in Fig. 17. Electron microprobe data from Nürnberg (1995) are marked black, white dots show ICP-OES data from this work and Meland et al. (2006). The grey shaded area indicates that ICP-OES and electron microprobe-derived Mg/Ca data deviate less than 0.2 mmol/mol between adjacent core tops.

even higher. However, after publication of this first systematic planktonic Mg/Ca temperature calibration study in 1995, various authors focused on the depth distribution and habitat migration of *N. pachyderma* (sin.) in the Nordic Seas (e.g. Kohfeld et al., 1996, Stangeew, 2001, Simstich et al., 2003). They found that the average depth of chamber formation and encrustation of *N. pachyderma* (sin.) is highly variable, reflecting water depths of up to 250 m off Norway but only about 50 m in the Arctic Domain challenging previous reference temperatures assuming constant calcification depths. Hence, the aim of this study is the reassessment of the Mg/Ca temperature equation for *N. pachyderma* (sin.) from Nordic Seas core top samples in combining previous electron microprobe data with new ICP-AES/OES Mg/Ca measurements. In order to constrain the calcification habitat, independent calcification temperatures are calculated by parallel measurements of $\delta^{44/40}$Ca ratios in

N. pachyderma (sin.) which are found to have a temperature sensitivity of 0.15 ‰/°C in net catches and 0.16 ‰/°C in core top samples (Hippler et al., 2004, Fig. 2, this work).

4.2. Material and Methods

Both Ca isotopes and Mg/Ca ratios were determined on the polar to subpolar planktonic foraminifer *N. pachyderma* (sin.) from sediment surface samples which have previously been used by Meland et al. (2006) for parallel Mg/Ca and $\delta^{18}O$ measurements and by Hohnemann (1996), Horwege (1987) and Simstich et al. (2003) for the determination of $\delta^{18}O$ ratios. A station chart of Nordic Seas sediment surface samples is presented in Fig. 12. AMS ^{14}C ages of 35 adjacent core tops are given in Simstich et al., 2003. Except for three ages, all others are significant younger than about 3000 years and therefore represent modern conditions. The sample preparation, Mg/Ca and $\delta^{44/40}Ca$ measurements were performed as described in chapter 3.2.2

For electron microprobe analyses, five to ten foraminiferal tests for each core top or multinet station were picked and cleaned ultrasonically, then imbedded in epoxy resin, ground and polished. Elemental analyses was carried out on a JOEL JXA8900 Superprobe electron microprobe at the Institut für Geowissenschaften, University Kiel, Germany. CaO, SiO_2, Al_2O_3, FeO, MnO, MgO, SrO and CO_2 were measured using a beam diameter of 5 µm and an accelerating voltage of 15 kV. Forsterite, Wollastonite (Micro-Analysis Consultants Limited, UK) and Fayalite (Smithsonian Institution, Washington) were chosen as analytical standards. As the thickness of the septa in tests of *N. pachyderma* (sin.) was less than 5 µm in most samples, electron microprobe measurements were performed on the outer wall and secondary crust only. To minimize the effect of intratest variations of metal:calcium ratios, foraminiferal Mg/Ca ratios were averaged from at least 17 single measurements from individual tests.

4.3. Results

4.3.1. High latitude Mg/Ca – $\delta^{44/40}Ca$ – $\delta^{18}O$ relation

Existing planktonic Mg/Ca data from Nürnberg (1995) determined by electron microprobe match the ‘new’ ICP-AES/OES data only in the central Norwegian Sea and southwest of Iceland with an offset of less than 0.2 mmol/mol (Fig 12, Table 5). However, in Arctic Domain and polar waters

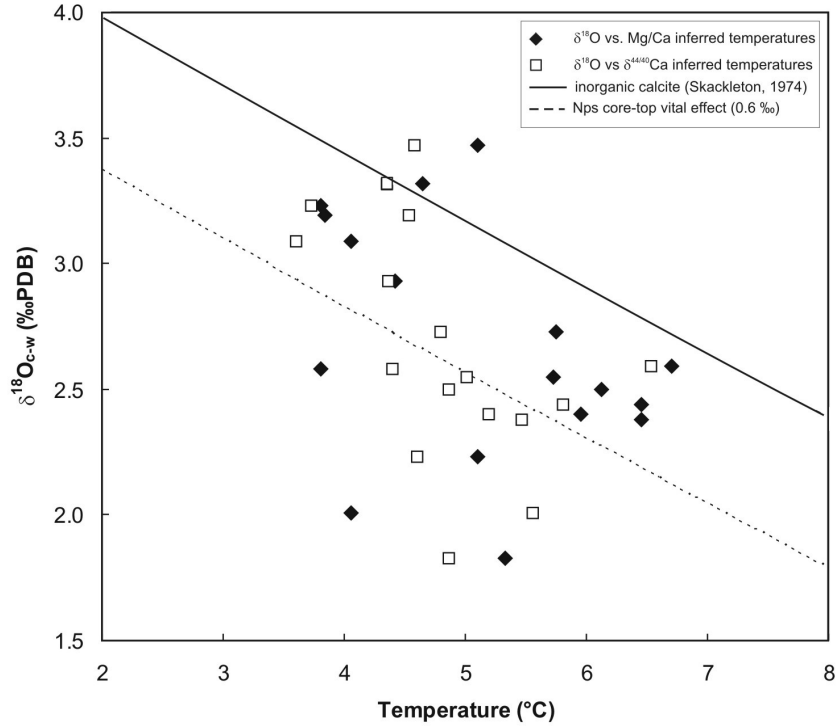

Fig. 13. Relationship between measured $\delta^{18}O_c$ versus Mg/Ca and $\delta^{44/40}$Ca-inferred temperatures of *N. pachyderma* (sin.) from Norwegian Sea core tops compared to the temperature- $\delta^{18}O_c$ equation of Shackleton, 1974: $T(°C) = 16.9 - 4.38*(\delta^{18}O_c - \delta^{18}O_w) + 0.1*(\delta^{18}O_c - \delta^{18}O_w)^2$. The dotted line is corrected for the δ^{18}O-vital effect of 0.6 ‰ found in Nordic Seas sediment surface samples (Simstich et al., 2003). A $\delta^{18}O_w$ of 0.24 ‰ [PDB] (averaged from modern data, see appendix) was assumed for the Norwegian Sea.

characterized by summer temperatures below about 3°C, ion microprobe derived Mg/Ca ratios are significantly lower than data obtained by the ICP-AES/OES technique but still higher than predicted by the Mg/Ca temperature calibrations of Mashiotta et al. (1999) and Elderfield and Ganssen (2000). This was already shown by Nürnberg (1995) who interpreted the high Mg-content in the Arctic Domain by effects related to the annual sea ice cover. A model demonstrating that the aberrant $\delta^{44/40}$Ca and Mg/Ca ratios in *N. pachyderma* (sin.) from cold, low saline waters can be interpreted by a two-step chemical modification of vacuolized seawater during its cytosolar transport to the calcification site is postulated in the second chapter of this work. For the purpose of a refined Mg/Ca temperature calibration, we focus on samples from the Norwegian Sea which show reasonable temperature to proxy responses.

In contrast to previous low latitude Mg/Ca temperature calibrations based on δ^{18}O calcification temperatures, the correlation between Mg/Ca and $\delta^{44/40}$Ca data with δ^{18}O ratios in the Norwegian Sea is poor (Fig. 14) and cannot be explained by salinity changes only. The relationship between

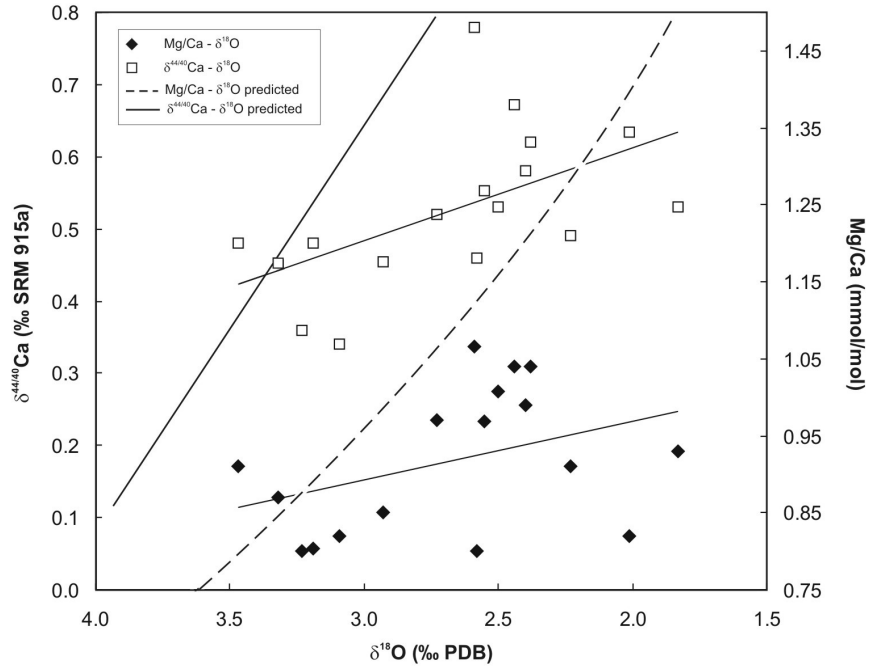

Fig. 14. Comparison of measured and predicted Mg/Ca and $\delta^{44/40}$Ca ratios of *N. pachyderma* (sin.) versus δ^{18}O. The predicted Mg/Ca – δ^{18}O relation was calculated using the palaeoequation of Shackleton et al., 1974 and the Mg/Ca calibration of Mashiotta et al., 1999 (see. Tab. 5). The $\delta^{44/40}$Ca – δ^{18}O relation comprises the Ca-isotope temperature equation of Hippler et al., (2004). A $\delta^{18}O_w$ of 0.24 ‰ [PDB] (averaged from modern data, see appendix) was assumed for the Norwegian Sea.

temperature, predicted and measured δ^{18}O ratios is shown in Fig 13. Assumed that the temperature equations are valid and δ^{18}O ratios reflect the same hydrographic conditions as Mg/Ca and $\delta^{44/40}$Ca data, measured δ^{18}O deviate up to 0.8 ‰ from the value predicted by Mg/Ca or $\delta^{44/40}$Ca temperature estimates. It is notably that summer salinity variation in most parts of the Norwegian Sea are almost negligible. In contrast to δ^{18}O, the correlation between Mg/Ca and $\delta^{44/40}$Ca ratios from Nordic Seas core *top N. pachyderma* (sin.) is excellent (Fig 15):

[6] Mg/Ca [mmol/mol] = 0.72 * $\delta^{44/40}$Ca [‰SRM 915a] + 0.5 (n = 20, R^2 = 0.75)

This consistency demonstrate that Mg/Ca and $\delta^{44/40}$Ca ratios are controlled by the same environmental parameter. As $\delta^{44/40}$Ca is calibrated independently based on net catches with corresponding water temperatures from CTD measurements (Hippler et al., 2004, Fig. 2, chapter 1), $\delta^{44/40}$Ca can be used to calculate true calcification temperatures and hence to recalibrate Mg/Ca ratios obtained by the ICP-AES/OES technique. The $\delta^{44/40}$Ca-temperature relationship on modern core top specimens and net catches of *N. pachyderma* (sin.) can be expressed as follows:

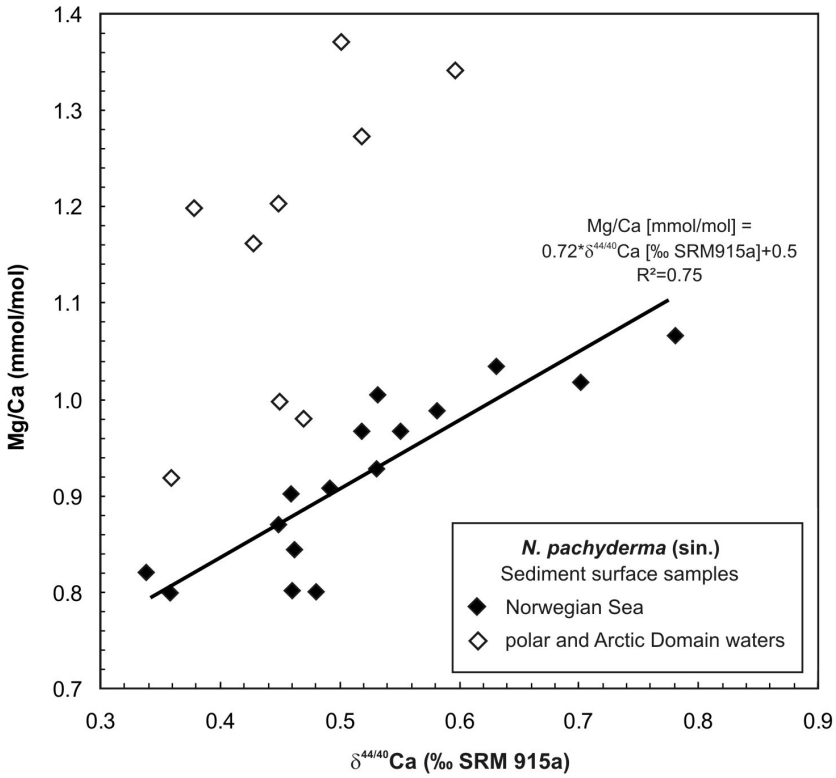

Fig. 15. Mg/Ca versus $\delta^{44/40}$Ca ratios from *N. pachyderma* (sin.) core top samples from the Nordic Seas. In the Norwegian Sea, Mg/Ca and $\delta^{44/40}$Ca ratios are positively correlated whereas both proxies deviate from the predicted trend in cold (< 3.5°C) low saline Arctic Domain and polar waters.

[7] $\delta^{44/40}$Ca [‰] = 0.16 (±0.09) * T [°C] – 0.18 (Hippler et al., 2004, Fig. 2, chapter 1)

4.3.2. Mg/Ca temperature recalibration based on parallel $\delta^{44/40}$Ca measurements

The refined Mg/Ca temperature equation for Norwegian Sea *N. pachyderma* (sin.) based on Ca-isotope temperature estimates is shown in Fig. 16:

[8] Mg/Ca [mmol/mol] = 0.12 * T [°C] + 0.42 (R^2 = 0.75, *n* = 20)

Parallel Mg/Ca and $\delta^{44/40}$Ca measurements reveal that the temperature range recorded in core top *N. pachyderma* (sin.) from the Norwegian Sea is strictly limited to a narrow range of about 3.5°C to 7°C whereas there is no consistent proxy to temperature relationship in the temperature interval below about 3.5°C. (Fig. 16). Hence, like other proxies available for polar waters, Mg/Ca is also affected by the 'cold-end error' (Weinelt et al., 2003). As we were not able to reproduce one single reliable Mg/Ca ratio below about 0.80 mmol/mol, we state that planktonic Mg/Ca temperature calibrations are limited to the temperature range above about 3.5°C. Although thermodynamic

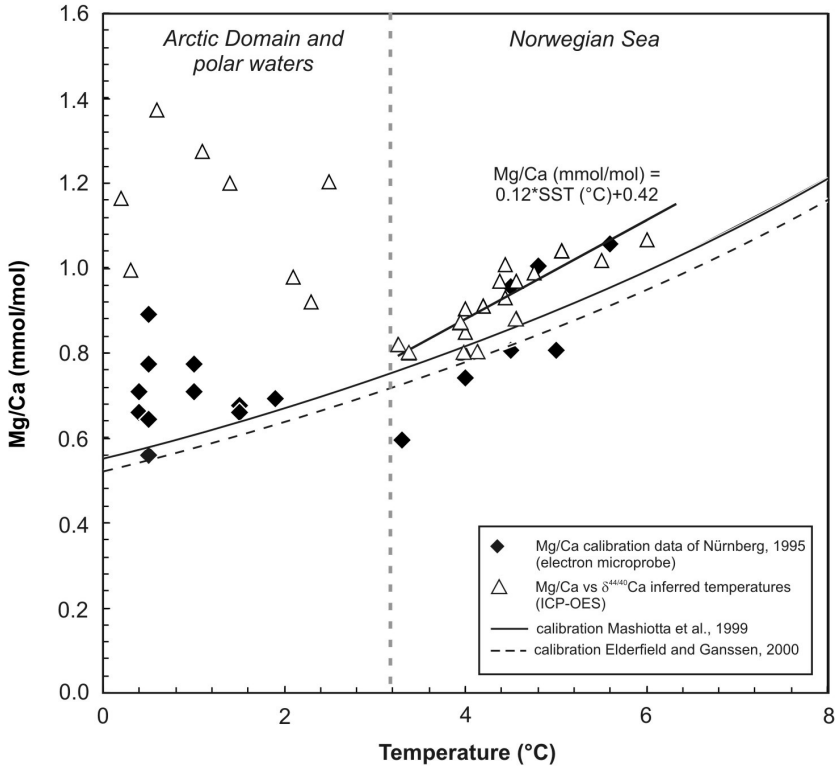

Fig. 16. Mg/Ca versus calcification temperatures for core top *N. pachyderma* (sin.) from the Nordic Seas. ICP-OES-derived Mg/Ca ratios are calibrated against $\delta^{44/40}$Ca temperature estimates for water temperatures higher than about 3.5°C. Due to the lack of reliable temperature proxies for planktic foraminifera from Arctic Domain and polar waters colder than about 3.5°C, these samples were calibrated against empirical temperature data according to Nürnberg, 1995. Note the offset between ICP-OES and electron microprobe derived data in cold waters.

considerations pretend an exponential increase in the Mg-content with temperature with a sensitivity of about 10 %°C^{-1}, we assume that in the narrow temperature range occupied by *N. pachyderma* (sin.) a linear temperature function is appropriate. Compared to previous Mg/Ca calibrations based on the data set of Nürnberg (1995), the refined Mg/Ca calibration comprises two major achievements: (i) calcification temperatures are measured in the same phase of foraminiferal calcite and promise reliable values due to the self-consistent excellent Mg/Ca – $\delta^{44/40}$Ca correlation and (ii) Mg/Ca data used for this calibration are derived from ICP-AES/OES instruments which is the common analytical approach in most laboratories running Mg/Ca measurements in marine carbonates today.

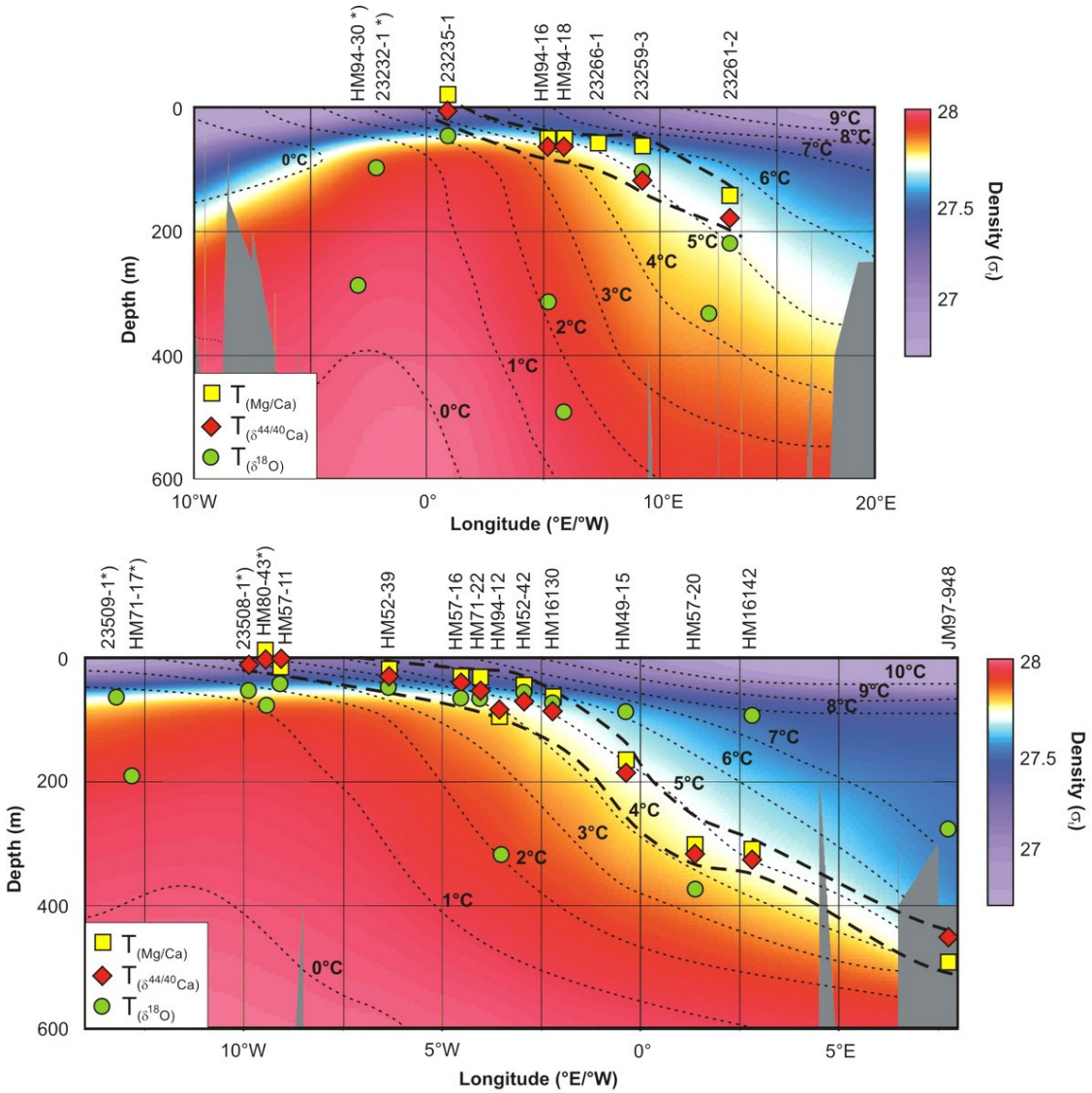

Fig. 17. Mg/Ca, $\delta^{44/40}$Ca and δ^{18}O – inferred temperatures from the transects defined in Fig. 12 projected meridionally to depth intervals with appropriate summer temperatures. a) Transect North, b) Transect South. δ^{18}O- inferred temperatures predict unrealistic average calcification depths, whereas Mg/Ca and $\delta^{44/40}$Ca temperature estimates closely follow the 27.7 isopycne (reduced to sea surface pressure). In Arctic Domain and polar waters, Mg/Ca and $\delta^{44/40}$Ca temperature estimates are higher than maximum summer SST's (core labels marked by asterisks). Isopycnals (reduced to surface pressure) are calculated with ODV (Schlitzer, 2006) based on data from the World Ocean Atlas, 2001 (www.nodc.noaa.gov/OC5/WOA01/pr_woa01.html).

4.3.3. Calcification habitat

It is well known from various studies that production in the Nordic Seas culminates from July to September (Kohfeld et al., 1996, Jensen et al., 1998, Schröder-Ritzrau et al., 2001). Hence, *N. pachyderma* (sin.) from Nordic Seas core top sediments reflect summer temperatures in distinct calcification depths. Based on paired oxygen isotope data of *N. pachyderma* (sin.) and

T. quinqueloba, Simstich et al. (2003) proposed that apparent calcification depths of *N. pachyderma* (sin.) are bound to pycnoclines, indicating water depth of about 20-50 m in the Arctic Domain and up to about 250 m off Norway. As a self-consistent confirmation of our data, Mg/Ca and $\delta^{44/40}$Ca proxy temperature estimates projected to water depth with corresponding summer temperatures show similar calcification depths (Fig. 17). Mg/Ca as well as $\delta^{44/40}$Ca – inferred temperatures reflect hydrographic conditions strongly bound to the isopycnal defined by the density σ_t of 27.7 to 27.8. This indicates that the habitat of *N. pachyderma* (sin.) in the Nordic Seas is either actively or passively controlled by water density. As a result of this habitat migration, the total amplitude of SST variations in the Nordic Seas recorded in the Mg/Ca and $\delta^{44/40}$Ca signal of *N. pachyderma* (sin.) is restricted to only about 4°, giving fairly constant values for the temperature difference between Late Holocene and LGM.

4.3.4. Consistency between ICP-AES/OES and electron microprobe data

As a consequence of the poor reproducibility of the existing electron microprobe dataset of Nürnberg (1995) with the ICP-AES/OES approach, we prepared three core top samples with existing ICP-OES data and thee samples from multinet stations which are not affected by contamination or diagenetic effects for electron microprobe analyses (Table 6). Within analytical error, core top Mg/Ca ratios determined by ICP-OES are indistinguishable from the 'new' electron microprobe measurements performed for this comparison. Hence, we can not explain the extremely low Mg/Ca ratios in the range down to 0.59 mmol/mol found by Nürnberg (1995) at almost identical sample locations. We have no simple explanation for this observation and surmise artefacts of different sample preparation techniques or some issues with the lower sensitivity of the electron microprobe which was an earlier model compared to the instrument we used for our studies. In contrast to core top samples witch match our expectations perfectly, Mg/Ca ratios from net catches determined by electron microbe are significantly higher than predicted by CTD-derived temperatures. Unfortunately, no ICP-AES/OES measurements for comparison are available for these samples due to an insufficient number of foraminiferal tests in net catches. However, Mg/Ca ratios from net catches vary in between 1.13 and 1.28 mmol/mol corresponding to water temperatures of about 7–9°C whereas instrumental derived temperatures from CTD measurements from the day of sampling do not exceed 4°C.

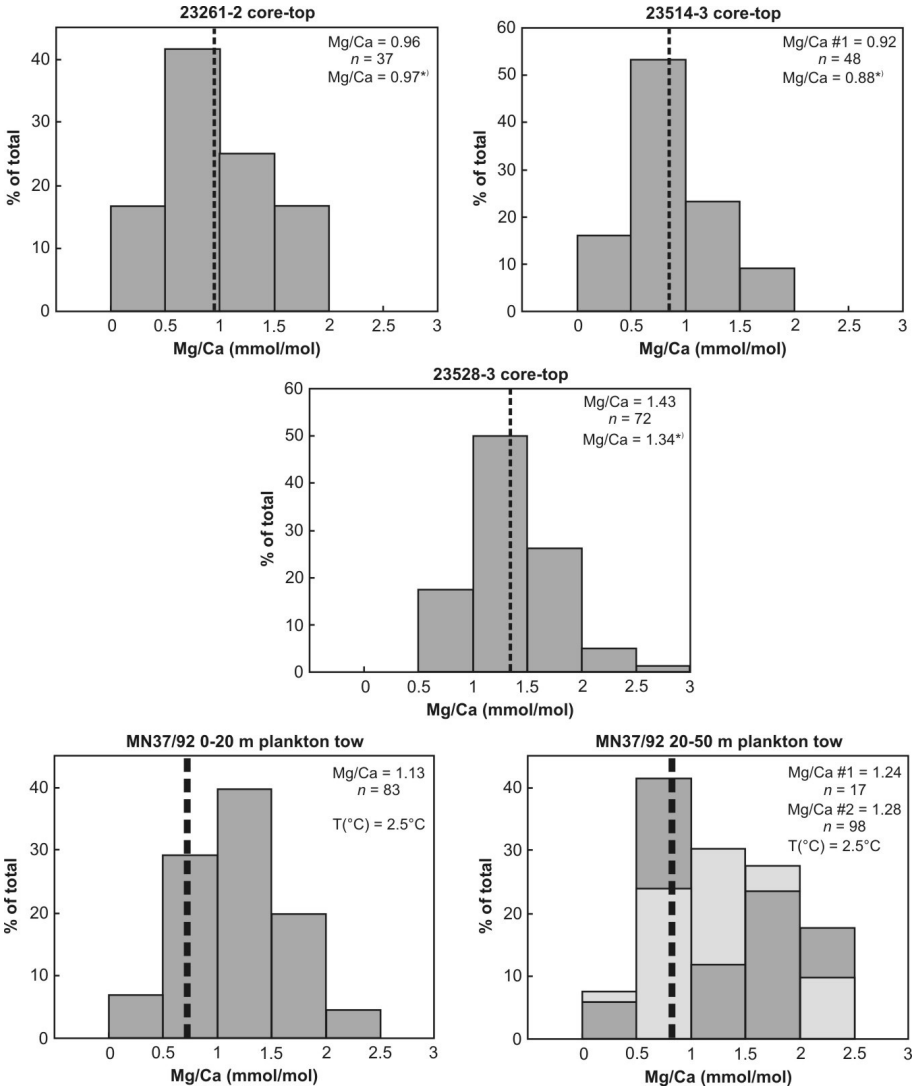

Fig. 18. Histograms of within-test Mg/Ca variations of Nordic Seas *N. pachyderma* (sin.) from sediment surface and net samples determined by electron microprobe. *n* is the total number of data points. Dotted lines show Mg/Ca ratios determined for comparison by ICP-OES from 40-60 homogenised tests. Mg/Ca ratios measured by ICP-OES are given in the plot marked by asterisks. Dotted lines in the histograms of the plankton-tow samples define the predicted Mg/Ca ratios calculated from water temperatures in the depth intervals measured by CTD.

4.4. Discussion

4.4.1. Offset between $\delta^{18}O$, $\delta^{44/40}Ca$ and Mg/Ca ratios

The correlation between $\delta^{18}O$ ratios and both $\delta^{44/40}Ca$ Mg/Ca data is poor, demonstrating that despite the low salinity variations in the Norwegian Sea, $\delta^{18}O$ should not be unambiguously converted to absolute temperature estimates. With respect to our data, it should be carefully

considered if $\delta^{18}O$- derived temperatures alone provide sufficient precision as reference temperatures for proxy- calibrations or the calculation of past hydrographic parameters such as palaeosalinity based on $\delta^{18}O$ and Mg/Ca only. Regarding oxygen isotopes, Nyland et al. (2006) made similar observations based on paired $\delta^{18}O$ and Mg/Ca data from *N. pachyderma* (dex) and *N. pachyderma* (sin.) from high resolution sediment cores from the Norwegian Sea, spanning the last 1200 years. They concluded that this discrepancy between these two proxies is based on variations in the oxygen isotopic composition of seawater during the late Holocene. Moreover, Mg/Ca ratios are normally determined on a significantly larger number of homogenised foraminiferal tests than oxygen isotopes, resulting in an effective filtering of short-term variations or aberrant signals of displaced specimens.

4.4.2. New ICP-OES Mg/Ca calibration versus previous electron microprobe data

Concerning our data, it is critical to use previous Mg/Ca temperature calibrations based on the electron microprobe dataset of Nürnberg (1995) for the conversion of ICP-AES/OES derived foraminiferal Mg/Ca ratios to absolute temperatures. The majority of the electron microbe data is at least 0.2 mmol/mol lower compared to Mg/Ca ratios derived from adjacent core tops with the ICP-AES/OES technique. Lowest Mg/Ca ratios derived by the ICP-AES/OES technique are in the range of about 0.80 mmol/mol whereas the existing electron microprobe data set contains various measurements in the range of 0.59 – 0.80 mol/mol from Nordic Seas core tops. Moreover, the Mg/Ca calibrations of Mashiotta (1999) and Elderfield and Ganssen (2000), which are both comprising the microprobe dataset of Nürnberg (1995) are extended to lowest water temperatures of about 0°, suggesting that Mg/Ca of planktonic foraminifera may be unambiguously applied as SST-proxy at the 'cold end'. This assumption is not straightforward as reliable planktonic Mg/Ca data in the temperature range <7°C are extremely sparse and fairly reproducible. Hence, we state that until a robust data-set for planktonic Mg/Ca cold-end calibrations is compiled, valid Mg/Ca-inferred proxy temperature estimates from high latitude planktonic foraminifera are limited to temperatures above about 3.5°C.

4.4.3. Implications of foraminiferal habitat migration for paleoceanographic reconstructions

The assumption that *N. pachyderma* (sin.) is either actively or passively bound to a narrow isopycnal range enlightens earlier finding of Meland et al., (2005, 2006) who found almost no offset in Mg/Ca ratios between *N. pachyderma* (sin.) from the Last Glacial Maximum (LGM) and samples reflecting the late Holocene. As water density is mainly a function of temperature and salinity, we would expect shallower dwelling depths of *N. pachyderma* (sin.) in glacial than in interglacial times. Hence, *N. pachyderma* (sin.) originating from the Nordic Seas are limiting the total temperature range recorded in their Mg/Ca and $\delta^{44/40}$Ca proxy signal by habitat migration to only about 4°C. It is notable that this assumption is only valid for core top samples comprising dozens of mature foraminiferal tests reflecting completed life cycles. In contrast, foraminiferal net catches represent various stages of ontogenetic development and may therefore deviate from the corresponding signal recorded in adjacent core top samples.

The knowledge of the mechanisms of non-spinose foraminifera to adjust their buoyancy is limited, mainly because their culturing in laboratories is challenging compared to spinose foraminiferal species (von Langen et al., 2005). In general, it is believed that foraminifera produce low-density lipids or gases to counter gravitational settling (Furbish et al., 1997). Many species of planktonic foraminifera need an active buoyancy control because they are confined to the photic zone due to their photosynthetic symbionts. In contrast, *N. pachyderma* (sin.) is known to be asymbiotic (Hemleben et al. 1987) and therefore probably mainly a passive drifter. This implies that the water mass stratification is preconditioning the average calcification depth of non-spinose or asymbiotic foraminifera more likely than that of spinose and symbiotic foraminifera which are supposed to have a more effective system to control their buoyancy. Anand et al. (2003) already found some indications that non-spinose foraminiferal species from the Sargasso Sea show a lower temperature sensitivity in their Mg/Ca signal than the spinose group. This effect may get amplified in high latitude oceans as a result of the stronger water mass stratification in these regions.

4.5. Conclusion

Based on parallel $\delta^{44/40}$Ca to Mg/Ca measurements, we found that *N. pachyderma* (sin.) in the Norwegian Sea is bound to a narrow isopycnal band reflecting water temperatures in the range of

about 3.5 to 7°C. As a result, the total temperature range is only party reflected in the Mg/Ca and $\delta^{44/40}$Ca proxy signal of core top *N. pachyderma* (sin.) from these water masses. At temperatures below about 3.5°C, the proxy to temperature relationship is not consistent anymore, implying that common Mg/Ca temperature calibrations are insufficient at the 'cold-end'. Mg/Ca ratios determined by both ICP-AES/OES instruments and electron microprobe are indistinguishable within errors but almost at least 0.2 mmol/mol higher than earlier electron microprobe measurements. Therefore, we suggest a new Mg/Ca temperature calibration for high latitude *N. pachyderma* (sin.) (Mg/Ca [mmol/mol] = 0.12 * T [°C] + 0.42) to take the higher Mg/Ca ratios measured by ICP-AES/OES instruments into account.

Acknowledgement

This study was supported by the German Science foundation within the Research Theme FOR 451 and the CASIOPEIA project (Ei272/20-1, DFG). We thank Peter Appel and Barbara Mader for technical assistance with sample preparation and the use of the electron microprobe. Mara Weinelt, Florian Böhm, Dirk Nürnberg and Ana Kolevica are acknowledged for their general support, interest and fruitful discussions concerning this project.

References

Anand, P., Elderfield, H., Conte, M.H., 2003. Calibration of Mg/Ca thermometry in planktonic foraminifera from a sediment trap time series. Paleoceanography 18.

Barker, S., Greaves, M., Elderfield, H., 2003. A study of cleaning procedures used for foraminiferal Mg/Ca paleothermometry. Geochem. Geophys. Geosyst 4.

de Villiers, S., Greaves, M., Elderfield, H., 2002. An intensity ratio calibration method for the accurate determination of Mg/Ca and Sr/Ca of marine carbonates by ICP-AES. Geochem. Geophys. Geosyst. 3.

Eggins, S., DeDeckker, P., Marshall, A.T. 2003. Mg/Ca variation in planktonic foraminiferal tests: implications for reconstructing palaeo-seawater temperature and habitat migration. Earth and Planetary Science Letters 212, 291–306.

Elderfield, H., Ganssen, G., 2000. Past temperature and delta-^{18}O of surface ocean waters inferred from foraminiferal Mg/Ca ratios. Nature 405, 442–445.

Furbish, D.J., Arnold, A.J., 1997: Hydrodynamic strategies in the morphological evolution of spinose planktonic foraminifera. GSA Bulletin 109, 1055–1072.

Hemleben, C., Anderson, O.R., Berthold, W., and Spindler, M., 1986, Calcification and chamber formation in Foraminifera - A brief overview. In Leadbeater, B.S.C., and Riding, R., eds., Biomineralization in lower plants and animals, 237–249.

Hohnemann, C., 1996. Zur Paläoozeanographie der südlichen Dänemarkstraße. Diploma Thesis, Geologisch-Paläontoloisches Institut, Christian-Albrechts-Universität, Kiel.

Horwege, S., 1987. Oberflächentemperaturen (und -strömungen) der Norwegisch- Grönländischen See im Abbild stabiler Kohlenstoff und Sauerstoffsotope rezenter planktischer Foraminiferen. Diploma Thesis, Geologisch-Paläontoloisches Institut, Christian-Albrechts Universität, Kiel.

Jensen, S., 1998. Planktische Foraminiferen im Europäischen Nordmeer: Verbreitung und Vertikalfluß sowie ihre Entwicklung während der letzten 15 000 Jahre. Berichte aus dem Sonderforschungsbereich 313, 75, Christian-Albrechts-Universität, Kiel.

Lea, D.W., Mashiotta, T.A., Spero, H.J., 1999. Controls on magnesium and strontium uptake in planktonic foraminifera determined by live culturing. Geochimica et Cosmochimica Acta 63, 2369–2379.

Mashiotta, T.A., Lea, D.W., Spero, H.J., 1999. Glacial-interglacial changes in Subantarctic sea surface temperature and δ^{18}O-water using foraminiferal Mg. Earth and Planetary Science Letters 170, 417–432.

Meland, M., Jansen, E., Elderfield, H., 2005. Constraints on SST estimates for the northern North Atlantic/Nordic Seas during the LGM. Quaternary Science Review, 24.

Meland, M. Y., Jansen, E., Elderfield, H., Dokken, T.M., Olsen, A., Bellerby R.G.J., 2006. Mg/Ca ratios in the planktonic foraminifer *Neogloboquadrina pachyderma* (sinistral) in the northern North Atlantic/Nordic Seas. Geochem. Geophys. Geosyst., 7.

McKenna, V.S., Prell, W.L., 2004. Calibration of the Mg/Ca of *Globorotalia truncatulinoides* (R) for the reconstruction of marine temperature gradients. Paleoceanography 19.

Kohfeld, K.E., Fairbanks, R.G., Smith, S.L., Walsh, I.D., 1996. *Neogloboquadrina pachyderma* (sinistral coiling) as paleoceanographic tracers in polar oceans: Evidence from Northeast Water Polynya plankton tows, sediment traps, and surface sediments. Paleoceanography 11, 679–699.

Nürnberg, D., 1995. Magnesium in tests of Neogloboquadrina pachyderma (sinistral) from high northern and southern latitudes. Journal of Foraminiferal Research 25, 350–368.

Nürnberg, D., Bijma, J., Hemleben, C., 1996. Assessing the reliability of magnesium in foraminiferal calcite as a proxy for water mass temperatures. Geochimica et Cosmochimica Acta 60, 803–814.

Nyland, B., Jansen, E., Elderfield, H., Andersson, C., 2006. Neogloboquadrina pachyderma (dex. and sin.) Mg/Ca and $\delta^{18}O$ records from the Norwegian Sea. Geochem. Geophys. Geosyst., 7.

Sadekov, A.Y., Eggins, S.M., DeDecker, P., 2005. Characterization of Mg/Ca distributions in planktonic foraminifera species by electron microprobe mapping. Geochem. Geophys. Geosyst., 6.

Schlitzer, R., Ocean Data View, http://odv.awi.de, 2006.

Schröder-Ritzrau, A., Andruleit, H., Jensen, S., Samtleben, C., Schäfer, P., Matthiessen, J., Hass, H.C., Kohly, A., Thiede, J., 2001. Distribution, export and alteration of fossilizable plankton in the Nordic Seas. In: Schäfer, P., Ritzrau, W., Schlüter, M., Thiede, J. (Eds.), The Northern North Atlantic. Springer, Berlin, pp. 81–104.

Simstich, J., Sarnthein, M., Erlenkeuser, H. 2003. Paired $\delta^{18}O$ signals of *Neogloboquadrina pachyderma* (s) and *Turborotalita quinqueloba* show thermal stratification structure in Nordic Seas. Mar. Micropaleontol. 48, 107–125.

Stangeew, E., 2001. Distribution and isotopic composition of living planktonic foraminifera *N. pachyderma* (sinsitral) and *T. quinqueloba* in the high latitude North Atlantic. PhD Thesis, Mathematisch-Naturwiss. Fakultät, Christian-Albrechts-Universiät, Kiel. http://e-diss.uni-kiel.de/diss_464/pp.

Von Langen, P.J., Pak, D.K., Spero, H.J., Lea, D.W., 2005. Effects of temperature on Mg/Ca in neogloboquadrinid shells determined by live culturing. Geochem. Geophys. Geosyst., 6.

Weinelt, M., Kuhnt, W., Sarnthein, M., Altenbach, A., Costello, O., Erlenkeuser, H., Matthiessen, J., Pflaumann, U., Simstich, J., Struck, U., Thies, A., Trauth, M., Vogelsang, E., 2001. Paleoceanographic proxies in the Northern North Atlantic. In: Schäfer, P., Ritzrau, W., Schlüter, M., Thiede, J. (Eds.), The Northern North Atlantic. Springer, Berlin, 319-352.

Appendix

Table 5: Core locations, $\delta^{44/40}$Ca, Mg/Ca and δ^{18}O records of *N. pachyderma* (sin.) and proxy temperature estimates

No	Core[1]	Latitude °N	Longitude °W/°E	Mg/Ca [mmol/mol][2]	$\delta^{44/40}$Ca [‰ SRM 915a]	$\delta^{18}O_{Nps}$ [‰ PDB][3]	$\delta^{18}O_{water}$ [‰ PDB][4]	$\delta^{18}O_{Nps}$ [‰ PDB][5]	$T_{\delta 18O}$[5]	$T_{Mg/Ca}$[6]	$T_{\delta 44/40Ca}$[7]
1	HM16130	65.10	-2.42	0.99	0.58 ± 0.11	2.40	0.27	2.40	5.7	6.0	5.2
2	HM16132	64.57	-0.72	0.80	0.46 ± 0.18	2.58	0.27	2.58	5.0	3.8	4.4
3	HM16142	63.25	2.60	0.93	0.53 ± 0.07	1.83	0.30	1.83	8.0	5.3	4
4	HM49-15	66.34	-0.36	0.91	0.49 ± 0.18	2.23	0.27	2.23	6.3	5.1	4.8
5	HM52-18	62.27	-14.14	0.82	0.34 ± 0.08	3.09	0.30	3.09	3.2	4.1	3.6
6	HM52-39	65.57	-6.79	0.97	0.52 ± 0.06	2.73	0.23	2.73	4.3	5.7	4.8
7	HM52-42	66.34	-2.80	1.04	0.62 ± 0.08	2.38	0.23	2.38	5.8	6.5	5.5
8	HM57-11	67.12	-8.30	0.80	0.48 ± 0.06	3.19	0.18	3.19	2.4	3.8	4.5
9	HM57-16	67.28	-4.37	1.07	0.78 ± 0.09	2.59	0.23	2.59	4.8	6.7	6.5
10	HM57-20	62.65	1.67	0.85	0.46 ± 0.05	2.92	0.30	2.92	3.8	4.4	4.4
11	HM71-17	70.00	-13.02	1.00	0.45 ± 0.11	3.40	0.18	3.40	1.5	6.0	4.3
12	HM71-22	69.34	-3.61	1.04	0.67 ± 0.14	2.44	0.23	2.44	5.4	6.5	5.5
13	HM80-43	72.25	-9.19	0.98	0.47 ± 0.08	3.50	-0.09	3.50	0.3	5.9	4.5
14	HM94-12	71.32	-3.55	0.80	0.36 ± 0.09	3.23	0.18	3.23	2.2	3.8	3.7
15	HM94-16	73.23	5.37	0.87	0.45 ± 0.06	3.32	0.23	3.32	2.1	4.7	4.3
16	HM94-18	74.50	5.70	0.91	0.48 ± 0.20	3.47	0.23	3.47	1.6	5.1	4.6
17	HM94-30	74.38	-2.00	0.92	0.36 ± 0.03	3.67	0.05	3.67	0.2	5.2	3.7
18	JM97-948	66.97	7.64	0.82	0.63 ± 0.05	2.01	0.27	2.01	7.2	4.1	5.5
19	HM133-21	61.62	-8.86	1.04	0.63 ± 0.09	-	0.30	-		6.5	5.5
20	HM133-24	61.42	-11.87	1.02	0.70 ± 0.03	-	0.30	-		6.2	6.0
21	23231-2	78.90	-3.99	1.17	0.43 ± 0.16	3.06	-0.13	3.06	1.7	7.6	4.2
22	23232-1	79.03	-1.62	1.27	0.52 ± 0.08	3.37	0.19	3.37	1.8	8.5	4.8
23	23233-1	79.41	6.88	1.20	0.45 ± 0.09	2.37	0.23	2.37	3.8	7.9	4.3
24	23235-1	78.87	1.39	0.90	0.46 ± 0.07	3.03	0.12	3.03	2.8	5.0	4.4
25	23259-3	72.02	9.3	1.01	0.53 ± 0.05	2.50	0.23	2.50	5.2	6.1	4.9
26	23261-2	72.18	13.11	0.97	0.55 ± 0.11	2.55	0.27	2.55	5.1	5.7	5.0
27	23508-1	73.86	-9.40	1.20	0.38 ± 0.20	3.35	-0.20	3.35	0.4	7.9	3.8
28	23509-1	73.83	-13.50	1.37	0.50 ± 0.08	3.41	-0.42	3.41	-0.4	9.3	4.7

[1] Samples 1 to 20 were provided from Meland et al., 2006, samples 21 to 28 were provided from Simstich et al., (2003) and references therein.

[2] Mg/Ca ratio measurements for samples 1 to 20 was performed in Cambridge, UK. Mg/Ca ratios of samples 21 to 28 were measured in Kiel, Germany.

[3] δ^{18}O values were taken from Hohnemann, 1996, Horwege, 1987, Meland et al. 2006 and Simstich et al., 2003

[4] Calculated after the salinity – δ^{18}O relation of Simstich et al., (2003): $\delta^{18}O_{water}$ [‰ SMOW] = -12.17 + 0.03*SAL

[5] Calculated after Shackleton, 1974: δ^{18}Ocalcite = [21.9–3.16*(31.061 + T)$^{0.5}$] + δ_w

[6] Mg/Ca temperature equation of Mashiotta, 1999 (Mg/Ca [mmol/mol] = 0.549*exp$^{0.099T}$).

[7] $\delta^{44/40}$Ca temperature equations of Hippler et al. 2004 ($\delta^{44/40}$Ca [‰] = 0.15 (±0.11)*SST [°C] – 0.20)

Table 6: Electron microprobe measurements and water column properties

Core tops, Norwegian Sea									
Core	Latitude °N	Longitude °W/°E	*n* Mg/Ca 0-0.5	*n* Mg/Ca 0.5-1	*n* Mg/Ca 1-1.5	*n* Mg/Ca 1.5-2	*n* Mg/Ca 2-2.5	*n* Mg/Ca 2.5-3	Mean (mmol/mol)
23514-3	66.67	-25.95	0	6	26	12	4	0	0.92
23528-3	63.16	-28.84	0	0	11	36	20	4	1.43
23261-2	72.18	13.11	0	6	14	19	7	0	0.96
Multi net catches MN 37/92, 75.00°N, 17.04°E, Norwegian Sea									
Core	Depth interval	T(°C) CTD[1)]	*n* Mg/Ca 0-0.5	*n* Mg/Ca 0.5-1	*n* Mg/Ca 1-1.5	*n* Mg/Ca 1.5-2	*n* Mg/Ca 2-2.5	*n* Mg/Ca 2.5-3	Mean (mmol/mol
MN37/92	0-20 m	2.3-2.5	0	6	25	34	14	4	1.13
MN37/92 #1	20-50 m	2.5-4.2	0	8	25	29	27	9	1.28
MN 37/92 #2	20-50 m	2.5-4.2	0	1	7	2	4	3	1.24

[1)] CTD profile from Jensen et al., 1998

Table 7: Supporting hydrographic data compiled from the WOA 2001 (www.nodc.noaa.gov/OC5/WOA01/pr_woa01.html)

Hydrographic conditions at core locations (July, compiled from the World Ocean Atlas, 2001)															
	0 m	50 m	mean	50 m	100 m	mean	100 m	150 m	mean	150 m	200 m	mean	200 m	250 m	mean
PS2638															
Temp [°C]	-1.4	-2.2	-1.8	-2.2	-1.7	-1.9	-1.7	-1.1	-1.4	-1.1	-0.4	-0.8			
S [psu]	30.0	33.9	32.0	33.9	34.3	34.1	34.3	34.5	34.4	34.5	34.5	34.6			
$\delta^{18}O_{water}$			-0.87			-0.09			0.01			0.09			
theoret. $\delta^{18}O_{calcite}$			3.93			4.75			4.7			4.59			
23071															
Temp [°C]	10.2	7.5	8.8	7.5	6.5	7.0	6.5	5.9	6.2	5.9	5.4	5.7	5.4	5.0	5.2
S [psu]	35.0	35.2	35.1	35.2	35.2	35.2	35.2	35.1	35.2	35.1	35.1	35.1	35.1	35.1	35.1
$\delta^{18}O_{water}$			0.27			0.3			0.28			0.27			0.27
theoret. $\delta^{18}O_{calcite}$			2.21			2.71			2.89			3.02			2.99
23231															
Temp [°C]	0.7	0.0	0.4	0.0	0.2	0.1	0.2	0.6	0.4	0.6	1.0	0.8	1.0	1.0	1.0
S [psu]	32.5	34.0	33.3	34.0	34.4	34.2	34.4	34.8	34.6	34.8	34.9	34.9	34.9	34.9	34.9
$\delta^{18}O_{water}$			-0.40			-0.06			0.09			0.18			0.19
theoret. $\delta^{18}O_{calcite}$			3.79			4.20			4.26			4.24			4.20
23232															
Temp [°C]	1.1	0.5	0.8	0.5	0.6	0.6	0.6	0.9	0.8	0.9	1.0	1.0	1.0	1.0	1.0
S [psu]	33.0	34.2	33.6	34.2	34.6	34.4	34.6	34.8	34.7	34.8	34.9	34.9	34.9	35.0	35.0
$\delta^{18}O_{water}$			-0.28			0.01			0.12			0.18			0.21
theoret. $\delta^{18}O_{calcite}$			3.78			4.15			4.20			4.20			4.22
23235															
Temp [°C]	2.0	1.3	1.7	1.3	1.3	1.3	1.3	1.4	1.4	1.4	1.4	1.4	1.4	1.3	1.4
S [psu]	33.5	34.6	34.1	34.6	34.8	34.7	34.8	34.9	34.9	34.9	35.0	35.0	35.0	35.0	35.0
$\delta^{18}O_{water}$			-0.11			0.12			0.18			0.21			0.23
theoret. $\delta^{18}O_{calcite}$			3.71			4.05			4.09			4.11			4.14
23259															
Temp [°C]	8.3	6.0	7.2	6.0	5.2	5.6	5.2	4.8	5.0	4.8	4.5	4.7	4.5	4.2	4.4
S [psu]	35.0	35.1	35.1	35.1	35.1	35.1	35.1	35.1	35.1	35.1	35.1	35.1	35.1	35.1	35.1
$\delta^{18}O_{water}$			0.25			0.27			0.27			0.27			0.27
theoret. $\delta^{18}O_{calcite}$			2.61			3.03			3.19			3.28			3.36
23261															
Temp [°C]	7.8	6.0	6.9	6.0	5.2	5.6	5.2	4.9	5.1	4.9	4.6	4.8	4.6	4.3	4.5
S [psu]	34.9	35.1	35.0	35.1	35.1	35.1	35.1	35.1	35.1	35.1	35.1	35.1	35.1	35.1	35.1
$\delta^{18}O_{water}$			0.23			0.27			0.27			0.27			0.27
$\delta^{18}O_{calcite}$			2.66			3.03			3.18			3.26			3.34
23347															
Temp [°C]	2.0	-0.2	0.9	-0.2	-0.5	-0.4	-0.5	-0.2	-0.4	-0.2	0.2	0.0	0.2	0.4	0.3
S [psu]	33.5	34.5	34.0	34.5	34.7	34.6	34.7	34.8	34.8	34.8	34.8	34.8	34.8	34.9	34.9
$\delta^{18}O_{water}$			-0.13			0.09			0.14			0.16			0.18
theoret. $\delta^{18}O_{calcite}$			3.91			4.47			4.53			4.45			4.38
23506															
Temp [°C]	3.7	0.3	2.0	0.3	0.2	0.3	0.2	0.3	0.3	0.3	0.2	0.3	0.2	0.0	0.1
S [psu]	33.8	34.7	34.3	34.7	34.9	34.8	34.9	34.9	34.9	34.9	34.9	34.9	34.9	34.9	34.9
$\delta^{18}O_{water}$			-0.04			0.16			0.19			0.19			0.19
theoret. $\delta^{18}O_{calcite}$			3.69			4.38			4.41			4.41			4.45

Hydrographic conditions at core locations (July, compiled from the World Ocean Atlas, 2001)

	0 m	50 m	mean	50 m	100 m	mean	100 m	150 m	mean	150 m	200 m	mean	200 m	250 m	mean
23509															
Temp [°C]	1.5	-0.6	0.5	-0.6	-0.5	-0.6	-0.5	-0.3	-0.4	-0.3	0.0	-0.2	0.0	0.0	0.0
S [psu]	32.0	34.2	33.1	34.2	34.5	34.4	34.5	34.6	34.6	34.6	34.7	34.7	34.7	34.8	34.8
$\delta^{18}O_{water}$			-0.45			0.00			0.07			0.10			0.14
theoret. $\delta^{18}O_{calcite}$			3.71			4.44			4.47			4.44			4.43
23514															
Temp [°C]	5.4	4.3	4.9	4.3	4.0	4.2	4.0	3.7	3.9	3.7	3.7	3.7	3.7	3.0	3.4
S [psu]	33.6	34.6	34.1	34.6	34.8	34.7	34.8	34.9	34.9	34.9	34.9	34.9	34.9	34.9	34.9
$\delta^{18}O_{water}$			-0.09			0.12			0.18			0.19			0.19
theoret. $\delta^{18}O_{calcite}$			2.87			3.27			3.40			3.46			3.56
23523															
Temp [°C]	9.5	7.5	8.5	7.5	6.6	7.1	6.6	6.4	6.5	6.4	6.2	6.3	6.2	6.0	6.1
S [psu]	35.0	35.0	35.0	35.0	35.1	35.1	35.1	35.1	35.1	35.1	35.1	35.1	35.1	35.1	35.1
$\delta^{18}O_{water}$			0.23			0.25			0.27			0.27			0.27
theoret. $\delta^{18}O_{calcite}$			2.25			2.64			2.80			2.85			2.90
23528-3															
Temp [°C]	9.2	7.5	8.4	7.5	6.7	7.1	6.7	6.5	6.6	6.5	6.3	6.4	6.3	6.2	6.3
S [psu]	34.8	35.0	34.9	35.0	35.1	35.1	35.1	35.1	35.1	35.1	35.1	35.1	35.1	35.1	35.1
$\delta^{18}O_{water}$			0.19			0.25			0.27			0.27			0.27
theoret. $\delta^{18}O_{calcite}$			2.26			2.63			2.77			2.83			2.86
23538															
Temp [°C]	10.6	8.3	9.5	8.3	7.1	7.7	7.1	6.4	6.8	6.4	6.0	6.2	6.0	5.3	5.7
S [psu]	35.2	35.2	35.2	35.2	35.2	35.2	35.2	35.1	35.2	35.1	35.1	35.1	35.1	35.1	35.1
$\delta^{18}O_{water}$			0.30			0.30			0.28			0.27			0.27
theoret. $\delta^{18}O_{calcite}$			2.09			2.53			2.75			2.88			3.02
23540															
Temp [°C]	11.5	8.8	10.2	8.8	7.5	8.2	7.5	6.9	7.2	6.9	6.5	6.7	6.5	5.7	6.1
S [psu]	35.2	35.2	35.2	35.2	35.2	35.2	35.2	35.2	35.2	35.2	35.1	35.2	35.1	35.1	35.1
$\delta^{18}O_{water}$			0.30			0.30			0.30			0.28			0.27
theoret. $\delta^{18}O_{calcite}$			1.92			2.41			2.66			2.77			2.90
HM 49-15															
Temp [°C]	9.8	6.9	8.4	6.9	5.6	6.3	5.6	4.9	5.3	4.9	4.3	4.6	4.3	3.9	4.1
S [psu]	35.1	35.1	35.1	35.1	35.1	35.1	35.1	35.1	35.1	35.1	35.0	35.1	35.0	35.0	35.0
$\delta^{18}O_{water}$			0.27			0.27			0.27			0.25			0.23
theoret. $\delta^{18}O_{calcite}$			2.33			2.86			3.12			3.28			3.39
HM 52-18															
Temp [°C]	10.2	9.3	9.8	9.3	8.4	8.9	8.4	8.2	8.3	8.2	8.1	8.2	8.1	8.0	8.1
S [psu]	35.1	35.2	35.2	35.2	35.2	35.2	35.2	35.2	35.2	35.2	35.2	35.2	35.2	35.2	35.2
$\delta^{18}O_{water}$			0.28			0.30			0.30			0.30			0.30
theoret. $\delta^{18}O_{calcite}$			2.00			2.24			2.38			2.41			2.44
HM 52-39															
Temp [°C]	8.0	4.6	6.3	4.6	3.2	3.9	3.2	2.6	2.9	2.6	2.1	2.4	2.1	1.8	2.0
S [psu]	34.9	35.0	35.0	35.0	35.0	35.0	35.0	34.9	35.0	34.9	34.9	34.6	34.9	34.9	34.9
$\delta^{18}O_{water}$			0.21			0.23			0.21			0.09			0.19
theoret. $\delta^{18}O_{calcite}$			2.80			3.45			3.70			3.72			3.94

Hydrographic conditions at core locations (July, compiled from the World Ocean Atlas, 2001)

	0 m	50 m	mean	50 m	100 m	mean	100 m	150 m	mean	150 m	200 m	mean	200 m	250 m	mean
HM 52-42															
Temp [°C]	9.4	6.0	7.7	6.0	4.5	5.3	4.5	3.9	4.2	3.9	3.4	3.7	3.4	3.1	3.3
S [psu]	35.1	35.1	35.1	35.1	35.0	35.1	35.0	35.0	35.0	35.0	35.0	34.6	35.0	35.0	35.0
$\delta^{18}O_{water}$			0.27			0.25			0.23			0.09			0.23
theoret. $\delta^{18}O_{calcite}$			2.49			3.11			3.37			3.37			3.62
HM 57-11															
Temp [°C]	6.6	2.9	4.8	2.9	1.6	2.3	1.6	1.4	1.5	1.4	1.2	1.3	1.2	1.2	1.2
S [psu]	34.8	34.9	34.9	34.9	34.9	34.9	34.9	34.9	34.9	34.9	34.9	34.6	34.9	34.9	34.9
$\delta^{18}O_{water}$			0.18			0.19			0.19			0.09			0.19
theoret. $\delta^{18}O_{calcite}$			3.17			3.86			4.06			4.01			4.15
HM 57-16															
Temp [°C]	8.1	4.8	6.5	4.8	3.4	4.1	3.4	3.0	3.2	3.0	2.6	2.8	2.6	2.4	2.5
S [psu]	35.0	35.0	35.0	35.0	35.0	35.0	35.0	35.0	35.0	35.0	34.9	35.0	34.9	34.9	34.9
$\delta^{18}O_{water}$			0.23			0.23			0.23			0.21			0.19
theoret. $\delta^{18}O_{calcite}$			2.78			3.39			3.63			3.72			3.79
HM 57-20															
Temp [°C]	11.7	8.6	10.2	8.6	7.7	8.2	7.7	7.3	7.5	7.3	6.9	7.1	6.9	6.5	6.7
S [psu]	34.6	35.2	34.9	35.2	35.2	35.2	35.2	35.2	35.2	35.2	35.2	35.2	35.2	35.2	35.2
$\delta^{18}O_{water}$			0.19			0.30			0.30			0.30			0.30
theoret. $\delta^{18}O_{calcite}$			1.81			2.41			2.58			2.68			2.78
HM 71-17															
Temp [°C]	4.2	0.8	2.5	0.8	0.1	0.5	0.1	0.1	0.1	0.1	0.2	0.2	0.2	0.1	0.2
S [psu]	34.4	34.7	34.6	34.7	34.8	34.8	34.8	34.9	34.9	34.9	34.9	34.9	34.9	34.9	34.9
$\delta^{18}O_{water}$			0.07			0.14			0.18			0.19			0.19
theoret. $\delta^{18}O_{calcite}$			3.66			4.30			4.44			4.44			4.44
HM 71-22															
Temp [°C]	7.6	4.5	6.1	4.5	3.4	4.0	3.4	3.0	3.2	3.0	2.7	2.9	2.7	2.5	2.6
S [psu]	35.0	35.0	35.0	35.0	35.0	35.0	35.0	35.0	35.0	35.0	35.0	34.6	35.0	35.0	35.0
$\delta^{18}O_{water}$			0.23			0.23			0.23			0.09			0.23
theoret. $\delta^{18}O_{calcite}$			2.88			3.43			3.63			3.58			3.80
HM 80-43															
Temp [°C]	3.5	0.2	1.9	0.2	0.0	0.1	0.0	0.1	0.1	0.1	0.1	0.1	0.1	0.0	0.1
S [psu]	33.6	34.7	34.2	34.7	34.8	34.8	34.8	34.9	34.9	34.9	34.9	34.6	34.9	34.9	34.9
$\delta^{18}O_{water}$			-0.08			0.14			0.18			0.09			0.19
theoret. $\delta^{18}O_{calcite}$			3.70			4.40			4.45			4.35			4.47
HM 94-12															
Temp [°C]	5.9	2.3	4.1	2.3	1.7	2.0	1.7	1.6	1.7	1.6	1.4	1.5	1.4	1.2	1.3
S [psu]	34.6	34.9	34.8	34.9	34.9	34.9	34.9	34.9	34.9	34.9	34.9	34.6	34.9	34.9	34.9
$\delta^{18}O_{water}$			0.14			0.19			0.19			0.09			0.19
theoret. $\delta^{18}O_{calcite}$			3.30			3.92			4.02			3.95			4.12
HM 94-16															
Temp [°C]	6.1	3.4	4.8	3.4	2.7	3.1	2.7	2.4	2.6	2.4	2.2	2.3	2.2	1.9	2.1
S [psu]	34.9	35.0	35.0	35.0	35.0	35.0	35.0	35.0	35.0	35.0	35.0	35.0	35.0	35.0	35.0
$\delta^{18}O_{water}$			0.21			0.23			0.23			0.23			0.23
theoret. $\delta^{18}O_{calcite}$			3.20			3.67			3.81			3.88			3.95
HM 94-18															
Temp [°C]	5.7	3.2	4.5	3.2	2.5	2.9	2.5	2.2	2.4	2.2	2.0	2.1	2.0	1.7	1.9
S [psu]	34.9	35.0	35.0	35.0	35.0	35.0	35.0	35.0	35.0	35.0	35.0	35.0	35.0	35.0	35.0
$\delta^{18}O_{water}$			0.21			0.23			0.23			0.23			0.23
theoret. $\delta^{18}O_{calcite}$			3.28			3.73			3.86			3.93			4.00

Hydrographic conditions at core locations (July, compiled from the World Ocean Atlas, 2001)

	0 m	50 m	mean	50 m	100 m	mean	100 m	150 m	mean	150 m	200 m	mean	200 m	250 m	mean
HM 94-30															
Temp [°C]	3.8	0.2	2.0	0.2	-0.2	0.0	-0.2	-0.1	-0.2	-0.1	-0.1	-0.1	-0.1	-0.2	-0.2
S [psu]	34.1	34.8	34.5	34.8	34.9	34.9	34.9	34.9	34.9	34.9	34.9	34.9	34.9	34.9	34.9
$\delta^{18}O_{water}$			0.03			0.18			0.19			0.19			0.19
theoret. $\delta^{18}O_{calcite}$			3.76			4.46			4.53			4.51			4.53
JM 97-948															
Temp [°C]	11.4	7.8	9.6	7.8	7.2	7.5	7.2	7.0	7.1	7.0	6.7	6.9	6.7	6.5	6.6
S [psu]	34.6	35.1	34.9	35.1	35.2	35.2	35.2	35.2	35.2	35.2	35.2	34.6	35.2	35.2	35.2
$\delta^{18}O_{water}$			0.18			0.28			0.30			0.09			0.30
theoret. $\delta^{18}O_{calcite}$			1.93			2.56			2.68			2.53			2.81
HM 133-21															
Temp [°C]	11.0	9.1	10.1	9.1	8.2	8.7	8.2	7.9	8.1	7.9	7.5	7.7	7.5	7.8	7.7
S [psu]	35.2	35.2	35.2	35.2	35.2	35.2	35.2	35.2	35.2	35.2	35.2	35.2	35.2	35.2	35.2
$\delta^{18}O_{water}$			0.30			0.30			0.30			0.30			0.30
theoret. $\delta^{18}O_{calcite}$			1.94			2.29			2.44			2.53			2.54
HM 133-24															
Temp [°C]	10.8	9.5	10.2	9.5	8.5	9.0	8.5	8.2	8.4	8.2	7.9	8.1	7.9	7.8	7.9
S [psu]	35.2	35.2	35.2	35.2	35.2	35.2	35.2	35.2	35.2	35.2	35.2	35.2	35.2	35.2	35.2
$\delta^{18}O_{water}$			0.30			0.30			0.30			0.30			0.30
theoret. $\delta^{18}O_{calcite}$			1.92			2.20			2.36			2.44			2.49
HM 16130															
Temp [°C]	9.6	6.7	8.2	6.7	5.3	6.0	5.3	4.5	4.9	4.5	3.9	4.2	3.9	3.3	3.6
S [psu]	35.1	35.1	35.1	35.1	35.1	35.1	35.1	35.1	35.1	35.0	35.0	34.6	35.0	35.0	35.0
$\delta^{18}O_{water}$			0.27			0.27			0.27			0.09			0.23
theoret. $\delta^{18}O_{calcite}$			2.38			2.93			3.22			3.22			3.53
HM 16132															
Temp [°C]	10.3	7.4	8.9	7.4	6.2	6.8	6.2	5.4	5.8	5.4	4.8	5.1	4.8	4.2	4.5
S [psu]	35.1	35.2	35.2	35.2	35.1	35.2	35.1	35.1	35.1	35.1	35.1	35.1	35.1	35.0	35.1
$\delta^{18}O_{water}$			0.28			0.28			0.27			0.27			0.25
theoret. $\delta^{18}O_{calcite}$			2.22			2.71			2.98			3.16			3.30
HM 16142															
Temp [°C]	11.6	8.5	10.1	8.5	7.6	8.1	7.6	7.1	7.4	7.1	6.6	6.9	6.6	6.1	6.4
S [psu]	34.6	35.2	34.9	35.2	35.2	35.2	35.2	35.1	35.2	35.1	35.1	35.1	35.1	35.1	35.1
$\delta^{18}O_{water}$			0.19			0.30			0.28			0.27			0.27
theoret. $\delta^{18}O_{calcite}$			1.83			2.44			2.60			2.71			2.84

Hydrographic conditions at core locations (August, compiled from the World Ocean Atlas, 2001)

	0 m	50 m	mean	50 m	100 m	mean	100 m	150 m	mean	150 m	200 m	mean	200 m	250 m	mean
PS2638															
Temp [°C]	-0.7	-2.1	-1.4	-2.1	-1.8	-2.0	-1.8	-0.9	-1.4	-0.9	0.0	-0.5	0.0	0.7	0.4
S [psu]	29.0	33.5	31.3	33.5	34.1	33.8	34.1	34.5	34.3	34.5	34.7	34.6	34.7	34.9	34.8
$\delta^{18}O_{water}$			-1.12			-0.20			-0.02			0.09			0.16
theoret. $\delta^{18}O_{calcite}$			3.57			4.65			4.65			4.50			4.35
23071															
Temp [°C]	11.4	8.3	9.9	8.3	7.2	7.8	7.2	6.6	6.9	6.6	6.0	6.3	6.0	5.5	5.8
S [psu]	34.9	35.2	35.1	35.2	35.2	35.2	35.2	35.2	35.2	35.2	35.2	35.2	35.1	35.1	35.1
$\delta^{18}O_{water}$			0.25			0.30			0.30			0.30			0.27
theoret. $\delta^{18}O_{calcite}$			1.94			2.52			2.73			2.89			2.99
23231															
Temp [°C]	1.0	0.2	0.6	0.2	0.4	0.3	0.4	0.7	0.6	0.7	1.0	0.9	1.0	1.1	1.1
S [psu]	32.3	34.1	33.2	34.1	34.5	34.3	34.5	34.8	34.7	34.8	34.9	34.9	34.9	35.0	35.0
$\delta^{18}O_{water}$			-0.42			-0.02			0.10			0.18			0.21
theoret. $\delta^{18}O_{calcite}$			3.70			4.18			4.24			4.23			4.21
23232															
Temp [°C]	1.6	0.7	1.2	0.7	0.8	0.8	0.8	1.0	0.9	1.0	1.2	1.1	1.2	1.1	1.2
S [psu]	32.7	34.3	33.5	34.3	34.7	34.5	34.7	34.9	34.8	35.0	35.0	35.0	35.0	35.0	35.0
$\delta^{18}O_{water}$			-0.31			0.05			0.16			0.23			0.23
theoret. $\delta^{18}O_{calcite}$			3.66			4.13			4.19			4.21			4.20
23235															
Temp [°C]	2.4	1.6	2.0	1.6	1.5	1.6	1.5	1.5	1.5	1.5	1.4	1.5	1.4	1.3	1.4
S [psu]	33.3	34.6	34.0	34.6	34.8	34.7	34.8	34.9	34.9	35.0	35.0	35.0	35.0	35.0	35.0
$\delta^{18}O_{water}$			-0.15			0.12			0.18			0.23			0.23
$\delta^{18}O_{calcite}$			3.58			3.98			4.04			4.11			4.14
23259															
Temp [°C]	9.2	6.5	7.9	6.5	5.3	5.9	5.3	4.8	5.1	4.8	4.4	4.6	4.4	4.2	4.3
S [psu]	35.0	35.1	35.1	35.1	35.1	35.1	35.1	35.1	35.1	35.1	35.1	35.1	35.1	35.1	35.1
$\delta^{18}O_{water}$			0.25			0.27			0.27			0.27			0.27
theoret. $\delta^{18}O_{calcite}$			2.44			2.95			3.18			3.30			3.37
23261															
Temp [°C]	8.8	6.5	7.7	6.5	5.4	6.0	5.4	5.0	5.2	5.0	4.7	4.9	4.7	4.3	4.5
S [psu]	35.0	35.0	35.0	35.0	35.0	35.0	35.0	35.0	35.0	35.0	35.0	35.0	35.0	35.0	35.0
$\delta^{18}O_{water}$			0.23			0.23			0.23			0.23			0.23
theoret. $\delta^{18}O_{calcite}$			2.47			2.91			3.10			3.19			3.29
23347															
Temp [°C]	2.9	0.0	1.5	0.0	-0.2	-0.1	-0.2	0.2	0.0	0.2	0.4	0.3	0.4	0.5	0.5
S [psu]	32.6	34.4	33.5	34.4	34.6	34.5	34.6	34.8	34.7	34.8	34.8	34.8	34.8	34.9	34.9
$\delta^{18}O_{water}$			-0.31			0.05			0.12			0.16			0.18
theoret. $\delta^{18}O_{calcite}$			3.57			4.37			4.41			4.36			4.34
23506															
Temp [°C]	4.5	0.4	2.5	0.4	0.5	0.5	0.5	0.5	0.5	0.5	0.4	0.5	0.4	0.1	0.3
S [psu]	33.5	34.7	34.1	34.7	34.9	34.8	34.9	34.9	34.9	34.9	34.9	34.9	34.9	34.9	34.9
$\delta^{18}O_{water}$			-0.09			0.16			0.19			0.19			0.19
theoret. $\delta^{18}O_{calcite}$			3.51			4.32			4.34			4.36			4.41

Hydrographic conditions at core locations (August, compiled from the World Ocean Atlas, 2001)

	0 m	50 m	mean	50 m	100 m	mean	100 m	150 m	mean	150 m	200 m	mean	200 m	250 m	mean
23509															
Temp [°C]	1.6	-0.4	0.6	-0.4	0.0	-0.2	0.0	0.3	0.2	0.3	0.5	0.4	0.5	0.5	0.5
S [psu]	32.0	34.3	33.2	34.3	34.6	34.5	34.6	34.7	34.7	34.7	34.8	34.8	34.8	34.9	34.9
$\delta^{18}O_{water}$			-0.44			0.03			0.10			0.14			0.18
theoret. $\delta^{18}O_{calcite}$			3.68			4.38			4.35			4.32			4.32
23514															
Temp [°C]	5.7	4.3	5.0	4.3	3.8	4.1	3.8	3.7	3.8	3.7	3.7	3.7	3.7	3.0	3.4
S [psu]	33.2	34.2	33.7	34.3	34.6	34.5	34.6	34.8	34.7	34.8	34.9	34.9	34.9	34.9	34.9
$\delta^{18}O_{water}$			-0.24			0.03			0.12			0.18			0.19
theoret. $\delta^{18}O_{calcite}$			2.69			3.21			3.38			3.45			3.56
23523															
Temp [°C]	10.1	8.0	9.1	8.0	6.7	7.4	6.7	6.5	6.6	6.5	6.3	6.4	6.3	6.2	6.3
S [psu]	35.0	35.0	35.0	35.0	35.1	35.1	35.1	35.1	35.1	35.1	35.1	35.1	35.1	35.1	35.1
$\delta^{18}O_{water}$			0.23			0.25			0.27			0.27			0.27
theoret. $\delta^{18}O_{calcite}$			2.12			2.56			2.77			2.83			2.86
23528															
Temp [°C]	9.8	7.8	8.8	7.8	6.8	7.3	6.8	6.5	6.7	6.5	6.3	6.4	6.3	6.2	6.2
S [psu]	34.9	35.0	35.0	35.0	35.0	35.0	35.0	35.0	35.0	35.0	35.0	35.0	35.0	35.0	35.0
$\delta^{18}O_{water}$			0.21			0.23			0.23			0.23			0.23
theoret. $\delta^{18}O_{calcite}$			2.16			2.56			2.72			2.80			2.83
23538															
Temp [°C]	11.9	9.5	10.7	9.5	8.3	8.9	8.3	7.9	8.1	7.9	7.7	7.8	7.7	7.0	7.4
S [psu]	35.2	35.2	35.2	35.2	35.2	35.2	35.2	35.3	35.3	35.3	35.3	35.3	35.3	35.2	35.3
$\delta^{18}O_{water}$			0.30			0.30			0.32			0.34			0.32
theoret. $\delta^{18}O_{calcite}$			1.79			2.23			2.45			2.54			2.64
23540															
Temp [°C]	11.5	8.7	10.1	8.7	7.4	8.1	7.4	6.8	7.1	6.8	6.3	6.6	6.3	5.7	6.0
S [psu]	35.1	35.2	35.2	35.2	35.2	35.2	35.2	35.2	35.2	35.2	35.2	35.2	35.2	35.1	35.2
$\delta^{18}O_{water}$			0.28			0.30			0.30			0.30			0.28
theoret. $\delta^{18}O_{calcite}$			1.91			2.44			2.68			2.82			2.95
HM 49-15															
Temp [°C]	10.6	7.3	9.0	7.3	5.8	6.6	5.8	5.1	5.5	5.1	4.4	4.8	4.4	3.9	4.2
S [psu]	35.1	35.1	35.1	35.1	35.1	35.1	35.1	35.1	35.1	35.1	35.0	35.1	35.0	35.0	35.0
$\delta^{18}O_{water}$			0.27			0.27			0.27			0.25			0.23
theoret. $\delta^{18}O_{calcite}$			2.18			2.79			3.07			3.24			3.38
HM 52-18															
Temp [°C]	11.4	9.7	10.6	9.7	8.6	9.2	8.6	8.3	8.5	8.3	8.2	8.3	8.2	8.0	8.1
S [psu]	35.1	35.2	35.2	35.2	35.2	35.2	35.2	35.2	35.2	35.2	35.2	35.2	35.2	35.2	35.2
$\delta^{18}O_{water}$			0.28			0.30			0.30			0.30			0.30
theoret. $\delta^{18}O_{calcite}$			1.80			2.16			2.34			2.39			2.43
HM 52-39															
Temp [°C]	9.1	5.0	7.1	5.0	3.4	4.2	3.4	2.7	3.1	2.7	2.3	2.5	2.3	1.9	2.1
S [psu]	34.9	35.0	35.0	35.0	35.0	35.0	35.0	34.9	35.0	34.9	34.9	34.9	34.9	34.9	34.9
$\delta^{18}O_{water}$			0.21			0.23			0.21			0.19			0.19
theoret. $\delta^{18}O_{calcite}$			2.60			3.37			3.33			3.79			3.90
52-42															
Temp [°C]	10.0	6.4	8.2	6.4	4.8	5.6	4.8	4.1	4.5	4.1	3.5	3.8	3.5	3.1	3.3
S [psu]	35.1	35.1	35.1	35.1	35.0	35.1	35.0	35.0	35.0	35.0	35.0	35.0	35.0	35.0	35.0
$\delta^{18}O_{water}$			0.27			0.25			0.23						
theoret. $\delta^{18}O_{calcite}$			2.37			3.01			3.30						

Hydrographic conditions at core locations (August, compiled from the World Ocean Atlas, 2001)

	0 m	50 m	mean	50 m	100 m	mean	100 m	150 m	mean	150 m	200 m	mean	200 m	250 m	mean
57-11															
Temp [°C]	7.7	3.2	5.5	3.2	1.7	2.5	1.7	1.4	1.6	1.4	1.2	1.3	1.2	1.0	1.1
S [psu]	34.8	34.9	34.9	34.9	34.9	34.9	34.9	34.9	34.9	34.9	34.9	34.9	34.9	34.9	34.9
$\delta^{18}O_{water}$			0.18			0.19			0.19			0.19			0.19
theoret. $\delta^{18}O_{calcite}$			2.98			3.80			4.05			4.12			4.17
HM 57-16															
Temp [°C]	8.9	5.1	7.0	5.1	3.6	4.4	3.6	2.9	3.3	2.9	2.5	2.7	2.5	2.2	2.4
S [psu]	35.0	35.0	35.0	35.0	35.0	35.0	35.0	35.0	35.0	35.0	34.9	35.0	34.9	34.9	34.9
$\delta^{18}O_{water}$			0.23			0.23			0.23			0.21			0.19
theoret. $\delta^{18}O_{calcite}$			2.63			3.33			3.62			3.75			3.83
HM 57-20															
Temp [°C]	12.6	9.0	10.8	9.0	8.0	8.5	8.0	7.5	7.8	7.5	7.2	7.4	7.2	6.9	7.1
S [psu]	34.6	35.2	34.9	35.2	35.2	35.2	35.2	35.2	35.2	35.2	35.2	35.2	35.2	35.2	35.2
$\delta^{18}O_{water}$			0.19			0.30			0.30			0.30			0.30
theoret. $\delta^{18}O_{calcite}$			1.65			2.33			2.52			2.62			2.69
HM 71-17															
Temp [°C]	4.0	0.4	2.2	0.4	0.2	0.3	0.2	0.3	0.3	0.3	0.4	0.4	0.4	0.2	0.3
S [psu]	33.4	33.6	33.5	33.6	34.8	34.2	34.8	34.8	34.8	34.8	34.9	34.9	34.9	34.9	34.9
$\delta^{18}O_{water}$			-0.31			-0.06			0.16			0.18			0.19
theoret. $\delta^{18}O_{calcite}$			3.37			4.15			4.38			4.37			4.40
HM 71-22															
Temp [°C]	8.3	4.8	6.6	4.8	3.5	4.2	3.5	3.1	3.3	3.1	2.7	2.9	2.7	2.4	2.6
S [psu]	34.9	35.0	35.0	35.0	35.0	35.0	35.0	35.0	35.0	35.0	35.0	35.0	35.0	35.0	35.0
$\delta^{18}O_{water}$			0.21			0.23			0.23			0.23			0.23
theoret. $\delta^{18}O_{calcite}$			2.73			3.38			3.61			3.71			3.81
HM 80-43															
Temp [°C]	3.8	0.2	2.0	0.2	0.4	0.3	0.4	0.5	0.5	0.5	0.4	0.5	0.4	0.2	0.3
S [psu]	33.2	34.6	33.9	34.6	34.9	34.7	34.9	34.9	34.9	34.9	34.9	34.9	34.9	34.9	34.9
$\delta^{18}O_{water}$			-0.17			0.13			0.18			0.19			0.19
theoret. $\delta^{18}O_{calcite}$			3.56			4.33			4.35			4.36			4.40
HM 94-12															
Temp [°C]	6.6	2.4	4.5	2.4	1.8	2.1	1.8	1.7	1.8	1.7	1.4	1.6	1.4	1.2	1.3
S [psu]	34.4	34.9	34.7	34.9	34.9	34.9	34.9	35.0	35.0	35.0	35.0	35.0	35.0	35.9	35.5
$\delta^{18}O_{water}$			0.10			0.19			0.21			0.23			0.39
theoret. $\delta^{18}O_{calcite}$			3.16			3.90			4.01			4.08			4.32
HM 94-16															
Temp [°C]	7.0	3.4	5.2	3.4	2.4	2.9	2.4	2.2	2.3	2.2	1.9	2.1	1.9	1.4	1.7
S [psu]	34.9	35.0	35.0	35.0	35.0	35.0	35.0	35.0	35.0	35.0	35.0	35.0	35.0	35.0	35.0
$\delta^{18}O_{water}$			0.21			0.23			0.23			0.23			0.23
theoret. $\delta^{18}O_{calcite}$			3.08			3.71			3.88			3.95			4.06
HM 94-18															
Temp [°C]	6.3	2.8	4.6	2.8	2.0	2.4	2.0	1.7	1.9	1.7	1.5	1.6	1.5	1.3	1.4
S [psu]	34.8	35.0	34.9	35.0	35.0	35.0	35.0	35.0	35.0	35.0	35.0	35.0	35.0	35.0	35.0
$\delta^{18}O_{water}$			0.19			0.23			0.23			0.23			0.23
theoret. $\delta^{18}O_{calcite}$			3.24			3.85			4.00			4.07			4.13

Hydrographic conditions at core locations (August, compiled from the World Ocean Atlas, 2001)

	0 m	50 m	mean	50 m	100 m	mean	100 m	150 m	mean	150 m	200 m	mean	200 m	250 m	mean
HM 94-30															
Temp [°C]	4.7	0.2	2.5	0.2	-0.1	0.1	-0.1	0.0	-0.1	0.0	-0.1	-0.1	-0.1	-0.3	-0.2
S [psu]	33.9	34.8	34.4	34.8	34.9	34.9	34.9	34.9	34.9	34.9	34.9	34.9	34.9	34.9	34.9
$\delta^{18}O_{water}$			0.00			0.18			0.19			0.19			0.19
theoret. $\delta^{18}O_{calcite}$			3.60			4.45			4.50			4.50			4.54
97-948															
Temp [°C]	11.8	8.2	10.0	8.2	7.5	7.9	7.5	7.1	7.3	7.1	6.8	7.0	6.8	6.5	6.7
S [psu]	34.4	35.1	34.8	35.1	35.2	35.2	35.2	35.2	35.2	35.2	35.2	35.2	35.2	35.2	35.2
$\delta^{18}O_{water}$			0.14			0.28			0.30			0.30			0.30
theoret. $\delta^{18}O_{calcite}$			1.79			2.47			2.63			2.72			2.80
HM 133-21															
Temp [°C]	11.2	9.7	10.5	9.7	8.5	9.1	8.5	8.1	8.3	8.1	7.7	7.9	7.7	8.0	7.9
S [psu]	35.2	35.2	35.2	35.2	35.2	35.2	35.2	35.2	35.2	35.2	35.2	35.2	35.2	35.2	35.2
$\delta^{18}O_{water}$			0.30			0.30			0.30			0.30			0.30
theoret. $\delta^{18}O_{calcite}$			1.84			2.18			2.38			2.48			2.49
HM 133-24															
Temp [°C]	11.4	9.9	10.7	9.9	8.6	9.3	8.6	8.3	8.5	8.3	8.1	8.2	8.1	7.8	8.0
S [psu]	35.2	35.2	35.2	35.2	35.2	35.2	35.2	35.2	35.2	35.2	35.2	35.2	35.2	35.2	35.2
$\delta^{18}O_{water}$			0.30			0.30			0.30			0.30			0.30
theoret. $\delta^{18}O_{calcite}$			1.79			2.14			2.34			2.40			2.46
HM 16130															
Temp [°C]	10.3	6.7	8.5	6.7	5.1	5.9	5.1	4.3	4.7	4.3	3.7	4.0	3.7	3.3	3.5
S [psu]	35.1	35.1	35.1	35.1	35.1	35.1	35.1	35.0	35.1	35.0	35.0	35.0	35.0	35.0	35.0
$\delta^{18}O_{water}$			0.27			0.27			0.25			0.23			0.23
theoret. $\delta^{18}O_{calcite}$			2.29			2.95			3.25			3.42			3.55
HM 16132															
Temp [°C]	10.9	7.6	9.3	7.6	6.1	6.9	6.1	5.4	5.8	5.4	4.6	5.0	4.6	4.2	4.4
S [psu]	35.1	35.1	35.1	35.1	35.1	35.1	35.1	35.1	35.1	35.1	35.0	35.1	35.0	35.0	35.0
$\delta^{18}O_{water}$			0.27			0.27			0.27			0.25			0.23
theoret. $\delta^{18}O_{calcite}$			2.10			2.71			2.99			3.17			3.31
HM 16142															
Temp [°C]	12.5	8.9	10.7	8.9	7.9	8.4	7.9	7.3	7.6	7.3	6.9	7.1	6.9	6.4	6.7
S [psu]	34.5	35.2	34.9	35.2	35.2	35.2	35.2	35.2	35.2	35.2	35.2	35.2	35.2	35.2	35.2
$\delta^{18}O_{water}$			0.18			0.30			0.30			0.30			0.30
theoret. $\delta^{18}O_{calcite}$			1.66			2.35			2.55			2.68			2.80

Hydrographic conditions at core locations (September, compiled from the World Ocean Atlas, 2001)

	0 m	50 m	mean	50 m	100 m	mean	100 m	150 m	mean	150 m	200 m	mean	200 m	250 m	mean
PS2638															
Temp [°C]	-0.9	-1.9	-1.4	-1.9	-0.9	-1.4	-0.9	0.1	-0.4	0.1	0.5	0.3	0.5	1.0	0.8
S [psu]	30.2	33.6	31.9	33.6	34.2	33.9	34.2	34.6	34.4	34.6	34.8	34.7	34.8	34.9	34.9
$\delta^{18}O_{water}$			-0.89			-0.17			0.01			0.3			0.18
theoret. $\delta^{18}O_{calcite}$			3.80			4.52			4.42			4.33			4.25
23071															
Temp [°C]	10.6	8.9	9.8	8.9	7.4	8.2	7.4	6.6	7.0	6.6	6.1	6.4	6.1	5.4	5.8
S [psu]	35.1	35.2	35.2	35.2	35.2	35.2	35.2	35.1	35.2	35.1	35.1	35.1	35.1	35.1	35.1
$\delta^{18}O_{water}$			0.28			0.30			0.28			0.27			0.27
theoret. $\delta^{18}O_{calcite}$			2.00			2.41			2.69			2.84			2.99
23231															
Temp [°C]	0.3	0.3	0.3	0.3	0.3	0.3	0.3	0.7	0.5	0.7	1.0	0.9	1.0	1.3	1.2
S [psu]	32.5	34.0	33.3	34.0	34.4	34.2	34.4	34.7	34.6	34.7	34.8	34.8	34.8	34.9	34.9
$\delta^{18}O_{water}$			-0.40			-0.06			0.07			0.14			0.18
theoret. $\delta^{18}O_{calcite}$			3.80			4.15			4.22			4.19			4.14
23232															
Temp [°C]	0.9	0.8	0.9	0.8	0.8	0.8	0.8	1.0	0.9	1.0	1.2	1.1	1.2	1.3	1.3
S [psu]	32.9	34.3	33.6	34.3	34.6	34.5	34.6	34.8	34.7	34.8	34.9	34.9	34.9	34.9	34.9
$\delta^{18}O_{water}$			-0.27			0.03			0.12			0.18			0.19
theoret. $\delta^{18}O_{calcite}$			3.78			4.10			4.16			4.16			4.13
23235															
Temp [°C]	1.8	1.8	1.8	1.8	1.5	1.7	1.5	1.5	1.5	1.5	1.6	1.6	1.6	1.5	1.6
S [psu]	33.5	34.5	34.0	34.5	34.8	34.7	34.8	34.9	34.9	34.9	34.9	34.9	34.9	34.9	34.9
$\delta^{18}O_{water}$			-0.13			0.10			0.18			0.19			0.19
theoret. $\delta^{18}O_{calcite}$			3.66			3.93			4.04			4.05			4.05
23259															
Temp [°C]	8.3	6.8	7.6	6.8	5.5	6.2	5.5	5.0	5.3	5.0	4.6	4.8	4.6	4.3	4.5
S [psu]	34.0	34.7	34.4	34.7	34.8	34.8	34.8	34.8	34.8	34.8	34.8	34.8	34.8	34.8	34.8
$\delta^{18}O_{water}$			0.00			0.14			0.16			0.16			0.16
theoret. $\delta^{18}O_{calcite}$			2.26			2.76			3.02			3.13			3.23
23261															
Temp [°C]	8.0	6.7	7.3	6.7	5.7	6.2	5.7	5.1	5.4	5.1	4.7	4.9	4.7	4.4	4.6
S [psu]	34.9	35.0	35.0	35.0	35.1	35.1	35.1	35.1	35.1	35.1	35.1	35.1	35.1	35.1	35.1
$\delta^{18}O_{water}$			0.22			0.25			0.27			0.27			0.27
theoret. $\delta^{18}O_{calcite}$			2.54			2.86			3.08			3.22			3.31
23347															
Temp [°C]	3.0	0.7	1.9	0.7	0.3	0.5	0.3	0.6	0.5	0.6	0.7	0.7	0.7	0.6	0.7
S [psu]	33.4	34.5	34.0	34.5	34.7	34.6	34.7	34.8	34.8	34.8	34.9	34.9	34.9	34.9	34.9
$\delta^{18}O_{water}$			-0.15			0.09			0.14			0.18			0.19
theoret. $\delta^{18}O_{calcite}$			3.62			4.23			4.30			4.28			4.30
23506															
Temp [°C]	3.8	1.3	2.6	1.3	0.7	1.0	0.7	0.6	0.7	0.6	0.4	0.5	0.4	0.2	0.3
S [psu]	33.9	34.7	34.3	34.7	34.8	34.8	34.8	34.9	34.9	34.9	34.9	34.9	34.9	34.9	34.9
$\delta^{18}O_{water}$			-0.02			0.14			0.18			0.19			0.19
theoret. $\delta^{18}O_{calcite}$			3.56			4.15			4.28			4.34			4.40

Hydrographic conditions at core locations (September, compiled from the World Ocean Atlas, 2001)

	0 m	50 m	mean	50 m	100 m	mean	100 m	150 m	mean	150 m	200 m	mean	200 m	250 m	mean
23509															
Temp [°C]	1.1	0.2	0.7	0.2	0.4	0.3	0.4	0.7	0.6	0.7	0.7	0.7	0.7	0.6	0.7
S [psu]	32.4	34.3	33.4	34.3	34.6	34.5	34.6	34.8	34.7	34.8	34.8	34.8	34.8	34.9	34.9
$\delta^{18}O_{water}$			-0.36			0.03			0.12			0.16			0.18
theoret. $\delta^{18}O_{calcite}$			3.74			4.24			4.26			4.25			4.28
23514															
Temp [°C]	4.8	4.2	4.5	4.2	3.9	4.1	3.9	3.7	3.8	3.7	3.6	3.7	3.6	3.6	3.6
S [psu]	33.1	34.0	33.6	34.0	34.5	34.3	34.5	34.7	34.6	34.7	34.8	34.8	34.8	34.5	34.7
$\delta^{18}O_{water}$			-0.29			-0.04			0.09			0.14			0.10
theoret. $\delta^{18}O_{calcite}$			2.76			3.14			3.33			3.42			3.40
23523															
Temp [°C]	9.5	8.6	9.1	8.6	6.9	7.8	6.9	6.6	6.8	6.6	6.4	6.5	6.4	6.4	6.4
S [psu]	35.0	35.0	35.0	35.0	35.1	35.1	35.1	35.1	35.1	35.1	35.1	35.1	35.1	35.1	35.1
$\delta^{18}O_{water}$			0.23			0.25			0.27			0.27			0.27
theoret. $\delta^{18}O_{calcite}$			2.12			2.46			2.73			2.80			2.83
23528															
Temp [°C]	9.0	8.0	8.5	8.0	6.9	7.5	6.9	6.7	6.8	6.7	6.4	6.6	6.4	6.4	6.4
S [psu]	34.8	35.0	34.9	35.0	35.0	35.0	35.0	35.0	35.0	35.0	35.0	35.0	35.0	35.0	35.0
$\delta^{18}O_{water}$			0.19			0.23			0.23			0.23			0.23
$\delta^{18}O_{calcite}$			2.22			2.52			2.69			2.75			2.79
23538															
Temp [°C]	11.0	10.1	10.6	10.1	8.7	9.4	8.7	8.4	8.6	8.4	7.9	8.2	7.9	7.3	7.6
S [psu]	35.2	35.2	35.2	35.2	35.2	35.2	35.2	35.3	35.3	35.3	35.2	35.3	35.2	35.2	35.2
$\delta^{18}O_{water}$			0.30			0.30			0.32			0.23			0.30
theoret. $\delta^{18}O_{calcite}$			1.82			2.10			2.33			2.43			2.55
23540															
Temp [°C]	10.7	9.5	10.1	9.5	8.0	8.8	8.0	7.4	7.7	7.4	6.8	7.1	6.8	6.0	6.4
S [psu]	35.1	35.2	35.2	35.2	35.2	35.2	35.2	35.2	35.2	35.2	35.1	35.2	35.2	35.1	35.2
$\delta^{18}O_{water}$			0.28			0.30			0.30			0.28			0.28
theoret. $\delta^{18}O_{calcite}$			1.91			2.26			2.53			2.66			2.84
HM 49-15															
Temp [°C]	10.0	8.2	9.1	8.2	6.3	7.3	6.3	5.4	5.9	5.4	4.8	5.1	4.8	4.2	4.5
S [psu]	35.1	35.1	35.1	35.1	35.1	35.1	35.1	35.1	35.1	35.1	35.1	35.1	35.1	35.0	35.1
$\delta^{18}O_{water}$			0.27			0.27			0.27			0.27			0.25
theoret. $\delta^{18}O_{calcite}$			2.14			2.61			2.97			3.16			3.30
HM 52-18															
Temp [°C]	11.1	10.3	10.7	10.3	9.1	9.7	9.1	8.8	9.0	8.8	8.7	8.8	8.7	8.5	8.6
S [psu]	35.1	35.2	35.2	35.2	35.2	35.2	35.2	35.2	35.2	35.2	35.2	35.2	35.2	35.2	35.2
$\delta^{18}O_{water}$			0.28			0.30			0.30			0.30			0.30
theoret. $\delta^{18}O_{calcite}$			1.76			2.03			2.21			2.26			2.30
HM 52-39															
Temp [°C]	8.5	6.0	7.3	6.0	3.9	5.0	3.9	3.0	3.5	3.0	2.6	2.8	2.6	2.1	2.4
S [psu]	34.9	35.0	35.0	35.0	35.0	35.0	35.0	35.0	35.0	35.0	35.0	35.0	35.0	35.0	35.0
$\delta^{18}O_{water}$			0.21			0.23			0.23			0.23			0.23
theoret. $\delta^{18}O_{calcite}$			2.55			3.17			3.57			3.74			3.86

Hydrographic conditions at core locations (September, compiled from the World Ocean Atlas, 2001)

	0 m	50 m	mean	50 m	100 m	mean	100 m	150 m	mean	150 m	200 m	mean	200 m	250 m	mean
52-42															
Temp [°C]	9.4	7.3	8.4	7.3	5.2	6.3	5.2	4.4	4.8	4.4	3.7	4.1	3.7	3.3	3.5
S [psu]	35.1	35.1	35.1	35.1	35.1	35.1	35.1	35.0	35.1	35.0	35.0	35.0	35.0	35.0	35.0
$\delta^{18}O_{water}$			0.27			0.27			0.25			0.23			0.23
theoret. $\delta^{18}O_{calcite}$			2.33			2.86			3.22			3.41			3.55
57-11															
Temp [°C]	7.0	3.9	5.5	3.9	2.0	3.0	2.0	1.5	1.8	1.5	1.2	1.4	1.2	1.2	1.2
S [psu]	34.8	34.9	34.9	34.9	34.9	34.9	34.9	34.9	34.9	34.9	34.9	34.9	34.9	34.9	34.9
$\delta^{18}O_{water}$			0.18			0.19			0.19			0.19			0.19
theoret. $\delta^{18}O_{calcite}$			2.98			3.67			3.99			4.10			4.15
HM 57-16															
Temp [°C]	8.5	5.9	7.2	5.9	3.7	4.8	3.7	3.1	3.4	3.1	2.8	3.0	2.8	2.5	2.7
S [psu]	35.0	35.0	35.0	35.0	35.0	35.0	35.0	35.0	35.0	35.0	35.0	35.0	35.0	35.0	35.0
$\delta^{18}O_{water}$			0.23			0.23			0.23			0.23			0.23
theoret. $\delta^{18}O_{calcite}$			2.58			3.21			3.58			3.70			3.78
HM 57-20															
Temp [°C]	11.3	9.8	10.6	9.8	8.4	9.1	8.4	7.9	8.2	7.9	7.6	7.8	7.8	7.2	7.5
S [psu]	34.7	35.2	35.0	35.2	35.2	35.2	35.2	35.2	35.2	35.2	35.2	35.2	35.2	35.2	35.2
$\delta^{18}O_{water}$			0.21			0.30			0.30			0.30			0.30
theoret. $\delta^{18}O_{calcite}$			1.73			2.18			2.41			2.52			2.58
HM 71-17															
Temp [°C]	4.1	1.4	2.8	1.4	0.6	1.0	0.6	0.6	0.6	0.6	0.5	0.6	0.5	0.4	0.5
S [psu]	33.9	34.7	34.3	34.7	34.8	34.8	34.8	34.9	34.9	34.9	34.9	34.9	34.9	34.9	34.9
$\delta^{18}O_{water}$			-0.02			0.14			0.18			0.19			0.19
theoret. $\delta^{18}O_{calcite}$			3.50			4.15			4.30			4.33			4.36
HM 71-22															
Temp [°C]	7.8	5.7	6.8	5.7	3.8	4.8	3.8	3.2	3.5	3.2	2.8	3.0	2.8	2.6	2.7
S [psu]	34.9	35.0	35.0	35.0	35.0	35.0	35.0	35.0	35.0	35.0	35.0	35.0	35.0	35.0	35.0
$\delta^{18}O_{water}$			0.21			0.23			0.23			0.23			0.23
theoret. $\delta^{18}O_{calcite}$			2.68			3.22			3.55			3.69			3.77
HM 80-43															
Temp [°C]	3.5	1.1	2.3	1.1	0.7	0.9	0.7	0.6	0.7	0.6	0.4	0.5	0.4	0.2	0.3
S [psu]	33.8	34.7	34.3	34.7	34.9	34.8	34.9	34.9	34.9	34.9	34.9	34.9	34.9	34.9	34.9
$\delta^{18}O_{water}$			-0.04			0.16			0.19			0.19			0.19
theoret. $\delta^{18}O_{calcite}$			3.61			4.19			4.30			4.34			4.40
Temp [°C]	6.0	3.3	4.7	3.3	2.0	2.7	2.0	1.7	1.9	1.7	1.4	1.6	1.4	1.3	1.4
S [psu]	34.6	34.9	34.8	34.9	34.9	34.9	34.9	34.9	34.9	34.9	34.9	34.9	34.9	34.9	34.9
$\delta^{18}O_{water}$			0.14			0.19			0.19			0.19			0.19
theoret. $\delta^{18}O_{calcite}$			3.16			3.75			3.97			4.05			4.10
HM 94-16															
Temp [°C]	6.3	4.1	5.2	4.1	2.7	3.4	2.7	2.3	2.5	2.3	2.1	2.2	2.1	1.9	2.0
S [psu]	35.0	35.0	35.0	35.0	35.0	35.0	35.0	35.0	35.0	35.0	35.0	35.0	35.0	35.0	35.0
$\delta^{18}O_{water}$			0.23			0.23			0.23			0.23			0.23
theoret. $\delta^{18}O_{calcite}$			3.10			3.58			3.82			3.91			3.96
HM 94-18															
Temp [°C]	5.7	3.5	4.6	3.5	2.2	2.9	2.2	1.8	2.0	1.8	1.6	1.7	1.6	1.4	1.5
S [psu]	34.9	35.0	35.0	35.0	35.0	35.0	35.0	35.0	35.0	35.0	35.0	35.0	35.0	35.0	35.0
$\delta^{18}O_{water}$			0.21			0.23			0.23			0.23			0.23
theoret. $\delta^{18}O_{calcite}$			3.24			3.73			3.96			4.04			4.10

Hydrographic conditions at core locations (September, compiled from the World Ocean Atlas, 2001)

	0 m	50 m	mean	50 m	100 m	mean	100 m	150 m	mean	150 m	200 m	mean	200 m	250 m	mean
HM 94-30															
Temp [°C]	3.8	1.0	2.4	1.0	0.1	0.6	0.1	0.1	0.1	0.1	-0.1	0.0	-0.1	-0.2	-0.2
S [psu]	34.3	34.8	34.6	34.8	34.9	34.9	34.9	34.9	34.9	34.9	34.9	34.9	34.9	34.9	34.9
$\delta^{18}O_{water}$			0.07			0.18			0.19			0.19			0.19
theoret. $\delta^{18}O_{calcite}$			3.69			4.31			4.45			4.48			4.53
97-948															
Temp [°C]	11.0	9.0	10.0	9.0	7.8	8.4	7.8	7.3	7.6	7.3	7.0	7.2	7.0	6.7	6.9
S [psu]	34.5	35.0	34.8	35.0	35.1	35.1	35.1	35.2	35.2	35.2	35.2	35.2	35.2	35.1	35.2
$\delta^{18}O_{water}$			0.14			0.25			0.28			0.30			0.28
theoret. $\delta^{18}O_{calcite}$			1.79			2.30			2.55			2.67			2.73
HM 133-21															
Temp [°C]	10.8	10.0	10.4	10.0	8.7	9.4	8.7	8.4	8.6	8.4	8.0	8.2	8.0	8.2	8.1
S [psu]	35.1	35.2	35.2	35.2	35.2	35.2	35.2	35.2	35.2	35.2	35.2	35.2	35.2	35.2	35.2
$\delta^{18}O_{water}$			0.28			0.30			0.30			0.30			0.30
theoret. $\delta^{18}O_{calcite}$			1.84			2.11			2.31			0.30			2.43
HM 133-24															
Temp [°C]	11.2	10.3	10.8	10.3	8.8	9.6	8.8	8.5	8.7	8.5	8.2	8.4	8.2	8.0	8.1
S [psu]	35.1	35.2	35.2	35.2	35.2	35.2	35.2	35.2	35.2	35.2	35.2	35.2	35.2	35..2	35.2
$\delta^{18}O_{water}$			0.28			0.30			0.30			0.30			0.30
theoret. $\delta^{18}O_{calcite}$			1.75			2.06			2.29			2.36			2.43
HM 16130															
Temp [°C]	9.6	7.6	8.6	7.6	5.6	6.6	5.6	4.7	5.2	4.7	4.0	4.4	4.0	3.5	3.8
S [psu]	35.1	35.1	35.1	35.1	35.1	35.1	35.1	35.0	35.1	35.0	35.0	35.0	35.0	35.0	35.0
$\delta^{18}O_{water}$			0.27			0.27			0.25			0.23			0.23
theoret. $\delta^{18}O_{calcite}$			2.27			2.77			3.13			3.33			3.49
HM 16132															
Temp [°C]	10.5	8.8	9.7	8.8	6.9	7.9	6.9	6.2	6.6	6.2	5.5	5.9	5.5	4.9	5.2
S [psu]	35.1	35.2	35.2	35.2	35.2	35.2	35.2	35.1	35.2	35.1	35.1	35.1	35.1	35.0	35.1
$\delta^{18}O_{water}$			0.28			0.30			0.28			0.27			0.25
theoret. $\delta^{18}O_{calcite}$			2.02			2.49			2.80			2.97			3.12
HM 16142															
Temp [°C]	11.3	9.7	10.5	9.7	8.3	9.0	8.3	7.7	8.0	7.7	7.2	7.5	7.2	6.6	6.9
S [psu]	34.7	35.2	35.0	35.2	35.2	35.2	35.2	35.2	35.2	35.2	35.2	35.2	35.2	35.1	35.2
$\delta^{18}O_{water}$			0.21			0.30			0.30			0.30			0.28
theoret. $\delta^{18}O_{calcite}$			1.74			2.20			2.45			2.59			2.71

Calculation of theoretical $\delta^{18}O$-profile based on the paleotemperature equation of Shackleton et al., 1974:

$T(°C) = 16.9 - 4.38*(\delta^{18}O_{calcite} - \delta^{18}O_{water}) + 0.1*(\delta^{18}O_{calcite} - \delta^{18}O_{water})^2$

$\delta^{18}O_{water}$ (SMOW) = –12.17+0.36*S (Simstich et al., 2003)

5. Danksagung

Mit der Fertigstellung dieser Arbeit möchte ich mich bei folgenden Personen bedanken, die maßgeblich zu deren Gelingen beigetragen haben:

Meinem Betreuer Herrn Prof. Anton Eisenhauer danke ich für die ausdauernde Betreuung, seine Hilfestellung, den roten Faden nicht zu verlieren, und seine zahlreichen Ideen, die mit in diese Arbeit eingeflossen sind.

Mara Weinelt danke ich für das unerschöpfliche Probenarchiv und die vielen interessanten Anregungen zu der ‚Cold-End'-Problematik.

Ebenso möchte ich mich bei Herrn Prof. Michael Sarnthein für seine zahlreichen hilfreichen Hinweise bedanken.

Ein großes Dankeschön auch an Jan Fietzke, Barbara Bock, Ana Kolevica sowie Nikolaus Gussone, die mich in die Geheimnisse der Massenspektrometrie sowie der Kalzium-Analytik eingeführt haben.

Florian Böhm wusste auf alle Fragen passende Antworten. Respekt und vielen Dank für die kritische Betrachtung meiner Ergebnisse.

Folkmar Hauff habe ich es zu verdanken, dass die TRITON Tag und Nacht zur Verfügung stand.

Ohne die tatkräftige Unterstützung von Barbara Mader und Peter Appel wären die Messungen an der Mikrosonde nicht möglich gewesen.

Ein Dankeschön auch an meine Freunde, die für so vieles Verständnis aufbrachten.

Ein Kompliment an Macho Amini, die es mit mir drei Jahre im Büro ausgehalten hat.

Und natürlich: last but not least ein herzliches Dankeschön an meine Eltern für ihre vielfältige Unterstützung.

Vielen Dank!